



FACULTAD DE CIENCIAS BIOLÓGICAS
PONTIFICIA UNIVERSIDAD CATÓLICA DE CHILE

Unveiling non canonical roles for RCOR1 and RCOR2 transcriptional co-repressors

A dissertation presented to Pontificia Universidad Católica de Chile in partial fulfillment of the requirements for the degree of Doctor of Philosophy in the subject of Biological Sciences with Specialization in Molecular and Cellular Biology.

By:

CARLOS ANDRÉS RIVERA ÁLVAREZ

Dissertation Advisor : **MARÍA ESTELA ANDRÉS COKE Ph.D.**
Dissertation Co-advisor : **MARCELA K. SJÖBERG HERRERA, Ph.D.**
International Sponsor : **JEANNIE T. LEE, M.D., Ph.D.**

NOVEMBER, 2020

ABSTRACT

The RCOR/CoREST family of transcriptional co-repressors comprises three proteins commonly associated to neurospecific gene silencing in non neuronal cells and early stages of neuronal differentiation. Their repressive role is mediated by their association to the enzymes LSD1 and HDAC1/2, which in turn erase transcriptional-permissive histone modifications. Although RCOR proteins have high identity on their functional domains, they evolved significant biochemical features that explain why their repressive capacity is different between them. Paradoxically, while RCOR complexes have been commonly linked to repression of transcription in different cellular contexts, the inhibition of their associated enzyme activities upregulates histone modifications that favor transcription, suggesting that the complex is acting at euchromatin domains.

The work presented in this thesis was designed to characterize the role of RCOR1 and RCOR2 in subnuclear domains associated to active gene expression. In chapter 2, I unveil RCOR1 as a global repressor of transcription that preferentially targets euchromatin domains and controls RNA Pol II activity. In chapter 3, I describe RCOR2 as a component of nuclear speckles which stabilizes these membrane-less organelles that concentrate pre-mRNA processing factors. In Chapter 4, I discuss the broader significance of my findings relating them to the state of the art in the field, as well as future steps to be taken. I conclude by proposing a model to explain a novel way to understand non canonical functions of transcription co-repressors in active regions of the genome.

RESUMEN

La familia de co-represores transcripcionales RCOR/CoREST comprende tres proteínas comúnmente asociadas a silenciamiento de genes neuronales en células no-neuronales y en etapas tempranas de la diferenciación neuronal. Su capacidad represora es llevada a cabo por las enzimas LSD1 y HDAC1/2, que remueven modificaciones post-traduccionales de histonas permisivas para la transcripción. Si bien las proteínas RCOR poseen alta identidad de secuencia en sus dominios funcionales, han evolucionado características bioquímicas específicas que explican por qué su capacidad represora es diferente. Paradójicamente, mientras los complejos de las proteínas RCOR han sido comúnmente asociadas a la represión de la transcripción en contextos celulares específicos, la inhibición de sus actividades enzimáticas asociadas genera un aumento en modificaciones de histonas que favorecen la transcripción, sugiriendo que el complejo actúa en dominios de eucromatina.

El presente trabajo fue diseñado para caracterizar el rol de las proteínas RCOR1 y RCOR2 en dominios intranucleares asociados a expresión génica activa. En el capítulo 2, revelo a RCOR1 como un represor global de la transcripción que se recluta en dominios de eucromatina y controla la actividad de la RNA Polimerasa II. En el capítulo 3, describo a RCOR2 como un componente de speckles nucleares que estabiliza dichos organelos no-membranosos. En el capítulo 4, discuto la significancia de mis hallazgos y los relaciono con el estado del arte del campo. Finalmente, concluyo proponiendo un modelo para comprender funciones no canónicas de co-represores de la transcripción en regiones activas del genoma.

TABLE OF CONTENTS AND FIGURES

ABSTRACT	iii
RESUMEN	iv
ACKNOWLEDGEMENTS	1
DEDICATION	4
ABBREVIATIONS	5
CHAPTER I	9
INTRODUCTION	9
CHROMATIN AND ITS DYNAMIC STRUCTURE	10
TRANSCRIPTION CO-REGULATORS	10
RCOR/COREST TRANSCRIPTIONAL CO-REPRESSORS	11
RCOR PROTEINS DISPLAY DIFFERENTIAL BIOCHEMICAL PROPERTIES	13
<i>Figure 1.</i>	15
RECRUITMENT OF RCOR PROTEINS TO CHROMATIN	16
CHROMATIN MODIFICATION EXERTED BY THE RCOR-LSD1-HDAC1/2 COMPLEX	17
RCOR FAMILY MEMBERS MARK DIFFERENT SUBNUCLEAR TERRITORIES ASSOCIATED WITH TRANSCRIPTIONALLY ACTIVE CHROMATIN REGIONS	19
<i>Figure 2.</i>	20
HYPOTHESIS	21
GENERAL AIM	22
SPECIFIC AIMS	22
CHAPTER II	24
<i>Unveiling RCOR1 as a rheostat at transcriptional permissive chromatin</i>	24

COVER LETTER	25
ABSTRACT	28
INTRODUCTION	29
RESULTS	32
Different RCOR1-containing complexes segregate inside cells and mostly enriched in the interchromatin space.....	32
RCOR1 is mostly enriched at transcriptionally permissive chromatin	35
The LSD1-RCOR1-HDAC1 complex marks proximal promoters in euchromatin	38
RCOR1 is preferentially enriched in highly expressed genes	40
RCOR1 physically interacts with RNA Polymerase II at transcription specific stages	41
RCOR1 is a fast-acting repressor of de novo transcription	43
DISCUSSION	46
A distribution equilibrium between cytosolic, nucleoplasm and chromatin for the RCOR1 complex subunits	46
Enrichment of RCOR1 at accessible and transcribed chromatin	47
Insights on the recruitment of RCOR1 at specific transcription stages.....	49
ACKNOWLEDGEMENTS	51
AUTHOR CONTRIBUTIONS	51
DECLARATION OF COMPETING INTERESTS	51
FIGURES	52
Figure 1. Three different subpopulations of the LSD1-RCOR1-HDAC1/2 complex coexist in cells.....	52
Figure 2. RCOR1 is enriched in accessible, transcriptionally permissive chromatin.....	54
Figure 3. RCOR1 is closer to H3K4me3 than H3K27me3 in 3D simulated chromosome 20.	56
Figure 4. RCOR1 is enriched in proximal promoters of active genes.....	58
Figure 5. RCOR1 occupancies are positively correlated with gene expression.	60
Figure 6. RCOR1 establishes an interaction with RNA Pol II after initiation and before elongation.	62
Figure 7. RCOR1 globally represses transcription of rapidly synthesized transcripts.	64
MATERIAL AND METHODS	67
Cell culture	67
Antibodies	67
Cell Immunofluorescence	68
Image analyses	68
Subcellular fractionation and sequential extraction of chromatin-bound proteins	69
Immunoprecipitation.	69
Western blot	70
MNase digestion and sucrose gradient ultracentrifugation	71
Analysis of ChIP-seq data sets.....	71
Analysis of genomic enrichment.....	71
Distance distribution analysis	71
High resolution chromosome modeling	71
Imaging of nascent transcripts	73
Exon Inclusion Frequency by Relative Quantity Fluorescent-PCR Analysis (Rqf-PCR).....	73
Statistical analyses	73
REFERENCES	75
SUPPLEMENTARY INFORMATION	82

Figure S1.....	83
Figure S2.....	84
Figure S3.....	85
Figure S4.....	86
Figure S5.....	87
Figure S6.....	88
CHAPTER III.....	90
<i>RCOR2 is a core component of nuclear speckles and stabilizes SRSF2</i>	90
COVER LETTER.....	91
ABSTRACT	94
INTRODUCTION	95
MATERIALS AND METHODS.....	98
Animals.....	98
Cell culture.....	98
Antibodies.....	98
Cell Immunofluorescence.....	98
Poly(A)-RNA In situ hybridization.....	99
Microscopy:	99
Image analyses.....	99
Immunoprecipitation.....	100
RNA immunoprecipitation (RIP).....	100
Subcellular fractionation and sequential extraction of chromatin-bound proteins.....	100
RNA interference.....	101
RESULTS	102
The RCOR2-LSD1 complex is specifically compartmentalized at nuclear speckles.....	102
RCOR2 associates with nuclear speckles inside its core region.....	103
RCOR2 recruitment to nuclear speckles is stabilized by RNA	105
Chemical perturbation of nuclear speckle architecture does not alter RCOR2 recruitment to nuclear speckles.....	106
RCOR2 stabilizes the architecture of nuclear speckles	108
DISCUSSION	109
Sub-nuclear distribution equilibrium of RCOR2 reflecting a novel non-canonical function.....	109
RCOR2 impact on gene expression: beyond chromatin?.....	110
An RNA component allows for the localization of RCOR2 at the core of nuclear speckles	112
Stability of nuclear speckle-bound RCOR2: even higher than splicing factors	113
RCOR2 stabilizes nuclear speckles.....	114
ACKNOWLEDGEMENTS.....	115
FUNDING:	115
DECLARATION OF COMPETING INTERESTS:.....	115
SUPPLEMENTARY DATA STATEMENT.....	115
FIGURES	116

Figure 1. RCOR2 colocalizes with nuclear speckles.....	116
Figure 2. RCOR2 associates with nuclear speckles at their core region.	118
Figure 3. An RNA component stabilizes RCOR2 at nuclear speckles.	121
Figure 4. RCOR2 nucleation in speckles is highly stable.	123
Figure 5. RCOR2 regulates SRSF2 stability.	125
REFERENCES	127
SUPPLEMENTARY INFORMATION.....	134
Figure S1.....	135
Figure S2.....	136
Figure S3.....	137
CHAPTER IV.....	139
GENERAL DISCUSSION	139
DISCUSSION	140
Insights from the evolution of co-repressor proteins	140
On the subcellular distribution of RCOR1 and RCOR2	141
On the interaction between RCOR1 and RNA Polymerase II	143
On the non-canonical role of RCOR1 in euchromatin gene repression.....	144
On the molecular assemblies of RCOR proteins.....	147
Conclusive remarks	148
UNCATEGORIZED REFERENCES	149

ACKNOWLEDGEMENTS

The degree of Doctor in Philosophy in the field of Biological Sciences is supposed to give graduate students their first certification to continue an academic life pursuing the goal of being an independent researcher. However, not all graduate students have the opportunity to perform their investigations with a degree of freedom that allows them to get prepared as independent researchers. In this regard, I am grateful to have had the opportunity to design and perform the present research with enough liberty to put my own style on it. In my opinion, this would not have been possible without the trust that Estela, Marcela and Jeannie put in me. I sincerely thank them for being great mentors in this process and teaching me strategies to perform consistent research. I thank Estela for accepting me in her laboratory and for always consider my suggestions on scientific discussions. She is a brilliant woman in science made in Chile, and I had the honor to count with her as my PhD mentor. I thank her for promoting horizontal relationships between investigators and students, for being transparent and honest on every advice she gives, and also for supporting me in all the decisions I did during my stay in the program. In addition, a big debt of gratitude is owed to Jeannie, I was happy to have had the chance to perform a short-term internship in her laboratory, which is one of the leaders in the field of epigenetics. Surprisingly, she gave me the wonderful opportunity to finish my Ph.D. in her laboratory, besides supporting the extension of my visa and offering a postdoctoral position in her lab. It is a real honor for me to have counted with her during this process. I thank

her for being one of these successful scientists who keep being humble, empathetic and human. I commit to perform my best to find exciting discoveries during my next steps in science guided by her as my principal mentor.

This process involves a series of responsibilities that significantly impact our mental health. I was not the exception, but without the support of my family and friends, I could have fallen into the abyss. I did not, so I thank my parents for always encouraging me to do my best to pursue my dreams. I wish I could have the opportunity to be with them during difficult times they have been dealing with, but somehow I know I contribute to their happiness just because they know I am following their advice, and so they contribute to my joy only by the fact I feel their love, even when we have been so far away during the final years of my Ph.D. I also thank my beautiful people who have always been giving me their support: Angélica Ovalle, Fernanda Cuevas, Paula García, Jeremy P. Marshall, Macarena Las Heras, Hugo Díaz, Gonzalo Jimenez, Pablo Veloso, Claudia Parra, Fabián Pinto, Pamela Rojas, Benjamín Cartes, Javier Castro, Karla Silva, Fernanda Herrera, Nico Guerrero, Paz Gutiérrez, Melissa Painemilla, Valentina Alarcón and Ester Otárola.

I feel lucky to have had a friendly environment of work where I could establish nice social interactions. Thanks to past and present members of both Estela Andrés and Jeannie T. Lee laboratories, especially to Verónica Noches, Marcela González, Duxan Arancibia, Fabián Guzmán, Danni Wang, Hun-Goo Lee, Katya Nizovtseva, Yesu Jeon and Rodrigo Aguilar.

I thank members of my advisory committee, Dr. Hugo Olgún and Dr. Luis Larrondo for critical advise and their helpful input. I especially thank Dr. Alejandra Loyola who beyond

being a member of the committee will always be my very first mentor in scientific research who motivated me to continue pursuing an academic career in the field of chromatin science.

DEDICATION

Some people think we find joy and peace when doing what we love to do. This work is dedicated to my parents, Corita and Marco. I will never find the same joy and peace as when I am with both of them. Their strength and resilience will guide my steps until the end of my days. Especial dedication is directed to my mother. She has been fighting for more than two years the dreadful pain of pancreatic cancer, unfortunately without the physical option to access any anti-tumoral therapy. However, her life has continued against any prognosis, without losing her willing to live. There is no distance nor borders that split the true love, so I am today and always with her.

ABBREVIATIONS

A.U.	:	Arbitrary units.
Act D	:	Actinomycin D.
ATP	:	Adenosine triphosphate
Bps	:	Base pairs.
CCF	:	Cross Correlation Function
CO ₂	:	Carbon dioxide
CoREST	:	Co-repressor of REST
Corin	:	CoREST complex inhibitor
DNA	:	Deoxyribonucleic acid
ELM2	:	Egl-27 and MTA1 homology 2
ENCODE	:	Encyclopedia of DNA Elements
EtBr	:	Ethidium bromide
EU	:	5-Ethynyl Uridine
EZH2	:	Enhancer of Zeste Homolog 2
GAPDH	:	Glyceraldehyde 3-Phosphate Dehydrogenase
HDAC1	:	Histone Deacetylase 1
HDAC2	:	Histone Deacetylase 2

HP1 α	:	Heterochromatin Protein 1
IgG	:	Immunoglobulin G
IP	:	Immunoprecipitation
KCl	:	Potassium Chloride
LSD1	:	Lysine Specific Demethylase 1
MALAT1	:	Metastasis-associated Lung Adenocarcinoma Transcript 1
MNase	:	Micrococcal Nuclease
NaCl	:	Sodium Chloride
PMSF	:	Phenylmethylsulfonyl Fluoride
Poly(A)-RNA	:	Poly-adenylated RNA
RCOR1	:	REST co-repressor 1
RCOR2	:	REST co-repressor 2
RCOR3	:	REST co-repressor 3
RDF	:	Radial Distribution Function
REST	:	RE1 Silencing Transcription Factor
RNA	:	Ribonucleic Acid
RNA Pol II	:	RNA Polymerase II
RNase A	:	Ribonuclease A

RPB1	:	RNA Polymerase II subunit B1
S2P	:	Serine 2 Phosphorylation
S5P	:	Serine 5 Phosphorylation
S7P	:	Serine 7 Phosphorylation
SANT	:	Swi3 Ada2 N-Cor and TFIIB
SDS	:	Sodium Dodecyl Sulphate
SEM	:	Standard error of measurement
siRNA	:	Small interfering RNA
SRSF2	:	Serine and Arginine Rich Splicing Factor 2
STD	:	Molecular Weight Standard
TCP	:	Tranlycypromine
TES	:	Transcription End Site
TSS	:	Transcription Start Site
μg	:	Microgram
μL	:	Microliter
μM	:	Micromolar
μm	:	Micrometer
UTR	:	Untranslated region

CHAPTER I

INTRODUCTION

INTRODUCTION

CHROMATIN AND ITS DYNAMIC STRUCTURE

The genetic information of eukaryotic organisms is stored as DNA. The native conformation of this nucleic acid is highly compacted inside the cell nuclei due to proteins and other factors that, once bound to it, generate a supramolecular, nucleoprotein structure known as chromatin (Butler 1983). The basic unit which confers the first level of chromatin compaction is the nucleosome (Kornberg 1974), a complex whose DNA distribution follows a repetitive nature. Each nucleosome is composed by an octamer of basic proteins called histones, over which 147 base pairs of DNA are supercoiled 1.75 times (Luger et al. 1997). Chromatin structure is dynamic, since it suffers global and local changes on its degree of compaction during replication, cell division, transcriptional cycles, co-transcriptional splicing, DNA repair and others. These changes are regulated by enzymes that post-translationally modify N-terminal histone tails, ATP-dependent chromatin remodeling complexes, non coding RNAs and histone chaperones that selectively incorporate different histone variants at specific genomic regions (Meller, Joshi, and Deshpande 2015; Rivera et al. 2014; Gurard-Levin, Quivy, and Almouzni 2014; Hamiche and Shuaib 2013; Kouzarides 2007; De Koning et al. 2007; Gunjan, Paik, and Verreault 2006; Benson et al. 2006; Loyola and Almouzni 2004; Vignali et al. 2000).

TRANSCRIPTION CO-REGULATORS

The access of the transcription machinery to specific chromatin regions can be regulated by molecular signals that activate the recruitment of transcription factors (TFs) that bind particular

response elements (REs) present along over the genome. TFs can further recruit co-regulator complexes, which can interact both with basal transcriptional machinery factors and enzymes that modify the local state of chromatin (Lee et al. 2001; McKenna, Lanz, and O'Malley 1999; McKenna and O'Malley 2001). According to their last activity on their target genes, co-regulators are classified as co-activator or co-repressor complexes. For instance, the P300 protein enhances estrogen receptor (ER)-mediated transcriptional activation over its target genes, given its lysine acetyltransferase activity, which can favor gene expression (Kraus and Kadonaga 1998). Similarly, NCOR proteins (Nuclear Receptor Co-repressors) associate to the retinoic acid receptor (RAR) to mediate basal transcriptional repression in the absence of RAR-ligands. This function is mediated, in part, by the association of NCOR to different histone deacetylases (HDACs) that further erase classical histone acetylations which favor transcriptional activity (Huang, Myers, and Dingledine 1999; Kao et al. 2000; Wen et al. 2000).

RCOR/COREST TRANSCRIPTIONAL CO-REPRESSORS

The REST/NRSF Co-repressor (RCOR) family of transcription co-repressors, which is also known as CoREST (Co-repressor of REST), comprises three paralogues genes that code for the proteins RCOR1, RCOR2 and RCOR3. RCOR1 was the first identified member of this family, and to date, the best characterized. The canonical role of RCOR1 is to act as transcription co-repressor of REST (Andres et al. 1999), a repressive transcription factor which silence the expression of neuronal genes in non-neuronal cells and neuronal precursor cells (Ballas et al. 2001; Andres et al. 1999). However, after RCOR1 was discovered, it has been shown that RCOR1 can also plays a transcriptional regulatory role in REST-independent cellular contexts. For instance, RCOR1 can bind the orphan receptor Nurr1 to regulate the expression of

proinflammatory genes in neuroglia (Saijo et al. 2009). In addition, RCOR1 can bind to the Steroid Receptor RNA Activator complex (SRA) to keep a basal silencing in SRA-targets (Vicent et al. 2013); and to Growth Factor Independence (Gfi) transcription factors to repress Gfi-target genes during hematopoietic differentiation (Saleque et al. 2007).

RCOR1-mediated repression is driven by the interaction it establishes with chromatin-remodeling proteins such as Histone H3 Lysine 4 specific Demethylase 1A (LSD1/KDM1) (You et al. 2001), Histone Deacetylases 1 and 2 (HDAC1/2, KDAC1/2) (Humphrey et al. 2001; You et al. 2001); the histone H3 lysine 9 methyl transferases G9a/KMT1C and EuHMT/KMT1D (Shi et al. 2003); subunits of the Switch/Sucrose Non-Fermentable (SWI-SNF) ATP-dependent chromatin remodeling complex (Battaglioli et al. 2002); and others. Among these interactions, the ones who define the biochemically-stable RCOR1 core-complex, resistant to multiple chromatography steps of purification, are LSD1 y HDAC1/2 (Ballas et al. 2001; Humphrey et al. 2001; You et al. 2001). In this context, there is substantial evidence emerging from structural studies showing a strong and stable interaction between RCOR1 and LSD1 (Forneris et al. 2007). Nevertheless, while there are no crystallographic data defining the structure of the ternary RCOR1-LSD1-HDAC1/2 complex, RCOR proteins have ELM2 and SANT1 contiguous conserved domains, suggesting they evolved classical HDAC-recruitment domains. It has been shown *in vitro* that these regions participate in the recruitment of HDAC1 and HDAC2 (Lee et al. 2006), and the crystal structure of the homologous ELM2-SANT domain present in the MTA1-HDAC1 complex (Millard, Watson, Celardo, et al. 2013) supports this feature. Recently, the first evidence characterizing the structure of the ternary complex emerged from Small-Angle X-Ray Scattering (SAXS) experiments and showed that the complex has a bilobed structure in which LSD1 and HDAC1 can not act in the same histone

substrate at a given time (Song et al. 2020).

Functionally, the subunits of the RCOR1-LSD1-HDAC1/2 complex can cross-regulate their activities to mediate a sequential action once recruited in chromatin. *In vitro* studies have shown that the LSD1 demethylase activity is reduced when HDAC activity is inhibited, suggesting that histone acetylation marks have to be erased prior to histone H3 lysine four demethylation (Lan, Nottke, and Shi 2008; Lan et al. 2007; Shi et al. 2005). On the other hand, it was recently shown that the catalytic mechanism of the complex does not follow a Michaelis-Menten behavior on its two enzymatic activities, and HDAC or LSD1 inhibitors can impact the efficiency of both enzymes, suggesting that LSD1 and HDAC1 have a coupled mechanism in the ternary complex (Song et al. 2020).

RCOR PROTEINS DISPLAY DIFFERENTIAL BIOCHEMICAL PROPERTIES

Both RCOR2 and RCOR3 were identified later than RCOR1, and there are few reports characterizing their biochemical properties. In mammals, the three RCOR proteins have a high degree of conservation of their primary structures. In fact, their homologs in murine species are 92%, 98%, and 97% identical for RCOR1, RCOR2, and RCOR3, respectively. In this context, RCOR2 and RCOR3 are significantly different from RCOR1. Furthermore, RCOR3 has different splicing variants that suggest functional specialization for each RCOR member (Saez et al. 2015).

The biggest identity among RCOR family members is present in three conserved domains:

ELM2, SANT1, and SANT2 (**Figure 1**), which are commonly found in co-repressor proteins that recruit chromatin-modifying enzymes. Interestingly, these domains participate in the recruitment of LSD1 and HDAC1 to RCOR complexes since the RCOR1-LSD1 interaction region maps from the RCOR1 linker region towards the first amino acids of the SANT2 domain. In the same way, the RCOR1-HDAC1 interaction occurs through the ELM2-SANT1 RCOR1 domains (You et al. 2001). Additional support emerged from evidence showing that the ELM2 domain is essential to stimulate the HDAC activity of the complex (Lee et al. 2006), while the SANT2 domain is necessary to enhance its demethylase activity in nucleosomal substrates (Shi et al. 2005). In addition, the SANT2 region establishes an interaction with the major groove of nucleosomal DNA, whose disruption abolishes LSD1 activity (Forneris et al. 2007). Altogether, these data suggest that RCOR proteins evolved specific domains to recruit and regulate the activity of enzymes that erase transcriptional-permissive modifications in chromatin.

It is noteworthy to mention that some RCOR3 isoforms lack the SANT2 domain, as the variant RCOR3C in the rat (Saez et al. 2015). Consequently, *in vitro* studies revealed that while RCOR1 and RCOR2 exert a stimulatory effect on LSD1 activity, RCOR3C lacks that property (Upadhyay et al. 2014). Regarding their repressive role, RCOR2 and RCOR3 display a significantly lower repressive capacity than RCOR1 (Barrios et al. 2014). Also, RCOR2-mediated repression is resistant to HDAC inhibitors because its interaction with HDACs is negligible compared to RCOR1 (Barrios et al. 2014). In summary, this evidence suggests that RCOR proteins evolved specialized biochemical properties to regulate their biological activity and gene expression differentially.

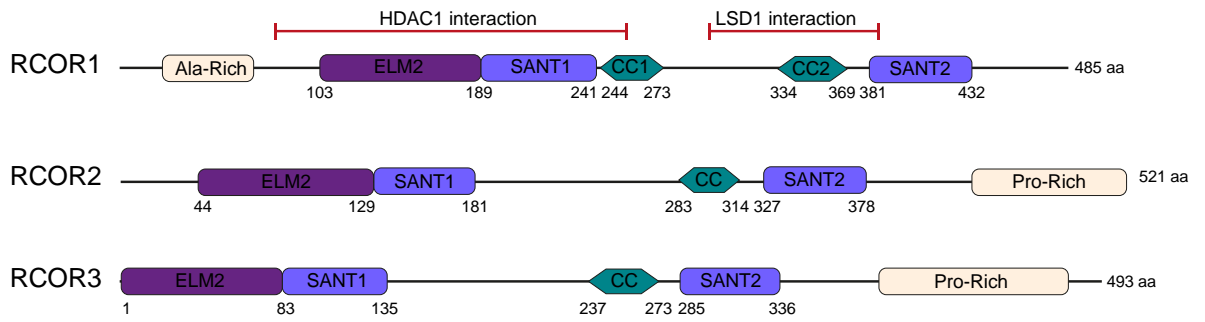


Figure 1. Representative scheme depicting conserved domains among RCOR proteins. CC: Coiled-coil domain. Included are compositional bias domains as Alanine and Proline-rich domains.

RECRUITMENT OF RCOR PROTEINS TO CHROMATIN

The mechanisms by which RCOR co-repressor proteins are targeted to chromatin remain as an unexplored topic. However, there are some insights from RCOR1-focused studies showing different chromatin-targeting mechanisms. Besides its binding to transcription factors such as REST (Andres et al. 1999), there are some RCOR1-target genes where their DNA methylation participates in recruiting RCOR1 through MECP2 (Methyl-CpG Binding Protein 2) (Ballas and Mandel 2005). A third possibility emerges from thermodynamic and structural evidence showing that the third alpha-helix structure residing inside the RCOR1 SANT2 domain binds directly to the major groove of nucleosomal DNA (Yang et al. 2006). This interaction is not favored by specific DNA sequences, and it is highly sensitive to ionic strength, suggesting it is mostly based on electrostatic interactions between RCOR1 and the DNA (Pilotto et al. 2015). Moreover, the affinity between RCOR1 and nucleosomes increases with the length of linker DNA harbored by the histone octamers, suggesting that RCOR1-binding to nucleosomes is stabilized by internucleosomal DNA (Kim et al. 2015). This suggests that once recruited to chromatin, the complex could move along the DNA until reaching a favorable conformation. In accordance with the previous statement, it also suggests that there could be RCOR-regulated genomic regions where the complex lacks the need for auxiliary proteins to be targeted to chromatin. Finally, while it is known that RCOR1 favors LSD1 activity towards nucleosomes (Forneris et al. 2007), LSD1 can also bind unmodified histone H3 (Forneris et al. 2005), suggesting that the complex could be recruited to chromatin in a demethylase-independent manner and/or that the complex could remain bound to chromatin after LSD1-mediated histone demethylation. Nevertheless, there is a need for studies that address this

phenomenon *in vivo*.

CHROMATIN MODIFICATION EXERTED BY THE RCOR-LSD1-HDAC1/2 COMPLEX

Different reports suggest key roles for RCOR proteins in neuronal, hematopoietic, and embryonic differentiation (Andres et al. 1999; Ballas et al. 2005b; Saleque et al. 2007; Upadhyay et al. 2014; Ballas and Mandel 2005; Lee et al. 2014), where chromatin is subject of global changes to reprogram gene expression towards the establishment of a new phenotype (Brero et al. 2005; Dixon et al. 2015; Tagoh et al. 2004). In addition, RCOR1 has been proposed as a mediator of global chromatin compaction. To understand this statement, it is necessary to consider the crosstalk mechanisms co-existing inside the chromatin template, especially at the histone modification levels, where the establishment of a single modification impacts the imposition or removal of another one (Suganuma and Workman 2008). For example, acetylation of histone H4 lysine 5,8 and 16 residues (H4K5ac, H4K8ac, and H4K16ac) can recruit the COMPASS (Complex Proteins Associated with Set1) complex, which further methylate lysine 4 of histone H3 (Zhao et al. 2013). This modification frequently colocalizes with proximal promoters and transcription start sites or gene bodies of actively expressed genes (Wang, Li, and Hu 2014; Zhang, Parvin, and Huang 2012). In this sense, considering that RCOR complexes act by erasing those histone modifications (Lan, Nottke, and Shi 2008; Lan et al. 2007; Shi et al. 2005), they could be playing a role in euchromatin by mediating crosstalk with the enzymes that impose transcription permissive histone marks. Indeed, it has been

reported that when the complex is inhibited by a small molecule inhibitor targeting both LSD1 and HDAC1 activities, multiple transcription permissive histone modifications are upregulated, suggesting that the complex is mediating a role in actively expressed chromatin domains (Anastas et al. 2019).

RCOR FAMILY MEMBERS MARK DIFFERENT SUBNUCLEAR TERRITORIES ASSOCIATED WITH TRANSCRIPTIONALLY ACTIVE CHROMATIN REGIONS

Comparative studies between RCOR co-repressors have been carried out by different laboratories, including ours. In regard to independent functions for each RCOR protein, exciting observations have been reported. On the one hand, RCOR stimulatory effect over LSD1 activity depends on which RCOR protein is binding to LSD1. While RCOR1 potentiates its activity, RCOR2 can exert that function but at concentrations ten times higher than RCOR1 (Upadhyay et al. 2014). Surprisingly, RCOR3C can block the RCOR1-mediated LSD1-stimulation by an unknown mechanism (Upadhyay et al. 2014). Furthermore, RCOR proteins cannot interact between them, as suggested by independent pull-down experiments where each RCOR protein was independently tagged (Barrios et al. 2014). In addition, unpublished data from our laboratory showed that RCOR proteins are occupying different subcellular territories, and they do not colocalize (**Figure 2**), supporting the aforementioned evidence. Interestingly, RCOR proteins are segregated from DNA dense regions, suggesting they are enriched in euchromatin.

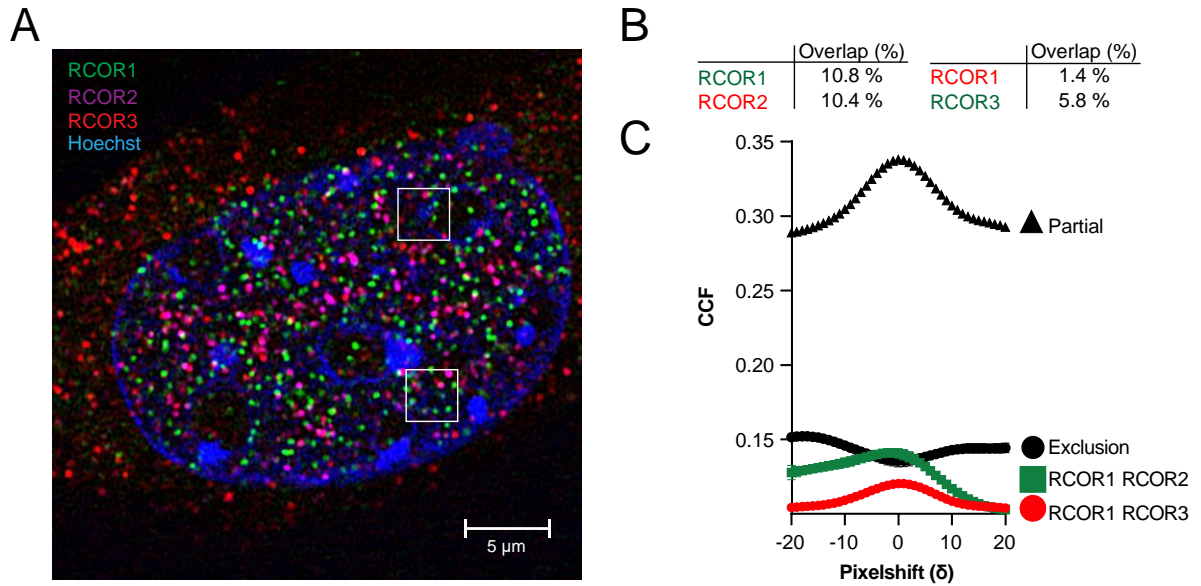


Figure 2. (A) RCOR proteins are segregated inside the cell, as seen in triple immunostaining performed on HT22 cells. (B) Overlapping of pixels shows that the colocalization between RCOR proteins is minimal, according to Mander's colocalization test. (C) Van Steensel's analysis of colocalization between RCOR proteins shows a low correlation between their fluorescent signals. (Rivera et al., unpublished).

HYPOTHESIS

State of the art commonly associates the function of repressor complexes to the establishment and maintenance of heterochromatin domains. For instance, the Suv39H1/HP1 (Suppressor of variegation 3-9 Homolog 1 / Heterochromatin Protein 1) complex is fundamental for the maintenance of pericentric heterochromatin as PRC1/2 (Polycomb Repressive Complex 1 and 2) is to facultative heterochromatin (Craig 2005; Probst and Almouzni 2008). However, little evidence has been reported to gain mechanistic insights about the potential roles of repressive enzymes in euchromatin. In this sense, both the evident repressive activity of RCOR proteins and their segregation in different subnuclear territories that are excluded from dense DNA regions make them an interesting model to characterize their role in euchromatin or in the nucleoplasmic space. Interestingly, reports from our laboratory and independent groups have shown RCOR2 immunostainings as a punctate pattern (Monaghan et al. 2017; Saez et al. 2015), suggesting it is recruited to some type of nuclear body close to euchromatin.

Given all the aforementioned evidence, the following hypothesis is presented:

“The transcriptional co-repressors RCOR1 and RCOR2 are playing differential roles in defined subnuclear compartments.”

GENERAL AIM

To unveil the roles of RCOR1 and RCOR2 beyond heterochromatin domains.

SPECIFIC AIMS

1. To characterize the role of RCOR1 in euchromatin.
 - a. To describe the subcellular and chromatin association properties of RCOR1.
 - b. To characterize the genomic distribution of RCOR1 in chromatin.
 - c. To evaluate if the modulation of RCOR1 levels impacts gene expression activity.

2. To characterize the role of RCOR2 in nucleoplasmic granules.
 - a. To identify the nuclear bodies where RCOR2 is recruited.
 - b. To evaluate if the modulation of RCOR2 levels impacts the function of these nuclear bodies.

CHAPTER II

Unveiling RCOR1 as a rheostat at transcriptional permissive chromatin

COVER LETTER

10/29/2020

Santiago, Chile

Manuscript Administration

Nature Communications - Editorial Office

4 Crinan Street

London N1 9XW

Dear editors:

We are pleased to submit the manuscript entitled “Unveiling RCOR1 as a rheostat a transcriptional permissive chromatin” by Carlos Rivera, Hun-Goo Lee, Anna Lappala, Verónica Noches, Montserrat Olivares-Costa, Marcela Sjöberg Herrera, Jeannie T. Lee and María Estela Andrés to be considered as original research Article. We strongly believe that our manuscript provides highly novel findings that will interest a large audience in the fields of Epigenetics, Transcriptional Dynamics, Chromatin Modifications and Gene Expression Regulation.

This investigation is the result of a successful collaboration with Dr. Jeannie T. Lee at Massachusetts General Hospital – Harvard Medical School, Boston, MA, USA. The aim of this work is to explore the mechanisms beyond a paradoxical finding showing that the classical neuronal-gene co-repressor RCOR1/CoREST, and its associated chromatin modifiers are preferentially enriched in transcriptionally active chromatin. With the use of high resolution

microscopy, biochemical approaches, bioinformatics and chromosome modeling techniques, we characterize this phenomena and discover that RCOR1 is recruited to the transcriptional machinery during the stage of promoter-proximal pausing and negatively regulates the speed of nascent-transcript synthesis. In addition, we show that the RCOR1-LSD1-HDAC1 complex is not only acting by removing histone modifications that favors transcription, since its inhibition led to an increase in the levels of lysine acetylation in the RNA polymerase II catalytic subunit, RPB1.

We could define a novel non-canonical function of RCOR1 beyond canonical ways to associate it to repressive compartments and provide a possible explanation to the paradox of the function of co-repressor complexes in euchromatin. We believe it will motivate further studies in the field. We declare this manuscript is original, it has not been published before nor it is being currently submitted to any other research journal. Finally, we thank you in advance for considering our manuscript and sincerely hope you will find it compelling.

Sincerely,

María Estela Andrés

Cellular and Molecular Biology Department

Pontifical Catholic University of Chile

Unveiling RCOR1 as a rheostat at transcriptional permissive chromatin

Carlos Rivera^{1,2,3,‡}, Hun-Goo Lee^{2,3,‡}, Anna Lappala^{2,3}, Verónica Noches¹, Montserrat Olivares-Costa¹, Marcela Sjöberg Herrera¹, Jeannie T. Lee^{2,3,#,*} & María Estela Andrés^{1,#,*}

¹ Department of Cellular and Molecular Biology, Faculty of Biological Sciences, Pontificia Universidad Católica de Chile. Santiago, 8330025, Chile.

² Department of Molecular Biology, Massachusetts General Hospital. Boston, MA 02114, USA.

³ Department of Genetics. The Blavatnik Institute, Harvard Medical School. Boston, MA 02114, USA.

[‡] These authors contributed equally to this work.

[#] These authors agreed to be considered as corresponding authors.

^{*} To whom correspondence should be addressed: María Estela Andrés, Ph.D. E-mail:

mandres@bio.puc.cl. Jeannie T. Lee, MD, Ph.D. E-mail: lee@molbio.mgh.harvard.edu

Keywords: RCOR1, LSD1, HDAC1, RPB1, RNA Pol II, Transcription, transcriptional co-repressor, euchromatin, histone modifications.

ABSTRACT

RCOR1 forms a stable complex with LSD1 and HDAC1/2 enzymes, which erase the transcriptionally-permissive histone modifications H3K4me1/2 and acetylation. RCOR1 is considered a crucial factor for the recruitment and positioning of LSD1 and HDAC1/2 on their chromatin substrates. Here, we examined the genome-wide role of RCOR1 in transcriptional regulation by using high-resolution microscopic, biochemical, and bioinformatics approaches. Unexpectedly, we found RCOR1 preferentially at accessible and transcriptionally-permissive chromatin. Metagenomic analyses of RCOR1 chromatin occupancy revealed RCOR1 peaks at transcriptionally-active chromatin and highly expressed genes. Finally, we demonstrated that RCOR1 controls RNA Polymerase II between transcription initiation and productive elongation, modulating the acetylation of its carboxy-terminal domain and de novo transcription speed on a short time scale. We conclude that RCOR1 is a transcriptional dampener in actively expressed genes.

INTRODUCTION

The process of gene expression on eukaryotic chromatin involves multiple layers of regulation. A key feature in this process is that transcription factors and chromatin-modifying enzymes must establish interactions with chromatin to exert transcriptional effects (Cusanovich et al. 2014; Liu and Tjian 2018). A critical factor influencing productive collisions with chromatin is the access to differentially compacted chromatin domains, such as open, actively transcribed (euchromatin), and highly compacted, repressed (heterochromatin) regions. Both types of domains require the activity of chromatin-modifying factors that participate in the establishment and maintenance of specific chromatin landscapes (Almouzni and Probst 2011; Trojer and Reinberg 2007). Thus, chromatin landscapes can be defined by histone modifications as di and tri-methylations of histone H3 lysine 4 (H3K4me_{2/3}) at transcriptionally-permissive chromatin, and tri-methylations of histone H3 lysine 9 and 27 (H3K9me₃ and H3K27me₃) marking constitutive and facultative heterochromatin (Almouzni and Probst 2011; Bannister and Kouzarides 2011; Trojer and Reinberg 2007). These specific chromatin signatures then aid or repress the RNA polymerase II (RNA Pol II) recruitment or its activity at target genes (Bannister and Kouzarides 2011; Kouzarides 2007).

The REST co-repressor 1 (RCOR1/CoREST1) was one of the first characterized co-repressor proteins based on its ability to induce transcriptional silencing of neuronal genes when interacting with RE1-Silencing Transcription Factor (REST) (Andres et al. 1999; Ballas et al. 2001). Among the three reported members of the RCOR family of proteins in mammals, RCOR1 has the highest repressive capacity over target reporter genes (Barrios et al. 2014). It can form a core co-repressor complex by associating with the lysine-specific demethylase 1A

(LSD1, KDM1A) (You et al. 2001) and Class I histone deacetylases 1 and 2 (HDAC1/2) (Ballas et al. 2001; Humphrey et al. 2001; Shi et al. 2003). Therefore, by the histone code hypothesis (Bannister and Kouzarides 2011; Jenuwein and Allis 2001; Strahl and Allis 2000), the LSD1-RCOR1-HDAC1/2 complex may be viewed as a biochemical entity that represses transcription by erasing transcriptionally-permissive histone modifications, such as mono and dimethylation of histone H3 lysine 4 (H3K4me1/2) and histone acetylation (Andres et al. 1999; Ballas et al. 2001; Humphrey et al. 2001; You et al. 2001). RCOR1 is the only RCOR family member that efficiently stimulate LSD1 and HDAC1 activities on nucleosomal substrates (Forneris et al. 2007; Lee et al. 2006; Shi et al. 2005; Yang et al. 2006), suggesting it is a necessary factor for efficient recruitment and function of these repressive enzymes.

RCOR1 structure encloses one ELM2 (Egl-27 and MTA1 homology 2) domain and two SANT (Swi3, Ada2, N-Cor, and TFIIB) domains. The first SANT domain localizes contiguously to the ELM2 domain, and both are required for RCOR1 interacting with HDAC1/2. Structural evidence has shown that the SANT2 domain establishes contacts between the RCOR1-LSD1 complex and the major groove of the nucleosomal DNA, suggesting it can interact with chromatin without a bonafide transcription factor (Pilotto et al. 2015). Interestingly, since RCOR1-LSD1 complex interaction either with naked DNA or with nucleosomes was abolished at high concentrations of monovalent ions and limited lengths of internucleosomal DNA (Pilotto et al. 2015), it has been suggested that electrostatic interactions and accessible nucleosome conformations could favor the recruitment of the complex to chromatin. Furthermore, a recent report described the first structural evidence for the ternary LSD1-RCOR1-HDAC1/2 complex, which shows a bilobed structure in which only one of the enzymes can interact with chromatin at a given time (Song et al. 2020), supporting that the

complex works in a sequential coordinated way to erase transcriptionally-permissive marks from histones (Forneris et al. 2005). This finding is consistent with classical biochemical observations where the LSD1 activity was shown to be weaker when HDACs were pharmacologically inhibited (Lan et al. 2007; Lan, Nottke, and Shi 2008; Shi et al. 2005).

Although some transcription factors such as REST and Gfi have been proposed as RCOR1 recruiters (Andres et al. 1999; Monaghan et al. 2017; Saijo et al. 2009; Vicent et al. 2013), the transcriptome regulated by RCOR1 is wider than theirs (Abrajano et al. 2010; Abrajano et al. 2009), suggesting RCOR1 plays additional independent roles in transcriptional regulation. The lack of evidence regarding how the LSD1-RCOR1-HDAC1/2 complex is endogenously distributed in the nucleus led us to explore its chromatin association properties and distribution features by biochemical, microscopical, and bioinformatics approaches. Here, we describe the existence of different subcellular variants of this complex. Surprisingly, we find RCOR1 enriched in actively expressed genes. We investigate this paradox and discuss how our findings might impact the canonical view of transcriptional regulation at active genes.

RESULTS

Different RCOR1-containing complexes segregate inside cells and mostly enriched in the interchromatin space

Based on reports showing that chromatin modifying factors and transcription factors establish interactions with chromatin (Cusanovich et al. 2014; Liu and Tjian 2018), we hypothesized that RCOR1 complexes, as a result of their collisions with chromatin, should display a distribution equilibrium between chromatin and nucleoplasm at steady state. To test this idea, we analyzed the subcellular distribution of RCOR1, LSD1, and HDAC1/2 in undifferentiated HT22 cells that express low amounts of the neuronal variant of LSD1 (**Figure S1A**). Immunostainings to double-label RCOR1 and each subunit of the complex were analyzed at high-confocal resolution using Airyscan confocal acquisition and super-resolution processing. We observed that the subunits of the complex were enriched inside the nucleus, although cytoplasmic localization was also detected (**Figure 1A**). As expected, we found RCOR1 establishing contacts or localizing in close proximity to its partners LSD1, HDAC1, and HDAC2. These observations were confirmed by measuring the 2D colocalization between RCOR1 and its partners. A significant and positive correlation of fluorescent signals was found for each pair of proteins (**Figure 1B**). This correlation analysis reached a maximum value of Pearson's coefficient at $\delta = 0$, indicating a significant correlation between the two fluorophores that is not due to random overlapping of fluorophore signals. We highlight that the correlation between RCOR1 and DNA reached a minimal value at $\delta = 0$, indicating a negative global

colocalization, or even exclusion, from dense DNA regions stained by Hoechst, which are mostly enriched in heterochromatin domains (Bucevicius et al. 2019; Holmquist 1975). These findings indicate that, while RCOR1 is concentrated in the nucleus, it is excluded from heterochromatin domains, suggesting that RCOR1 localizes at euchromatin domains or at the nucleoplasmic compartment. To examine this intriguing possibility, we performed biochemical fractionations of HT22 cell extracts that allow to obtain DNA-free soluble cytosolic and nuclear fractions, and a chromatin insoluble fraction (**Figure S1B**). The fraction markers, GAPDH and H3, were enriched as expected, on cytosolic and chromatin fractions, respectively, and Lamin B1 was mostly enriched in the chromatin-insoluble fraction (**Figure 1C**). Under these conditions, we found that RCOR1, LSD1, and HDAC1/2 showed similar distribution pattern and were enriched in the nuclear fractions (**Figure 1C**).

Given that we detected all the subunits of the LSD1-RCOR1-HDAC1/2 complex in the three cell fractions, we aimed to test whether they correspond to different subcellular populations. To this end, we performed sequential nuclear extractions using increasing concentrations of NaCl, and analyzed the distribution of proteins among the different fractions obtained. We observed that RCOR1, LSD1, and HDAC1/2 were distributed in three different subcellular populations: a cytosolic one, a nuclear soluble that was efficiently extracted between 250-300 mM NaCl, and an additional population that resisted all the salt-induced extractions and remained enriched in chromatin (**Figure 1D**). We found that EZH2 was distributed in two subnuclear populations, one that was efficiently extracted at higher ionic strength than RCOR1 (300-350 mM NaCl) and another one that remained on chromatin like RCOR1. On the other hand, HP1 α resisted all the extractions, reflecting its strong binding to chromatin, as we could

only detect it on the final chromatin pellet (**Figure 1D**). Thus, we confirmed that the presence of RCOR1, LSD1, and HDAC1/2 in the different subcellular fractions evidenced three specific subpopulations of the complex subunits. Furthermore, given the higher extractability shown by the RCOR1-related soluble nuclear species compared to factors that are classical markers of heterochromatin, it suggests that RCOR1 complexes might be located at different chromatin and/or nucleoplasmic domains than EZH2 and HP1 α .

To check if RCOR1 is forming complexes with LSD1 and HDAC1/2 in the three different subcellular populations, we performed LSD1 immunoprecipitation on cytosolic, nuclear soluble, and chromatin soluble fractions. As expected, we found that LSD1 co-precipitated RCOR1 and HDAC2 in the three analyzed fractions (**Figure 1E**), confirming the three detected RCOR1-subpopulations form complexes inside subcellular environments with and without chromatin. Finally, we tested whether RCOR1 nuclear populations display detectable interactions with nucleosomes. We performed MNase treatments on HT22 nuclei, and soluble products from the digestion – containing between 1 and 10 nucleosomes – were cleared and subjected to RCOR1 immunoprecipitation. We found that under efficient immunoprecipitation of RCOR1, it co-precipitated its bonafide binding partner LSD1 and also histone H3 (**Figure 1F**), confirming that nuclear populations of RCOR1 are forming stable complexes with nucleosomes in chromatin. Altogether, these data show that RCOR1 complexes are distributed in different cell compartments and its association to chromatin is weaker than canonical repressive complexes.

RCOR1 is mostly enriched at transcriptionally permissive chromatin

Previous results prompted us to characterize the properties of RCOR1 interaction with nucleosomes in the context of chromatin. To this end, we carried out MNase treatments on HT22 nuclei and RCOR1 immunoprecipitations on solubilized products (**Figure S2A**) to analyze the histone modifications that co-precipitate with it. We detected interactions with transcriptionally-permissive H3 modifications such as H3K4me1, H3K4me2, and H3K9ac (**Figure 2B**), supporting that nuclear RCOR1 interacts with euchromatin. Next, we tested whether RCOR1 is enriched at accessible chromatin. Therefore, we scaled-up the MNase digestion procedure, and the solubilized products were loaded on a 5 to 50% sucrose gradient and then subjected to ultracentrifugation (**Figure 2A**). The gradient showed an efficient separation of nucleosome-free nuclear fractions (**Figure 2C, Fractions 03-13**), mononucleosomes (**Fraction 19**), dinucleosomes (**Fraction 23**), and oligonucleosomes between 3 and 6 nucleosome units (**Fractions 27-35**). Under these conditions, most of the non-histone proteins from the loaded nuclear material were separated in nucleosome-free fractions while histones were consistently distributed among the fractions enriched in nucleosomal DNA (**Figure S2B**).

RCOR1 was distributed at fractions between 70 and 350 kDa (**Figure 2D**), indicating the co-existence of monomers and distinct RCOR1-containing complexes. A considerable amount of RCOR1 sedimented at fractions containing mono and dinucleosomes (**Figure 2D, Fractions 17-23**), suggesting that RCOR1 is mostly enriched at MNase-accessible chromatin. To confirm this data, we compared its sedimentation equilibrium with EZH2, which besides

showing a peak at accessible chromatin (**Fraction 19**), it also showed a second peak at denser fractions than RCOR1 (**Fraction 33**). Thus, RCOR1 is mostly enriched at chromatin domains more accessible than the heterochromatin marker EZH2.

To further validate our results, we performed immunofluorescence assays to visualize if RCOR1 is localized closer to transcriptionally-permissive chromatin. To this end, we double stained RCOR1 with H3K18ac and H3K4me3 as euchromatin markers, or with H3K9me3 and H3K27me3 as heterochromatin markers. We found that RCOR1 is closer and establishes more frequent contacts with H3K18ac and H3K4me3 than with H3K9me3 and H3K27me3 (**Figure 2E**). Quantitative analyses of colocalization revealed a higher partial colocalization of RCOR1 with transcriptionally-permissive histone modifications than with repressive ones (**Figure 2F**).

To have a global view of this finding, we created a high-resolution 3D model of chromosome 20 of human K562 cells. We conducted Monte Carlo simulations by representing the 63 Mb of chromosome 20 as a polymer made of 12,592 beads spanning 5 Kb each. The simulation folded chromosome 20 (**Figure 3A**) guided by 3D contacts as constraints were obtained from public datasets of Hi-C on the same cells. Localization of H3K4me3 and H3K27me3 ChIP-seq peaks derived from ENCODE datasets on K562 cells was assessed to distinguish transcriptionally active and repressed compartments (**Figure 3B**). Next, we compared the 3D distribution of RCOR1 ChIP-seq peaks to these histone modifications (**Figure 3C, 3D**). We observed that RCOR1 colocalized more frequently with H3K4me3 rather than H3K27me3 (**Figure 3E**), and this observation was significantly distinguishable, as radial distribution functions of RCOR1 and each histone modification showed RCOR1 closer to

H3K4me3 rather than H3K27me3 (**Figure 3F**). We conclude that RCOR1 is primarily found in accessible, actively-transcribed chromatin.

The LSD1-RCOR1-HDAC1 complex marks proximal promoters in euchromatin

The provided microscopical and biochemical evidence suggested a preferential, but paradoxical association between RCOR1 and euchromatin. This was most unexpectedly, given that LSD1-RCOR1-HDAC complexes have primarily been associated with transcriptional repression (Lakowski, Roelens, and Jacob 2006). Thus, we worked towards evaluating this association by performing bioinformatic analyses of available RCOR1, LSD1, and HDAC1 ChIP-seq datasets from the ENCODE project on human K562 cells. Our analysis showed that 35,885 out of 38,117 LSD1 peaks (94.1%) are co-occupied with RCOR1 (**Figure 4A**). In addition, 46,163 out of 112,641 HDAC1 peaks (41.0%) are co-occupied with RCOR1. Notably, 32,786 out of 47,329 LSD1/RCOR1 or HDAC1/RCOR1 shared peaks were co-occupied by the three subunits of the complex, highlighting the significant co-occupancy of the core RCOR1 complex components in genome-wide levels. Next, we explored the genomic elements where RCOR1 occupancy was enriched. We tested the relative enrichment of RCOR1 in different genomic features over genomic background. We found that RCOR1 peaks were significantly over-represented at promoters and 5' UTR. Interestingly, bidirectional promoters were also enriched (**Figure 4B and 4C**). Similar results were observed in CH12 cells (**Figure S3**).

In order to determine the features of chromatin where RCOR1 is enriched, we generated 4 clusters of RCOR1 genes by the k-means clustering approach (**Figure 4D**). In conditions where the genomic distributions of LSD1 and HDAC1, as bonafide RCOR1 interactors, were

similar, we observed a positive correlation between RCOR1 and markers of transcriptionally-permissive chromatin such as RNA Polymerase II, the acetyltransferase P300, H3K4me3, H3K9ac, and H3K27ac. In addition, we detected a negative correlation between RCOR1 peaks and markers of heterochromatin, such as H3K27me3 and H3K9me3, suggesting that RCOR1 is preferentially enriched at euchromatin domains. To confirm these findings, we regrouped RCOR1 peaks into quartiles (Q) according to the RCOR1 binding level and verified that occupancy of RCOR1 correlated with high occupancy of H3K4me3, H3K9ac, and P300 (**Figure 4E**).

Intriguingly, the clustering analysis revealed two different patterns of RCOR1 binding. While clusters I, II, and III showed a clear enrichment of RCOR1 around the TSS (**Figure 4D**), cluster I, which contained 849 target-genes, also showed an occupancy significantly higher on gene body regions. A representative example of this cluster is the FKBP2 gene, where RCOR1 is distributed at its TSS as well as downstream on its gene body, along with RNA pol II and other active-transcription markers (**Figure S4A**). On the other hand, we observed that genes with bidirectional promoters were overrepresented in cluster II, suggesting a novel role for RCOR1 on the regulation of this kind of genes, as exemplified by the SNX5/MGME1 promoter (**Figure S4B**). When we analyzed the distance between the TSS of the genes on each cluster and their nearest bidirectional transcripts, we found that the median distance measured for cluster II was two orders of magnitude lower than the other clusters, suggesting that the 2282 RCOR1 regulated genes in cluster II are located very near to their neighboring divergent genes (**Figure 5C**). Altogether, these data show that LSD1-RCOR1-HDAC1 complex preferentially binds TSS regions, gene bodies and bidirectional promoters in euchromatin.

RCOR1 is preferentially enriched in highly expressed genes

The positive correlation between RCOR1 and markers of actively-transcribed chromatin prompted us to examine whether RCOR1 peaks were enriched in genes that are actually being transcribed. For this purpose, we performed a cross-examination between ChIP-seq and RNA-seq from ENCODE datasets by analyzing the correlation between RCOR1 ChIP-seq data and RNA-seq data (**Figure 5A**). Genes were sorted according to RNA-seq data and grouped into four quartiles, and, as expected, they positively correlated to euchromatin markers such as RNA Pol II and H3K9ac (**Figure 5B**). Importantly, the highly-expressed genes (Quartiles Q1 and Q2) were more enriched in RCOR1 than the less-expressed ones (Quartiles Q3 and Q4). To further inquire about the functions related to RCOR1-regulated genes, we performed a Gene Ontology (GO) analysis for RCOR1 clusters I and II (**Figure 5D, 5E**), which revealed significant enrichment in actively expressed genes such as histones, ATP synthase, translation-related proteins and others. Altogether, bioinformatics analyses suggest that RCOR1 is preferentially positioned in proximal promoters of highly expressed genes in euchromatin.

RCOR1 physically interacts with RNA Polymerase II at transcription specific stages

We asked why RCOR1 associates with highly expressed genes. Given the colocalization with RNA Pol II within gene bodies of actively transcribed loci, we studied the functional relationship to RNA Pol II. We studied its largest subunit, RNA Polymerase Subunit B1 (RPB1) (Cramer et al. 2008), which also harbors the catalytic function for DNA-directed RNA synthesis and its C-terminal domain contains the heptapeptide tandem YSPTSPS repeats that are actively phosphorylated at different stages of the transcription cycle (Harlen and Churchman 2017; Zaborowska, Egloff, and Murphy 2016).

We performed RCOR1 immunoprecipitation experiments from native HT22 extracts, and we observed that both the hypo (II A) and hyper (II O) phosphorylated RPB1 isoforms co-precipitated with it (**Figure 6A**). Independent immunoprecipitations showed immunocomplexes between RCOR1 and specific RPB1 phosphorylations at serine 2, 5, and 7 on its C-terminal domain. This observation suggested that RCOR1 interacts with the active transcriptional holoenzyme. We also detected RPB1 as an LSD1 and HDAC1 interactor (**Figure 6B**), suggesting that the binding of RCOR1 to RNA Pol II involves its associated enzymes. In addition, RCOR1-RPB1 interaction was detectable on solubilized, MNase-treated chromatin (**Figure 6C**). To confirm this novel RCOR1 interaction, we transiently overexpressed an HA conjugated N-terminal tagged RCOR1 construct on HEK293T cells. HA-pulldown experiments demonstrated that RPB1 was co-precipitated only when HA-RCOR1

was transfected (**Figure 6D**), confirming the specificity of this interaction. To complement these findings, we observed by high-resolution confocal microscopy that RCOR1 is positively correlated with RPB1 phosphorylation states (**Figure S5A**).

Finally, to further determine at which stage of the transcription cycle RCOR1 is recruited to the transcriptional machinery, we treated HT22 cells with THZ1, Flavopiridol, and Cordycepin or Actinomycin D for 1 hour, in order to inhibit transcription before initiation, at promoter pausing, before productive elongation or at elongation, respectively (**Figure 6E**) (Steurer et al. 2018). These treatments cause global variations on the phosphorylation degree of RPB1 since THZ1 and Flavopiridol accumulate the hypo-phosphorylated variants while Cordycepin and Actinomycin D accumulate RPB1 in the hyper-phosphorylated state (Steurer et al. 2018). We carried out RCOR1 immunoprecipitations and noticed that its interaction with RPB1 was dependent on transcription stages. Under conditions where the immunoprecipitated amount of RCOR1 was similar between different extracts, we observed that THZ1 treatment abolished its interaction with RPB1 (**Figure 6F, Figure S5B**), suggesting that RCOR1 is recruited to the transcriptional machinery after premature initiation. On the other hand, the interaction was detectable at similar levels to the control when Flavopiridol was used, suggesting that RCOR1 starts to interact with RPB1 before serine 2 phosphorylation is imposed, presumably at the promoter pausing stage of transcription. Moreover, when productive elongation was inhibited by Cordycepin and Actinomycin D, we detected an enrichment in the RCOR1-RPB1 immunocomplexes, confirming that RCOR1 physically contacts RNA Pol II before productive elongation. These drug-inhibition experiments show that RCOR1 is recruited to active genes following formation of the pre-initiation complex (PIC) and load during

promoter-proximal pausing.

Based on these results, we hypothesized that RCOR1 presence in chromatin would be sensitive to transcriptional changes. To test this idea, we performed a sequential salt-extraction of nuclear proteins in THZ1 and Actinomycin D-treated cells. We found that THZ1 enriched hypophosphorylated RPB1 in the cytosol while RCOR1 did not experience significant changes in subcellular distribution (**Figure 6G, 6H**). However, Actinomycin D treatment “trapped” Pol II in chromatin on its hyper-phosphorylated state. In these conditions, RCOR1 nuclear subpopulation was extracted at higher salt concentrations compared to the DMSO treated cells (**Figure 6G, 6H**). This data supports the idea that if a fraction of RCOR1 is trapped in chromatin when elongation is blocked, RCOR1 might be acting before and during transcriptional elongation. Altogether, our data show that RCOR1 is recruited to the transcriptional machinery at early stages of gene expression.

RCOR1 is a fast-acting repressor of de novo transcription

With knowledge that RCOR1 engages RPB1 during promoter-proximal pausing, we reasoned that RCOR1 could play an inhibitory function by enhancing RNA Pol II pausing. We asked whether RCOR1 functions as a co-activator or a co-repressor at actively expressed genes. To this end, we modulated the steady-state RCOR1 protein levels by transient overexpression (**Figure 7A, 7B**), or by post-transcriptional silencing with siRNA in HeLa cells (**Figure 7A, 7E**). Twenty four hours after transfection, we incubated cells with a 30-minute pulse of 1 mM 5 Ethynyl Uridine (EU), which is incorporated into nascent RNA molecules and that in the

presence of divalent copper ions can then be tagged by a chemical reaction with fluorophore-conjugated azide groups (Jao and Salic 2008). Therefore, we were able to label and visualize transcripts that were synthesized for 30 minutes in cells. When RCOR1 was overexpressed, we detected a dramatic decrease in the fluorescence intensity of nascent transcripts (**Figure 7C, 7D**). This difference was rescued when Corin, a dual inhibitor for LSD1 and HDAC1/2 was added to the cells 2 hours prior EU labeling, suggesting RCOR1 associated enzymes are responsible for that repression of global transcription. To check if LSD1 or HDACs were responsible of this response, we added TCP (LSD1 inhibitor) or Entinostat (HDAC1/2 inhibitor) 2 hours prior EU labeling. We saw that Entinostat rescued transcriptional activity in a similar way than Corin did, suggesting that RCOR1 is repressing de novo transcription mostly by its associated HDAC activity.

When RCOR1 was knocked down (**Figure 7E**), we observed a significant increase in the fluorescent signal (**Figure 7F, 7G**), suggesting that RCOR1 might be regulating the speed of de novo transcription. Similar results were obtained when HT22 cells were treated with Corin (**Figure S6**). To confirm this, we blocked transcription in promoter-proximal pausing using Flavopiridol in RCOR1 KD cells for 2 hours, and after washing it out we followed EU incorporation at 0, 20 and 40 minutes (**Figure 7H, 7I**). We found that the recovery of transcriptional activity was significantly faster in RCOR1-deficient cells. These data supports RCOR1 as a fast repressor of gene expression and altering its levels can impact de novo transcription globally.

Finally, to gain more mechanistic insights, we wondered if the enzymatic activities of the complex could impact RPB1 acetylation or methylation, which are modifications that are enriched in early stages of transcription (Schroder et al. 2013; Dias et al. 2015). Thus, we carried out immunoprecipitation of acetylated or dimethylated proteins in cells treated with Corin (**Figure 7J**). We found that Corin treatment did not change the dimethylation levels of RPB1 (**Figure 7K**), but increased RPB1 acetylation. Altogether, our data indicate that RCOR1 can modulate de novo transcription by regulating histone modifications and RNA Pol II acetylation.

DISCUSSION

Here we have unveiled RCOR1 as a transcriptional rheostat. Although a repressor of transcription acting in concert with HDAC1/2, we first observed a paradoxical association with highly expressed genes and euchromatin in general. Further investigation revealed specific enrichment at promoters-proximal regions. Biochemical analyses then demonstrated a specific engagement of RCOR1 to the transcriptional machinery after promoter clearance. Importantly, we were able to detect that RCOR1 represses de novo transcription by regulating RNA Pol II speed. This is probably mediated by RCOR1 associated deacetylase activity which can impact histones and, importantly, RNA Pol II itself (**Figure 7M**).

A distribution equilibrium between cytosolic, nucleoplasm and chromatin for the RCOR1 complex subunits

As we hypothesized that RCOR1 complexes must establish transient interactions with chromatin, we were able to confirm they are distributed in cytosolic and nuclear soluble fractions, in addition to their chromatin-bound state. Since we detected the complex subunits both in cytosol and nucleus in single cells by microscopy, the biochemical subpopulations detected by fractionations reflect the co-existence of different complex states inside cells, possibly as the result of a dynamic distribution equilibrium between soluble cell compartments and chromatin at steady state. Curiously, the colocalization of RCOR1 with Hoechst was mostly negligible, suggesting that the distribution equilibrium of RCOR1 complexes must be occurring mostly at euchromatin regions. Since we detected an abundant chromatin-bound RCOR1 pool

which resisted high-salt extractions, further work will be needed to determine how the complex is stabilized in chromatin. In the same way, future studies will explore if their presence in cytosolic fractions is due to the synthesis of new complex-subunits and/or it is playing a non-canonical role on extranuclear demethylation and deacetylation reactions occurring on newly synthesized histones (Loyola et al. 2006; Rivera et al. 2015; Saavedra et al. 2017) as well as on non-histone cytosolic proteins (Narita, Weinert, and Choudhary 2019; Zhang, Wen, and Shi 2012).

Enrichment of RCOR1 at accessible and transcribed chromatin

When chromatin is digested by MNase, the digestion reaction preferentially occurs at nucleosome-free regions. Kinetically, the first products are chromatosomes (nucleosomes containing histone H1), which are then further digested to produce free nucleosomes, releasing histone H1 and short sequences of linker DNA (Ocampo et al. 2016; Simpson 1978). However, since chromatin architecture is not homogeneous, MNase-accessible genomic regions are digested first, and their products are enriched in partially digested chromatin (Chereji, Bryson, and Henikoff 2019; Mieczkowski et al. 2016). We showed that RCOR1 was mostly distributed in fractions spanning nucleosome-free regions, mono and di nucleosomes, suggesting that a substantial population of RCOR1 complexes is enriched in MNase-accessible chromatin, and it might be stabilized by linker DNA and/or by histone H1. In this context, it was shown that linker DNA stabilizes the binding of the RCOR1-LSD1 complex to nucleosomal substrates (Pilotto et al. 2015), and a recent report showed structural evidence of LSD1 direct binding to internucleosomal DNA (Kim, Zhu, et al. 2020). How this complex would display crosstalk with factors that bind linker DNA remains unexplored.

In addition to its prevalence on MNase-accessible chromatin, we presented biochemical, microscopical and chromosome 3D modeling evidence showing that RCOR1 interacts and colocalizes with nucleosomes harboring transcriptionally-permissive histone modifications. Our findings may reflect a common role of RCOR1 complexes since bioinformatic analyses on human K562 cells revealed that the complex is enriched at proximal promoters and 5'UTRs of chromatin marked by co-activators and histone modifications that are permissive to transcription. Consistently, we found a positive correlation between RCOR1 occupancy and gene expression, suggesting that the genes that contain higher levels of RCOR1 are more frequently transcribed. We also showed a negative correlation with heterochromatin marks, supporting the exclusion of the complex from heterochromatin domains.

Many questions emerged regarding the paradoxical role of a co-repressor complex at euchromatin domains. It has been previously suggested that the presence of different HDAC enzymes at active genes can reflect the need of histone deacetylation reactions to reset genes after transcription, since HDAC inhibition increases histone acetylation on active promoters (Wang et al. 2009). In addition, as we detected RCOR1 occupying gene body segments on genes with the highest RCOR1 occupancy, we can propose that the complex could be acting on the resetting of histone modifications after transcription in regions where transcription elongation occurs. In this sense, it has been shown that H3K9ac can recruit factors required for RNA Pol II-mediated elongation, and HDAC inhibition leads to impaired transcriptional elongation (Gates et al. 2017; Greer et al. 2015). Interestingly, NuRD, another co-repressor complex that functions with histone deacetylation, has also been detected at active regions as an acetylation regulator (Kraushaar et al. 2018; Zhang et al. 2018). In this regard, the dual

inhibition of LSD1 and HDAC1 in the context of the RCOR1 complex by Corin has revealed increased H3K27ac and H3K4me1 levels on both the TSS and gene body segments of active genes (Anastas et al. 2019). Since Corin rescued the loss of de novo transcription produced by overexpression of RCOR1, and also impacted the acetylation of RPB1, additional studies are needed to test if the RCOR1 complex is regulating nascent transcripts by modulating RPB1 acetylation, histone modifications, or both.

Insights on the recruitment of RCOR1 at specific transcription stages

Our study revealed a specific interaction between RCOR1 and RNA Pol II occurring in chromatin, which provides a biochemical basis of RCOR1 recruitment to active genes. Interestingly, this interaction was sensitive to chemical inhibition of different transcription stages and suggested that RCOR1 interacts with RNA Pol II after initiation and before productive elongation. These data support a model where the RCOR1 complex might be participating in the removal of histone modifications and RNA Pol II acetylation in a co-transcriptional way. The acetylation of lysine residues in CTD-YSPTSPK non-canonical repeats of RPB1 has been detected both in promoter-proximal paused RNA Pol II and in elongating RNA Pol II (Schroder et al. 2013; Ali et al. 2019), which makes RCOR1 a candidate to regulate this modification at different stages of transcription.

Given that the chemical inhibition of the RCOR1 complex by Corin results in an increase of transcriptionally permissive marks on its target genes (Kalin et al. 2018; Anastas et al. 2019), and our results suggested that RCOR1 may have a role regulating transcription of genes that are highly expressed, we studied the effect of modulating RCOR1 protein levels on transcripts

that were synthesized in a short time scale (30 min). We showed that RCOR1 upregulation globally represses transcription. This observation suggests that RCOR1 may work as a negative global regulator of highly expressed genes by presumably slowing down the transcription speed or other parameters of transcriptional bursting, such as burst size or frequency, as it has been reported for HDACs (Dar et al. 2012). According to the transcriptional bursting hypothesis, mammalian gene expression occurs in pulses known as bursts as genes can switch from an inactive to an active state depending on stochastic collisions of chromatin regulators of transcription rather than relying on the deterministic nature of biochemical pathways we can infer from cell population studies (Larson 2011; Lenstra et al. 2016; Tunnaclyffe and Chubb 2020). The cascade of events that marks the transition from the ON to OFF state in active transcription has not been clarified yet, but our evidence suggests that RCOR1 might be playing a role in it. Finally, we highlight our discovery of non-canonical roles for RCOR1 arising from its interaction with active RNA Pol II, which expands the scope of processes where RCOR1 can be involved in, from chromatin remodeling to regulation of transcription kinetics.

ACKNOWLEDGEMENTS: We thank Dr. Paola Merino, Dr. Francisco Saavedra and Dr. Yesu Jeon for critical comments on this work. Thanks to Massachusetts General Hospital (MGH) Program in Membrane Biology (PMB) Microscopy Core Facility for the use of confocal imaging instruments. We acknowledge funding support from FONDECYT Regular Grants #1150200 and #1191152 to MAE. CONICYT/ANID Ph.D. Fellowship #21161044 to CR. CONICYT/ANID Ph.D. Fellowship #21140438 to M.O.C. CONICYT/ANID. FONDECYT Postdoctoral Grant#3160308 to VN. CONICYT/FONDECYT/REGULAR No.1171004 to MSH. FRAXA grant to H.L. and J.T.L., and N.I.H (R01-HD097665) to J.T.L.

AUTHOR CONTRIBUTIONS: C.R., H.L., M.S.H., J.T.L. and M.E.A. designed research, analyzed data and wrote the manuscript. C.R. designed and performed biochemical fractionations and microscopy experiments. H.L. designed and performed bioinformatic analyses. A.L. performed high resolution chromosome modeling and 3D colocalization analyses. M.O.C. performed gene ontology analyses. V.N. analyzed neuronal LSD1 levels in HT22 cells.

DECLARATION OF COMPETING INTERESTS: J.T.L. is a co-founder of Translate Bio and Fulcrum Therapeutics, and also serves as Advisor to Skyhawk Therapeutics.

FIGURES

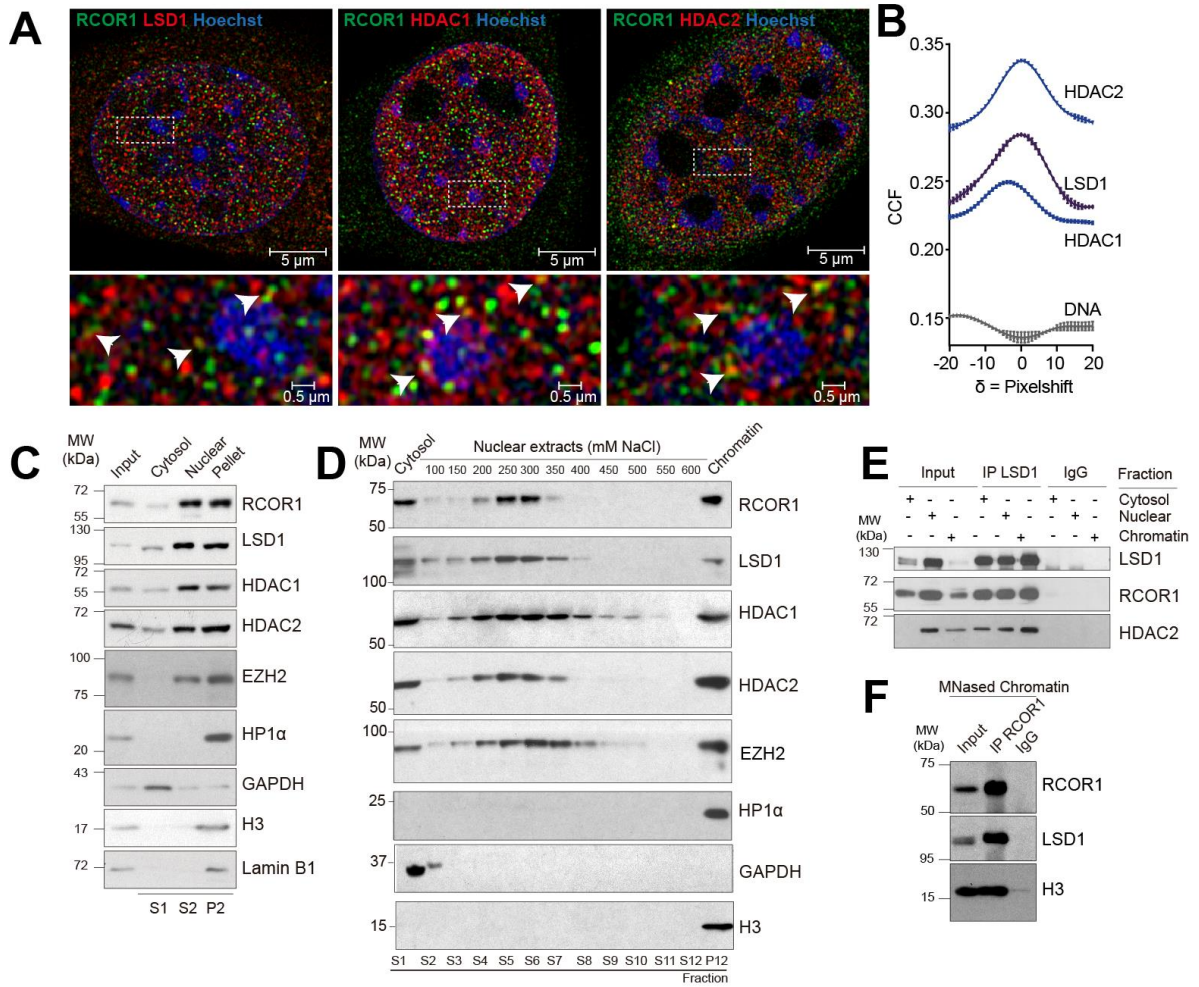


Figure 1. Three different subpopulations of the LSD1-RCOR1-HDAC1/2 complex coexist in cells

Figure 1. Three different subpopulations of the LSD1-RCOR1-HDAC1/2 complex coexist in cells

- (A) HT22 cells were stained with double immunolabeling of RCOR1 (green) and LSD1, HDAC1 or HDAC2 as shown in red. Bottom panels show magnified regions of original images highlighted inside dashed rectangles. White arrows indicate regions where RCOR1 and its binding partners are colocalizing.
- (B) Van Steensel's plot of 2D colocalization between RCOR1 and each co-stained protein or DNA. CCF: Cross correlation function.
- (C) Western blot analysis of subcellular fractionation in HT22 cells. GAPDH, H3 and Lamin B1 were assayed as cytosolic, chromatin and nuclear lamina markers, respectively. S: Supernatant. P: Pellet. MW: Molecular weight. kDa: Kilodalton.
- (D) Western blot analysis of sequential salt extractions of nuclear contents in HT22 cells. GAPDH and H3 were assayed as cytosolic and chromatin markers, respectively.
- (E) Western blot analysis of the immunoprecipitation of LSD1 in cytosolic, nuclear soluble and chromatin fractions. IP: Immunoprecipitation. IgG: Immunoglobulin.
- (F) Western blot analysis of the immunoprecipitation of RCOR1 on MNase-treated chromatin.

Western blots are representative of 2 or more biological replicates.

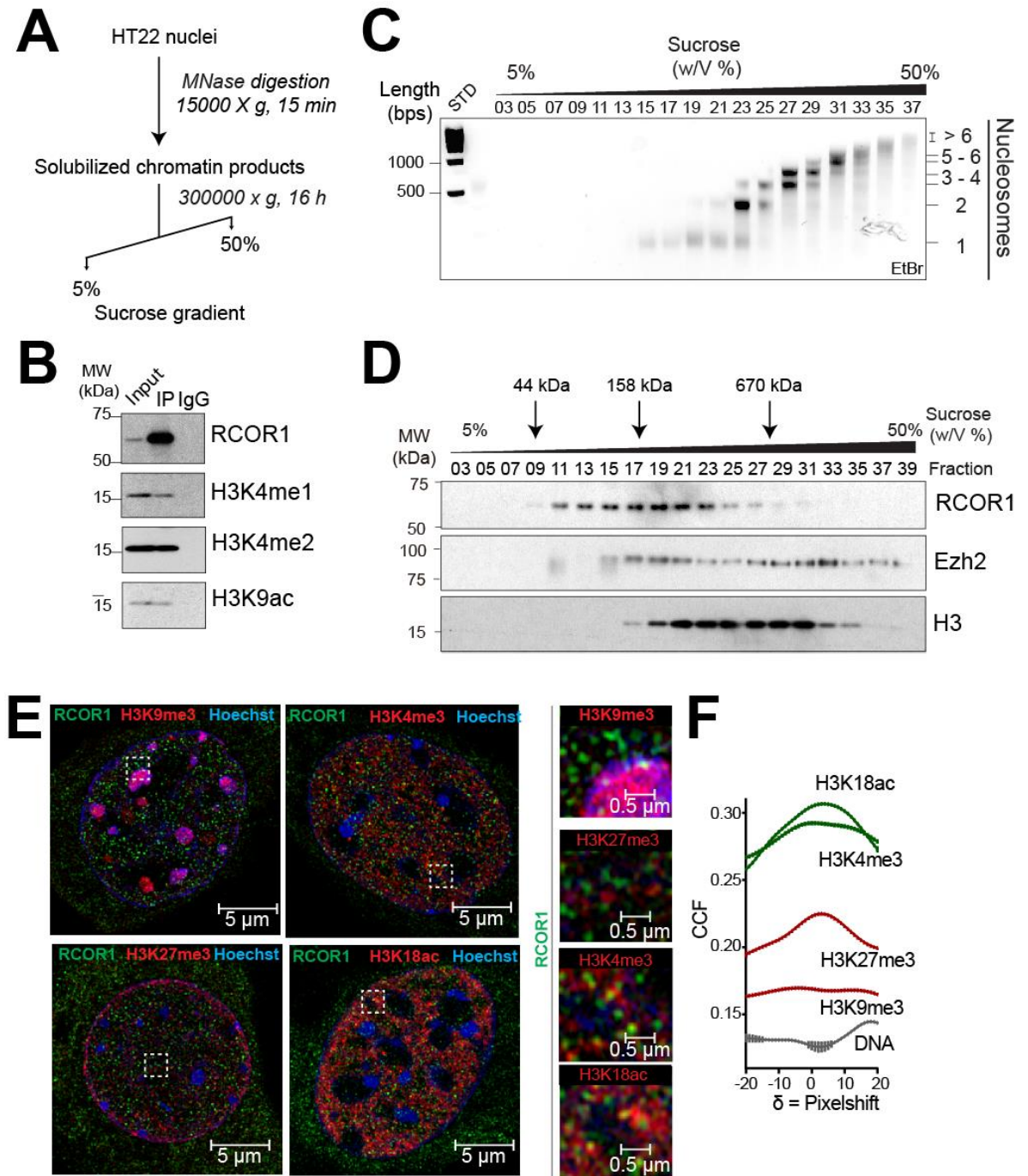


Figure 2. RCOR1 is enriched in accessible, transcriptionally permissive chromatin

Figure 2. RCOR1 is enriched in accessible, transcriptionally permissive chromatin

- (A) Scheme depicting the MNase digestion of chromatin coupled to ultracentrifugation for chromatin accessibility assays.
- (B) Western blot analysis of RCOR1 coimmunoprecipitated histone H3 modifications from MNased chromatin extracts.
- (C) Agarose gel showing the distribution of DNA fragments among the different fractions obtained from the ultra-centrifuged chromatin products. Bps: base pairs. STD: DNA Ladder. EtBr: Ethidium Bromide.
- (D) Western blot analyses of distribution of RCOR1, EZH2 and H3 in the sucrose gradient sedimentation equilibria. Upper arrows indicate standard molecular sizes resolved by this method.
- (E) HT22 cells were stained with double immunolabeling of RCOR1 (green) and different histone modifications as shown in red. Right panels show magnified regions of original images highlighted inside dashed squares.
- (F) Van Steensel's plot of 2D colocalization between RCOR1 and each co-stained histone modification or DNA. CCF: Cross correlation function.

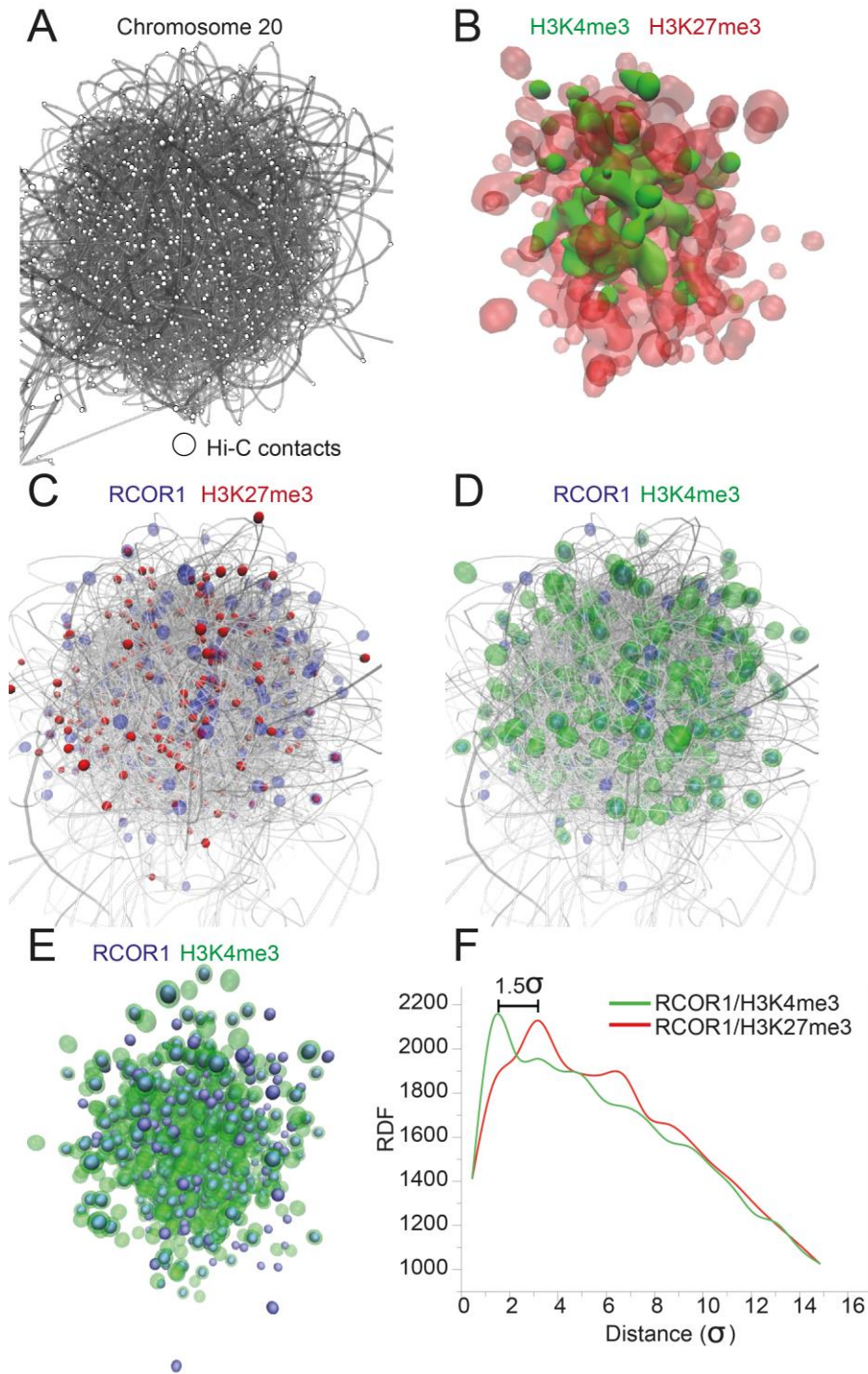


Figure 3. RCOR1 is closer to H3K4me3 than H3K27me3 in 3D simulated chromosome 20.

Figure 3. RCOR1 is closer to H3K4me3 than H3K27me3 in 3D simulated chromosome 20.

- (A) High-resolution 3D model generated by Monte Carlo simulations with Hi-C contacts as constraints. White dots represent Hi-C contacts.
- (B) H3K4me3 and H3K27me3 ChIP-seq positions were mapped into the 3D model of chromosome 20 and highlighted with different colors to show the segregation of active and repressive chromosome compartments.
- (C) RCOR1 and H3K27me3 ChIP-seq positions mapped.
- (D) RCOR1 and H3K4me3 ChIP-seq positions mapped.
- (E) Representative image of the significant colocalization between RCOR1 and H3K4me3 in 3D.
- (F) Radial distribution function analysis of the 3D colocalization between RCOR1 and histone modifications. RDF: Radial distribution function.

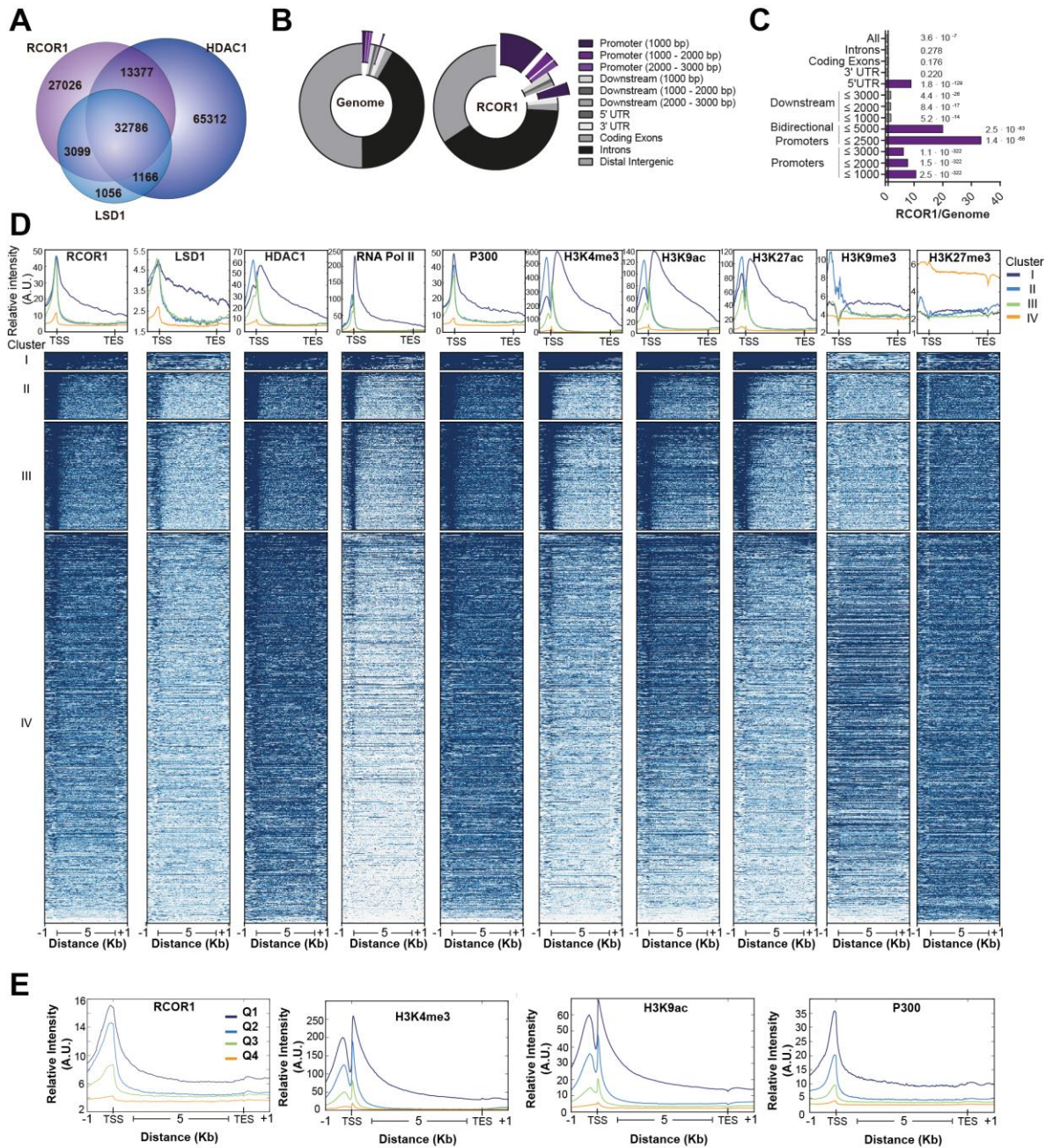


Figure 4. RCOR1 is enriched in proximal promoters of active genes.

Figure 4. RCOR1 is enriched in proximal promoters of active genes.

- (A) Venn diagram showing the number of ChIP-seq peaks of RCOR1, LSD1 and HDAC1 on K562 cells.
- (B) Pie chart of relative abundance of DNA elements in the genome (left) and the occupancy of RCOR1 ChIP-seq peaks on each DNA element.
- (C) Enrichment of ChIP-seq peaks on DNA elements over the natural abundance of these elements across the genome. P values are shown next to each bar.
- (D) Genomic meta-profiling of RCOR1, LSD1, HDAC1, RNA Pol II, P300 and histone modifications in K562 cells. Upper plots show the normalized occupancies of each protein or modification analyzed in different RCOR1 clusters.
- (E) Quartile-based comparison of relative occupancies of RCOR1, H3K4me3, H3K9ac and P300 on RCOR1-sorted genes.

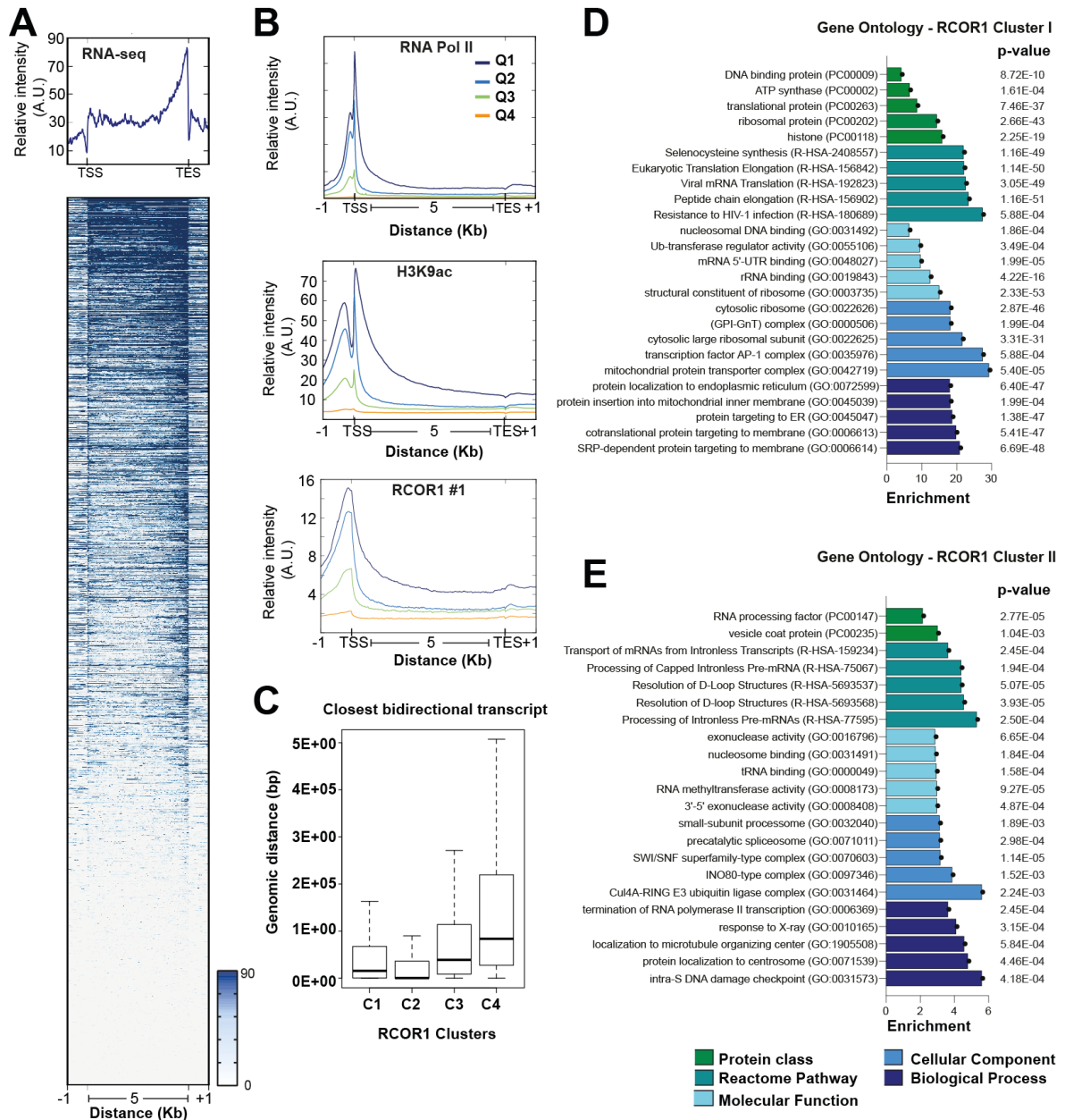


Figure 5. RCOR1 occupancies are positively correlated with gene expression.

Figure 5. RCOR1 occupancies are positively correlated with gene expression.

(A) Profiling of RNA-seq reads in K562 cells. Lower diagram shows the RNA-seq reads ordered by intensity.

(B) Quartile-based comparison of relative RNA Pol II, H3K9ac and RCOR1 occupancies on RNA-seq-sorted genes. Two different RCOR1 datasets were analyzed.

(C) Analysis of closest bidirectional transcript on the 4 clusters of RCOR1 ChIP-seq data.

(D)(E) Gene ontology analysis of RCOR1 clusters I and II, respectively. Bar colors represent different ontology categories, highlighted at the bottom.

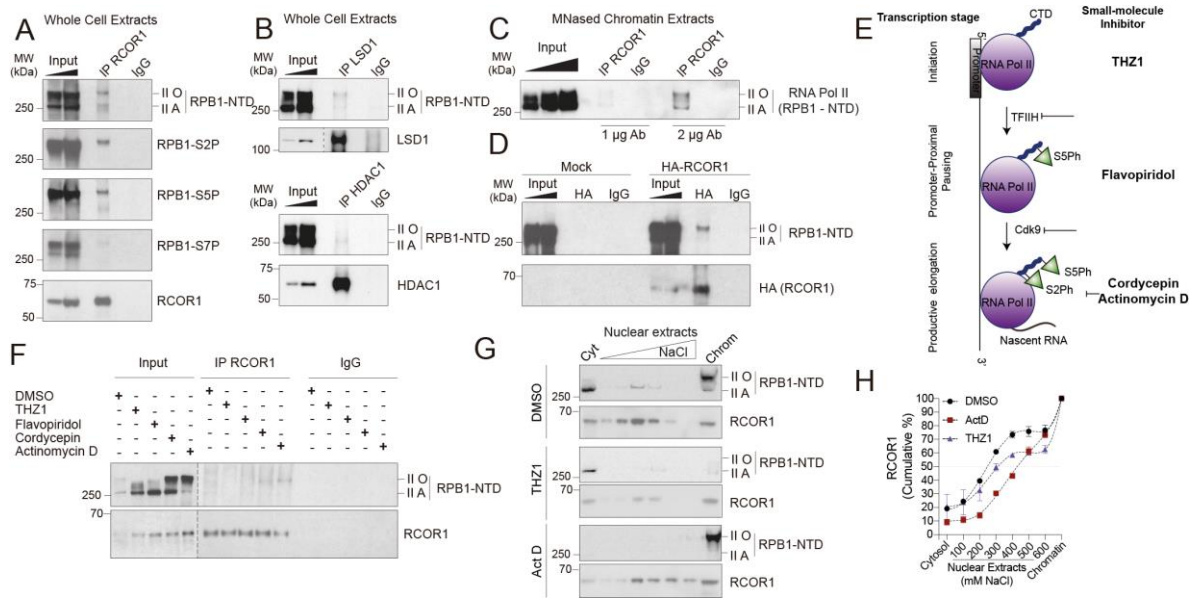


Figure 6. RCOR1 establishes an interaction with RNA Pol II after initiation and before elongation.

Figure 6. RCOR1 establishes an interaction with RNA Pol II after initiation and before elongation.

- (A) Western blot analyses of immunoprecipitation of RCOR1 and co-precipitation of RPB1 and its phosphorylated isoforms from whole cell extracts. II-O: Hyperphosphorylated isoforms. II-A: Hypophosphorylated isoforms.
- (B) Western blot analyses of immunoprecipitation of LSD1 (top) or HDAC1 (bottom) and co-precipitation of RPB1
- (C) Western blot analysis of immunoprecipitation of RCOR1 and RNA Pol II from MNased chromatin using 2 different RCOR1 antibody concentrations.
- (D) HA-Pulldown on extracts derived from empty-vector and HA-RCOR1 overexpressing HEK293 cells.
- (E) Scheme depicting different stages of eukaryotic RNA Pol II transcription. It highlights the steps that are inhibited by THZ1, Flavopiridol, Cordycepin and Actinomycin D. CTD: Carboxy-terminal domain. S5Ph: Phosphorylated serine 5. S2Ph: Phosphorylated serine 2.
- (F) Western blot analyses of RCOR1 immunoprecipitation and RPB1 co-precipitation under inhibition of transcription at different steps.
- (G) Western blot analyses of RPB1 and RCOR1 profiles on sequential salt-gradient extractions when THZ1 or Actinomycin D were used to inhibit elongation.
- (H) Cumulative protein levels of RCOR1 on each fraction of (F), expressed as percent of the total detected levels. Western blots are representative of at least 2 biological replicates.

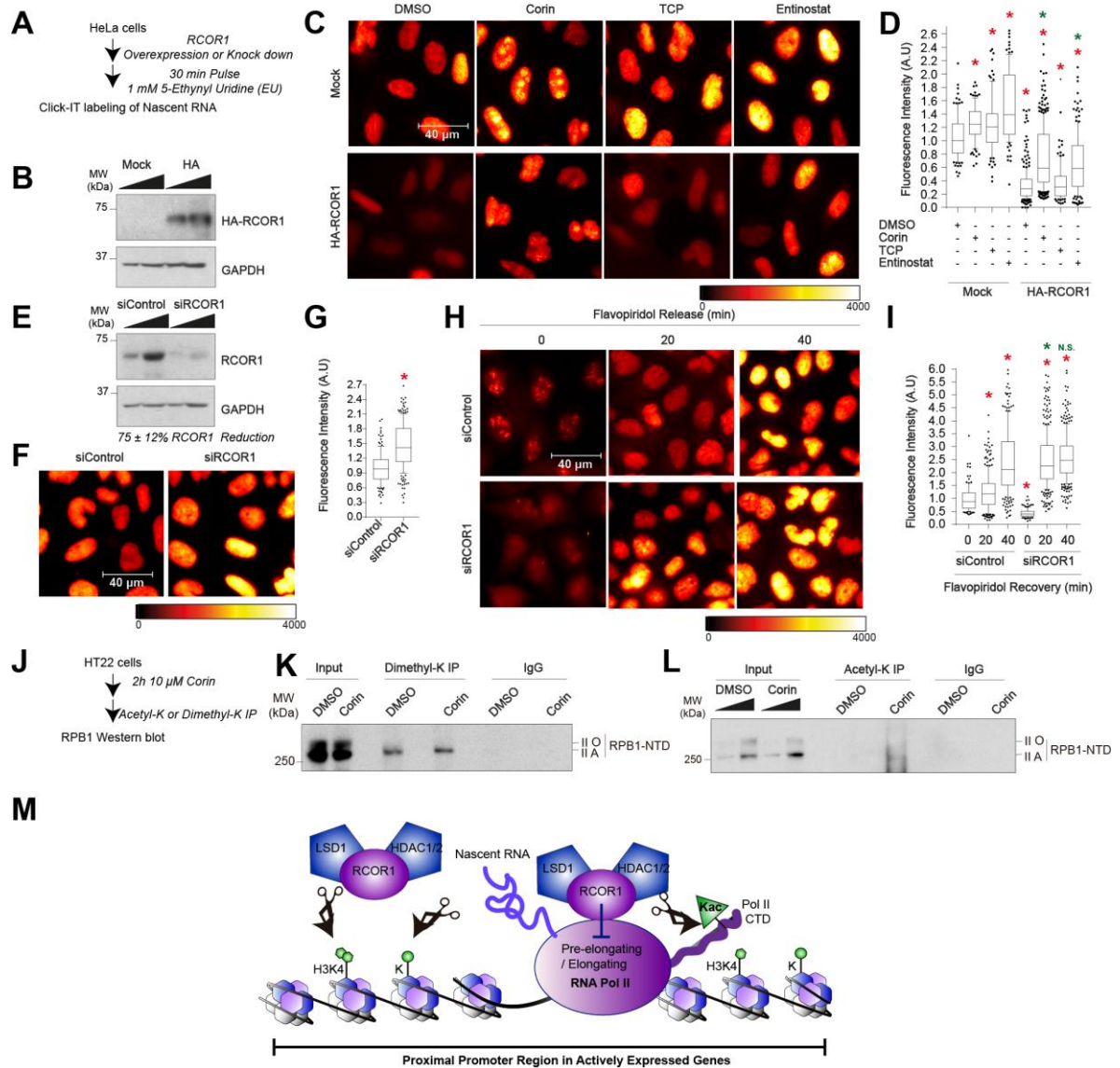


Figure 7. RCOR1 globally represses transcription of rapidly synthesized transcripts.

Figure 7. RCOR1 globally represses transcription of rapidly synthesized transcripts.

- (A) Workflow depicting the followed steps for imaging of newly synthesized RNAs under RCOR1 overexpression or knock down in HeLa cells.
- (B) Western blot analysis of HA-RCOR1 overexpression. GAPDH was assayed as a loading control.
- (C) Pseudocolored images of labeled transcripts under HA-RCOR1 overexpression. Scale bar represents 40 μm .
- (D) Box plots showing the quantitation of the relative fluorescent intensities per cell on each condition. Red asterisks indicate $p < 0.005$ respect to Mock-DMSO control. Green asterisks indicate $p < 0.005$ as significant rescue of the decreased transcription produced by RCOR1 overexpression.
- (E) Western blot analysis of RCOR1 knock down efficiency. GAPDH was assayed as loading control. Average is indicative of 3 biological replicates.
- (F) Pseudocolored images of labeled transcripts under RCOR1 knock down. Scale bar represents 40 μm .
- (G) Box plots showing the quantitation of the relative fluorescent intensities per cell under RCOR1 knock down conditions.
- (H) Pseudocolored images of labeled nascent transcripts when RCOR1 knock down cells were subjected to recovery after washing out flavopiridol at 0, 20 and 40 minutes. Scale bar represents 40 μm .

- (I) Box plots showing the quantitation of the relative fluorescent intensities per cell after 0, 20 or 40 minutes of washing out Flavopiridol in RCOR1 knock down cells. Red asterisks represent $p < 0.005$ with respect to siControl cells at time 0 minutes. Green asterisks represent $p < 0.005$ significantly different nascent transcription between the two groups at 20 minutes.
- (J) Scheme depicting strategy used to analyze RPB1 post-translational modifications after Corin treatment.
- (K)(L) Analyses of RPB1 dimethylation and acetylation under Corin treatment.
- (M) Working model

MATERIAL AND METHODS

Cell culture. HT22, HeLa and HEK293-T cells were cultured in Dulbecco's Modified Eagle's Medium (DMEM, Gibco) supplemented with 10% fetal bovine serum (FBS, Gibco) and 1% Penicillin/Streptomycin. Cells grew at 37°C in an atmosphere containing 5% CO₂. Transfections were carried out using Lipofectamine 3000® (Invitrogen) according to the manufacturer's instructions. Plasmids and Lipofectamine were mixed in ratios of 3 µL Lipofectamine per µg of DNA, and the resulting complexes were dropped to growing cells after 20 min incubation at room temperature. Cells were harvested at 24 hours after transfection. For knockdown experiments, cells were transfected for 24h with RCOR1 siRNA mix (Dharmacon, M-014076-01-0010). siRNAs were transfected at a ratio of 33 pmol every µL of Lipofectamine 2000®. Then, western blots were performed to check protein levels. For chemical inhibition of different stages of transcription 1 hour treatments with THZ1, Flavopiridol, Cordycepin or Actinomycin D were performed as previously described(Steurer et al. 2018).

Antibodies. Mouse anti-RCOR1 (NeuroMab, 75-039); Mouse anti-RCOR1 (BD Biosciences, #612146), rabbit anti-LSD1/KDM1 (Abcam, ab17721); rabbit anti-HDAC1 (Abcam, ab7028); mouse anti-HDAC2 (Abcam, ab51832); rabbit anti-EZH2 (Cell Signaling Technology #5246), rabbit anti-HP1α (Cell Signaling Technology, #2616), rabbit anti-RPB1 NTD (Cell Signaling Technology, #14958), rabbit anti-phospho-RPB1 CTD (Ser2) (Cell Signaling Technology, #13499), rabbit anti-phospho-RPB1 CTD (Ser5) (Cell Signaling Technology, #13523), rabbit anti phospho-RPB1 CTD (Ser7) (Cell Signaling Technology, #13780), rabbit anti-H3 (Novus

Biologicals, NB500-171), rabbit anti-H3K4me1 (Cell Signaling Technology, #5326), rabbit anti-H3K4me2 (Cell Signaling Technology, #9725); rabbit anti-H3K4me3 (Cell Signaling Technology, #9751), rabbit anti-H3K9me3 (Abcam, ab8898); rabbit anti-H3K27me3 (Active Motif, #39055), rabbit anti-H3K9ac (Cell Signaling Technology, #9649), rabbit anti-H3K18ac (Cell Signaling Technology, #13998), mouse anti-GAPDH (Cell Signaling Technology, #5174), rabbit anti-HA tag (Cell Signaling Technology, #3724).

Cell Immunofluorescence. Coverslips-grown cells were fixed with 4% paraformaldehyde in PBS for 15 min. After three washes with PBS, cells were permeabilized by 5 min incubation with 0.25% Triton-X100 in PBS and blocked by 1-hour incubation with 3% BSA in PBS. After extensive washes in 1X PBS, coverslips were incubated with secondary anti-rabbit IgG conjugated to Alexa 488 and anti-mouse IgG conjugated Alexa 594, respectively. All incubations were performed at room temperature and primary/secondary antibodies incubations were done in humid chambers. Coverslips were mounted on DAKO Fluorescence Mounting Medium (Agilent) after counterstaining with 1 $\mu\text{g}/\text{mL}$ Hoechst 33342. Images were acquired on a Zeiss LSM 800 Airyscan confocal microscope, with Airyscan acquisition mode and super-resolution processing was performed.

Image analyses. Colocalization analyses were performed using ImageJ software (NIH, Baltimore, MD) by using the JACoP (Just another colocalization plugin) plugin (Bolte and Cordelieres 2006) to determine Van Steensel parameters for single Z-stacks of images. Fluorescence intensity was measured from images using the raw integrated densities of each cell over background measurements. Intensities were normalized as the percentage of total fluorescence counts.

Subcellular fractionation and sequential extraction of chromatin-bound proteins Cells were washed twice in 1X PBS and collected by trypsinization. Trypsin was inactivated with complete growth media. Then, cells were centrifuged and washed twice in 1X PBS. The cell pellet was incubated for 10 minutes in 5 volumes of hypotonic buffer (10 mM Tris, pH 7.9, 1.5 mM MgCl₂, 10 mM KCl, 0.5 mM DTT and 0.2 mM PMSF and 1X protease inhibitor complex (Roche)), cells were then centrifuged, resuspended in 2 volumes of hypotonic buffer and finally lysed by mechanical homogenization. The supernatant was supplemented with additional 30 mM Tris pH 7.9, 140 mM KCl and 3 mM MgCl₂, then it was cleared by centrifugation at 15000 x g for 30 min at 4 °C and stored as a cytosolic extract. Nuclei were collected and washed 3 times in hypotonic buffer, then were sequentially resuspended in nuclear extraction buffers (20 mM Tris, pH 7.9, 25% glycerol, 1.5 mM MgCl₂, 0.2 mM EDTA, 0.5 mM DTT, 0.5 mM PMSF and 1X protease inhibitor complex (Roche)), starting with 100 mM NaCl and increasing salt concentration by steps of 100 mM until 600 mM NaCl was reached. For each step, nuclei were incubated for 7 minutes at 4 °C and then centrifuged at 4000 x g for 5 additional minutes. Supernatants were collected and cleared by centrifugation at 15000 x g for 30 minutes at 4 °C. Fractions were analyzed by western blot, loading equal volumes of each one.

Immunoprecipitation. Cells were lysed in Immunoprecipitation buffer (20 mM Tris-HCl pH 7.5, 150 mM NaCl, 1 mM EDTA, 1 mM EGTA, 1% NP40, 1 mM PMSF, 1 µg/mL leupeptin and 1 µg/mL aprotinin). Sonication was applied to improve the solubilization of chromatin-bound material, and the homogenate was cleared by centrifugation at 12,000 x g for 20 min at 4 °C. Immunoprecipitation was performed using 50 µL SureBeads Protein A Magnetic beads (BioRad) and 1-2 µg of primary antibody every 700 µg of protein. Immunocomplexes were magnetically separated after 12 hours of incubation. Then, beads were extensively washed

against CoIP buffer and immunocomplexes were eluted by boiling the beads in 1X Laemmli Sample Buffer (60 mM Tris-HCl pH 6.5, 2% SDS, 5% glycerol and 1.8 M β -mercaptoethanol).

Western blot. Whole-cell extracts were prepared by homogenization in RIPA buffer (Millipore) in the presence of 1 mM PMSF, 1 μ g/mL leupeptin, and 1 μ g/mL aprotinin as protease inhibitors. Sonication was applied to optimize lysis and protein extraction. Protein content was measured by the Micro-BCA method (Thermo-Scientific). Protein samples were mixed with 5X Laemmli Buffer and denatured at 100 °C for 5 min. SDS-PAGE was run at constant 80-100 V in denaturing running buffer (25 mM Tris, 200 mM glycine, 1% SDS) and transferred to 0.45 μ m pore-sized PVDF membranes at constant current 400 mA in transfer buffer (25 mM Tris, 200 mM glycine). Membranes were blocked 1 hr with 5% non-fat dry milk in TBS-Tween 20 buffer (25 mM Tris-HCl pH 7.6, 275 mM NaCl, 0.1% Tween 20). Incubation with primary antibodies was carried out overnight at 4 °C, and secondary antibody incubation was performed for 1 hour at room temperature. Chemiluminescence development (ECL, Amersham) was used to detect protein bands.

MNase digestion and sucrose gradient ultracentrifugation. 2×10^8 HT22 nuclei were partially digested with 20 U micrococcal nuclease (Worthington, LS004798) during 15 minutes at RT in 20 mM Tris-HCl pH 7.5, 70 mM NaCl, 20 mM KCl, 5 mM MgCl₂, 3 mM CaCl₂ and protease inhibitor cocktail (Roche). The reaction was stopped by adding 2 mM EDTA. Digestion products were extracted by incubating the suspension with 300 mM NaCl and centrifuged at 15000 x g during 15 minutes at 4 °C. Supernatants were loaded on 5-50% sucrose gradients and ultracentrifuged at an average speed of 300000 x g during 16 hours.

Analysis of ChIP-seq data sets. RCOR1, LSD1, HDAC1, p300, Pol-II, and various histone marks ChIP-seq data and peak information for K562 cell line were obtained from ENCODE project. Deeptools program was used for clustering and sorting ChIP-seq data(Ramirez et al. 2014). Peak overlap analysis between RCOR1, LSD1 and HDAC1 was performed using the R package ChIPpeakAnno(Zhu et al. 2010).

Analysis of genomic enrichment. The analysis of enrichment of RCOR1 peaks over genomic features (promoters, intergenic, etc) was done by mapping peaks to the annotated genome with CEAS Python package 1.0.2.(Shin et al. 2009)

Distance distribution analysis. The distance distribution analysis of nearest bidirectional gene transcription start site (TSS) or nearest bidirectional transcript for each cluster was done by calculating the distance from the TSS of each annotated gene to the closest bidirectional gene TSS. Box plots were drawn by R.

High resolution chromosome modeling. Simulations described in this work were performed using the Large-Scale Atomic/Molecular Massively Parallel Simulator (LAMMPS)(PLIMPTON 1995). The initial structure consisted of N=12592 beads that form a

linear polymer chain as a result of a self-avoiding random walk (SARW); these beads correspond to ~63 Mb. Experimental HiC constraints were used directly to form harmonic bonds between interacting particles, and those were forced to form connected pairs via the Monte Carlo algorithm. Once all the bonding constraints were satisfied, the bonds are preserved, and the structure was allowed to equilibrate using Brownian Dynamics with implicit solvent. Defined for the simulation were pair interactions between bonded particles using FENE and Lennard-Jones potentials:

$$U_{\text{FENE-LJ}} = -\frac{1}{2}\kappa R_0^2 \ln \left[1 - (r/R_0)^2 \right] + \begin{cases} 4\varepsilon^* \left[(\sigma/r)^{12} - (\sigma/r)^6 + \varepsilon^* \right], & r \leq 2^{1/6}\sigma \\ 0, & r > 2^{1/6}\sigma \end{cases} \quad (1)$$

where σ is a dimensionless quantity that characterizes distance, and the optimal parameter set of the maximum bond length $R_0 = 20\sigma$ and the spring constant $\kappa = 30\varepsilon^*/\sigma^2$. We choose the repulsive LJ strength $\varepsilon^* = 1$ in non-dimensional units for this bonded potential, which makes the equilibrium bond length $r_{\text{bond}} = 0.99\sigma$ yet allowing the bond to be stretched up to 20σ .

For nonbonded atoms, only the repulsive part of the Lennard-Jones interaction potential was used:

$$U_{\text{LJ}} = \begin{cases} 4\varepsilon \left[(\sigma/r)^{12} - (\sigma/r)^6 + 1/4 \right], & r \leq 2^{1/6}\sigma \\ 0, & r > 2^{1/6}\sigma \end{cases} \quad (2)$$

Finally, we used harmonic constraints originating from experimental HiC data, $U_{\text{HiC}} = K(r - r_0)^2$, where $K = 1 \varepsilon/\sigma^2$ and $r_0 = 2.2 \sigma$. This ensures that the initial random structure of the polymer chain converges and satisfies the constraints originating from Hi-C experiments. The

average simulation temperature was controlled by the Langevin thermostat (kept constant at $T_{\text{start}} = T_{\text{end}} = 1$ in dimensionless units, with the damping coefficient set to $1 \tau^{-1}$). A timestep of 0.01τ was used, where τ is the reduced (Lennard-Jones) time—a measure of how long it takes for the particle to move across its own size, defined as $\tau = \sigma\sqrt{(m/u)}$, where m is the characteristic mass, and u is the intrinsic energy of the system that is the same as parameter ε^* in the spring constant κ .

Imaging of nascent transcripts. Cells were seeded on coverslips at 50% confluency. 16 hours later, cells were incubated with 1 mM 5 ethynyl uridine (EU) during 30 minutes. Right after 30 minutes, cells were fixed in 4% paraformaldehyde - PBS and permeabilized in 0.5% Triton X100 – PBS at RT. Coverslips were then washed with PBS and biotinylation reactions were proceeded with Alexa Fluor 594 – conjugated sodium azide in the presence of CuSO_4 . Finally, coverslips were extensively washed, counterstained with Hoechst and mounted with DAKO. Image acquisition was performed on a Nikon 90i Microscope equipped with 603/1.4 NA. VC Objective lens, Orca ER CCD Camera (Hamamatsu) and Volocity Software (Perkin Elmer).

Exon Inclusion Frequency by Relative Quantity Fluorescent-PCR Analysis (Rqf-PCR).

Total RNA was isolated from HT22 and mice hippocampus, and mice PFC using Trizol reagent (Invitrogen Life Technologies), and reverse transcribed using MMuIV (Thermo Scientific). Rqf-PCR was performed as previously described (Zibetti et al. 2010). qPCR primers were designed to amplify 8a exon region: Ex8_FW: 6-Fam-5'TCCCATGGCTGTCGTCAGCA3'; Ex11_RV: 5'CTACCATTTCATCTTTTTCTTTGG 3'. The ratio of uLSD1/nLSD1 was analyzed by peak scanner software v.1.0.

Statistical analyses. Plotted data were reported in terms of its mean \pm standard error of the

mean (SEM). For experiments comparing two different conditions, Student's t-tests were used to analyze statistical significance. The number of replicates and calculated p-values is stated in figure legends.

REFERENCES

1. Cusanovich, D.A., Pavlovic, B., Pritchard, J.K. & Gilad, Y. The functional consequences of variation in transcription factor binding. *PLoS Genet* **10**, e1004226 (2014).
2. Liu, Z. & Tjian, R. Visualizing transcription factor dynamics in living cells. *J Cell Biol* **217**, 1181-1191 (2018).
3. Almouzni, G. & Probst, A.V. Heterochromatin maintenance and establishment: lessons from the mouse pericentromere. *Nucleus* **2**, 332-8 (2011).
4. Trojer, P. & Reinberg, D. Facultative heterochromatin: is there a distinctive molecular signature? *Mol Cell* **28**, 1-13 (2007).
5. Bannister, A.J. & Kouzarides, T. Regulation of chromatin by histone modifications. *Cell Res* **21**, 381-95 (2011).
6. Kouzarides, T. Chromatin modifications and their function. *Cell* **128**, 693-705 (2007).
7. Andres, M.E. et al. CoREST: a functional co-repressor required for regulation of neural-specific gene expression. *Proc Natl Acad Sci U S A* **96**, 9873-8 (1999).
8. Ballas, N. et al. Regulation of neuronal traits by a novel transcriptional complex. *Neuron* **31**, 353-65 (2001).
9. Barrios, A.P. et al. Differential properties of transcriptional complexes formed by the CoREST family. *Mol Cell Biol* **34**, 2760-70 (2014).
10. You, A., Tong, J.K., Grozinger, C.M. & Schreiber, S.L. CoREST is an integral component of the CoREST- human histone deacetylase complex. *Proc Natl Acad Sci U S A* **98**, 1454-8 (2001).

11. Humphrey, G.W. et al. Stable histone deacetylase complexes distinguished by the presence of SANT domain proteins CoREST/kiaa0071 and Mta-L1. *J Biol Chem* **276**, 6817-24 (2001).
12. Shi, Y. et al. Coordinated histone modifications mediated by a CtBP co-repressor complex. *Nature* **422**, 735-8 (2003).
13. Jenuwein, T. & Allis, C.D. Translating the histone code. *Science* **293**, 1074-80 (2001).
14. Strahl, B.D. & Allis, C.D. The language of covalent histone modifications. *Nature* **403**, 41-5 (2000).
15. Forneris, F., Binda, C., Adamo, A., Battaglioli, E. & Mattevi, A. Structural basis of LSD1-CoREST selectivity in histone H3 recognition. *J Biol Chem* **282**, 20070-4 (2007).
16. Lee, M.G. et al. Functional interplay between histone demethylase and deacetylase enzymes. *Mol Cell Biol* **26**, 6395-402 (2006).
17. Shi, Y.J. et al. Regulation of LSD1 histone demethylase activity by its associated factors. *Mol Cell* **19**, 857-64 (2005).
18. Yang, M. et al. Structural basis for CoREST-dependent demethylation of nucleosomes by the human LSD1 histone demethylase. *Mol Cell* **23**, 377-87 (2006).
19. Pilotto, S. et al. Interplay among nucleosomal DNA, histone tails, and co-repressor CoREST underlies LSD1-mediated H3 demethylation. *Proc Natl Acad Sci U S A* **112**, 2752-7 (2015).
20. Song, Y. et al. Mechanism of Crosstalk between the LSD1 Demethylase and HDAC1 Deacetylase in the CoREST Complex. *Cell Rep* **30**, 2699-2711 e8 (2020).
21. Forneris, F., Binda, C., Vanoni, M.A., Battaglioli, E. & Mattevi, A. Human histone demethylase LSD1 reads the histone code. *J Biol Chem* **280**, 41360-5 (2005).

22. Lan, F. et al. Recognition of unmethylated histone H3 lysine 4 links BHC80 to LSD1-mediated gene repression. *Nature* **448**, 718-22 (2007).
23. Lan, F., Nottke, A.C. & Shi, Y. Mechanisms involved in the regulation of histone lysine demethylases. *Curr Opin Cell Biol* **20**, 316-25 (2008).
24. Monaghan, C.E. et al. REST co-repressors RCOR1 and RCOR2 and the repressor INSM1 regulate the proliferation-differentiation balance in the developing brain. *Proc Natl Acad Sci U S A* **114**, E406-E415 (2017).
25. Saijo, K. et al. A Nurr1/CoREST pathway in microglia and astrocytes protects dopaminergic neurons from inflammation-induced death. *Cell* **137**, 47-59 (2009).
26. Vicent, G.P. et al. Unliganded progesterone receptor-mediated targeting of an RNA-containing repressive complex silences a subset of hormone-inducible genes. *Genes Dev* **27**, 1179-97 (2013).
27. Abrajano, J.J. et al. co-repressor for element-1-silencing transcription factor preferentially mediates gene networks underlying neural stem cell fate decisions. *Proc Natl Acad Sci U S A* **107**, 16685-90 (2010).
28. Abrajano, J.J. et al. REST and CoREST modulate neuronal subtype specification, maturation and maintenance. *PLoS One* **4**, e7936 (2009).
29. Bucevicius, J., Keller-Findeisen, J., Gilat, T., Hell, S.W. & Lukinavicius, G. Rhodamine-Hoechst positional isomers for highly efficient staining of heterochromatin. *Chem Sci* **10**, 1962-1970 (2019).
30. Holmquist, G. Hoechst 33258 fluorescent staining of Drosophila chromosomes. *Chromosoma* **49**, 333-56 (1975).

31. Lakowski, B., Roelens, I. & Jacob, S. CoREST-like complexes regulate chromatin modification and neuronal gene expression. *J Mol Neurosci* **29**, 227-39 (2006).
32. Cramer, P. et al. Structure of eukaryotic RNA polymerases. *Annu Rev Biophys* **37**, 337-52 (2008).
33. Harlen, K.M. & Churchman, L.S. The code and beyond: transcription regulation by the RNA polymerase II carboxy-terminal domain. *Nat Rev Mol Cell Biol* **18**, 263-273 (2017).
34. Zaborowska, J., Egloff, S. & Murphy, S. The pol II CTD: new twists in the tail. *Nat Struct Mol Biol* **23**, 771-7 (2016).
35. Steurer, B. et al. Live-cell analysis of endogenous GFP-RPB1 uncovers rapid turnover of initiating and promoter-paused RNA Polymerase II. *Proc Natl Acad Sci U S A* **115**, E4368-E4376 (2018).
36. Jao, C.Y. & Salic, A. Exploring RNA transcription and turnover in vivo by using click chemistry. *Proc Natl Acad Sci U S A* **105**, 15779-84 (2008).
37. Schroder, S. et al. Acetylation of RNA polymerase II regulates growth-factor-induced gene transcription in mammalian cells. *Mol Cell* **52**, 314-24 (2013).
38. Dias, J.D. et al. Methylation of RNA polymerase II non-consensus Lysine residues marks early transcription in mammalian cells. *Elife* **4**(2015).
39. Loyola, A., Bonaldi, T., Roche, D., Imhof, A. & Almouzni, G. PTMs on H3 variants before chromatin assembly potentiate their final epigenetic state. *Mol Cell* **24**, 309-16 (2006).
40. Rivera, C. et al. Methylation of histone H3 lysine 9 occurs during translation. *Nucleic Acids Res* **43**, 9097-106 (2015).

41. Saavedra, F. et al. PP32 and SET/TAF-Ibeta proteins regulate the acetylation of newly synthesized histone H4. *Nucleic Acids Res* **45**, 11700-11710 (2017).
42. Narita, T., Weinert, B.T. & Choudhary, C. Functions and mechanisms of non-histone protein acetylation. *Nat Rev Mol Cell Biol* **20**, 156-174 (2019).
43. Zhang, X., Wen, H. & Shi, X. Lysine methylation: beyond histones. *Acta Biochim Biophys Sin (Shanghai)* **44**, 14-27 (2012).
44. Ocampo, J., Cui, F., Zhurkin, V.B. & Clark, D.J. The proto-chromatosome: A fundamental subunit of chromatin? *Nucleus* **7**, 382-7 (2016).
45. Simpson, R.T. Structure of the chromatosome, a chromatin particle containing 160 base pairs of DNA and all the histones. *Biochemistry* **17**, 5524-31 (1978).
46. Chereji, R.V., Bryson, T.D. & Henikoff, S. Quantitative MNase-seq accurately maps nucleosome occupancy levels. *Genome Biol* **20**, 198 (2019).
47. Mieczkowski, J. et al. MNase titration reveals differences between nucleosome occupancy and chromatin accessibility. *Nat Commun* **7**, 11485 (2016).
48. Kim, S.A., Zhu, J., Yennawar, N., Eek, P. & Tan, S. Crystal Structure of the LSD1/CoREST Histone Demethylase Bound to Its Nucleosome Substrate. *Mol Cell* **78**, 903-914 e4 (2020).
49. Wang, Z. et al. Genome-wide mapping of HATs and HDACs reveals distinct functions in active and inactive genes. *Cell* **138**, 1019-31 (2009).
50. Gates, L.A. et al. Acetylation on histone H3 lysine 9 mediates a switch from transcription initiation to elongation. *J Biol Chem* **292**, 14456-14472 (2017).
51. Greer, C.B. et al. Histone Deacetylases Positively Regulate Transcription through the Elongation Machinery. *Cell Rep* **13**, 1444-1455 (2015).

52. Kraushaar, D.C. et al. The gene repressor complex NuRD interacts with the histone variant H3.3 at promoters of active genes. *Genome Res* **28**, 1646-1655 (2018).
53. Zhang, T. et al. A variant NuRD complex containing PWWP2A/B excludes MBD2/3 to regulate transcription at active genes. *Nat Commun* **9**, 3798 (2018).
54. Anastas, J.N. et al. Re-programing Chromatin with a Bifunctional LSD1/HDAC Inhibitor Induces Therapeutic Differentiation in DIPG. *Cancer Cell* **36**, 528-544 e10 (2019).
55. Ali, I. et al. Crosstalk between RNA Pol II C-Terminal Domain Acetylation and Phosphorylation via RPRD Proteins. *Mol Cell* **74**, 1164-1174 e4 (2019).
56. Kalin, J.H. et al. Targeting the CoREST complex with dual histone deacetylase and demethylase inhibitors. *Nat Commun* **9**, 53 (2018).
57. Dar, R.D. et al. Transcriptional burst frequency and burst size are equally modulated across the human genome. *Proc Natl Acad Sci U S A* **109**, 17454-9 (2012).
58. Larson, D.R. What do expression dynamics tell us about the mechanism of transcription? *Curr Opin Genet Dev* **21**, 591-9 (2011).
59. Lenstra, T.L., Rodriguez, J., Chen, H. & Larson, D.R. Transcription Dynamics in Living Cells. *Annu Rev Biophys* **45**, 25-47 (2016).
60. Tunnacliffe, E. & Chubb, J.R. What Is a Transcriptional Burst? *Trends Genet* **36**, 288-297 (2020).
61. Bolte, S. & Cordelieres, F.P. A guided tour into subcellular colocalization analysis in light microscopy. *J Microsc* **224**, 213-32 (2006).
62. Ramirez, F., Dundar, F., Diehl, S., Gruning, B.A. & Manke, T. deepTools: a flexible platform for exploring deep-sequencing data. *Nucleic Acids Res* **42**, W187-91 (2014).

63. Zhu, L.J. et al. ChIPpeakAnno: a Bioconductor package to annotate ChIP-seq and ChIP-chip data. *BMC Bioinformatics* **11**, 237 (2010).
64. Shin, H., Liu, T., Manrai, A.K. & Liu, X.S. CEAS: cis-regulatory element annotation system. *Bioinformatics* **25**, 2605-6 (2009).
65. PLIMPTON, S. FAST PARALLEL ALGORITHMS FOR SHORT-RANGE MOLECULAR-DYNAMICS. *Journal of Computational Physics* **117**, 1-19 (1995).
66. Zibetti, C. et al. Alternative splicing of the histone demethylase LSD1/KDM1 contributes to the modulation of neurite morphogenesis in the mammalian nervous system. *J Neurosci* **30**, 2521-32 (2010).

SUPPLEMENTARY INFORMATION**Unveiling RCOR1 as a rheostat at
transcriptional permissive chromatin**

Carlos Rivera^{1,2,3,‡}, Hun-Goo Lee^{2,3,‡}, Anna Lappala^{2,3}, Verónica Noches¹, Montserrat

Olivares-Costa¹, Marcela Sjöberg Herrera¹, Jeannie T. Lee^{2,3,#,*} & María Estela Andrés^{1,#,*}

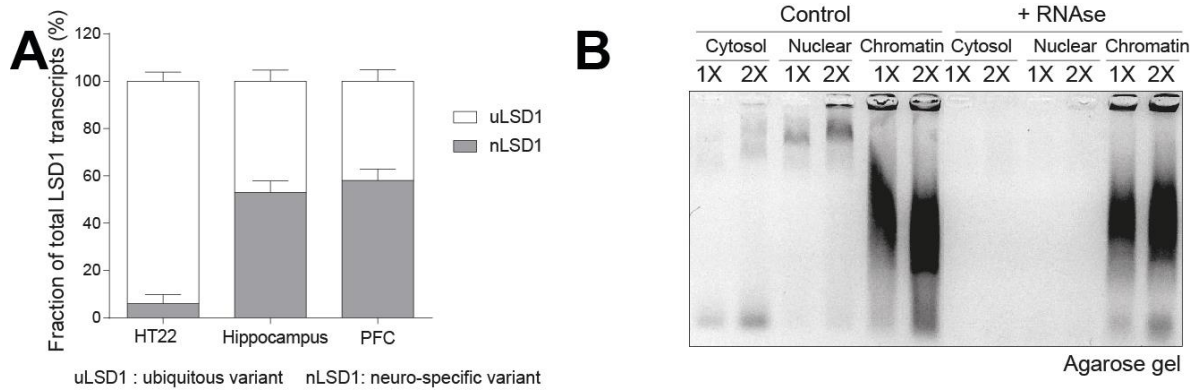


Figure S1.

(A) Ratio of LSD1/nLSD1 transcripts, expressed as percentage of total LSD1 transcripts on HT22 cells, mouse hippocampus and mouse prefrontal cortex (PFC).

(B) Subcellular fractionation control. Agarose gel analyzing the presence of nucleic acids in cytosolic, nuclear soluble and chromatin fractions. As expected, nucleic acids in soluble fractions disappeared after RNase A treatment, confirming our protocol yields chromatin-free soluble fractions.

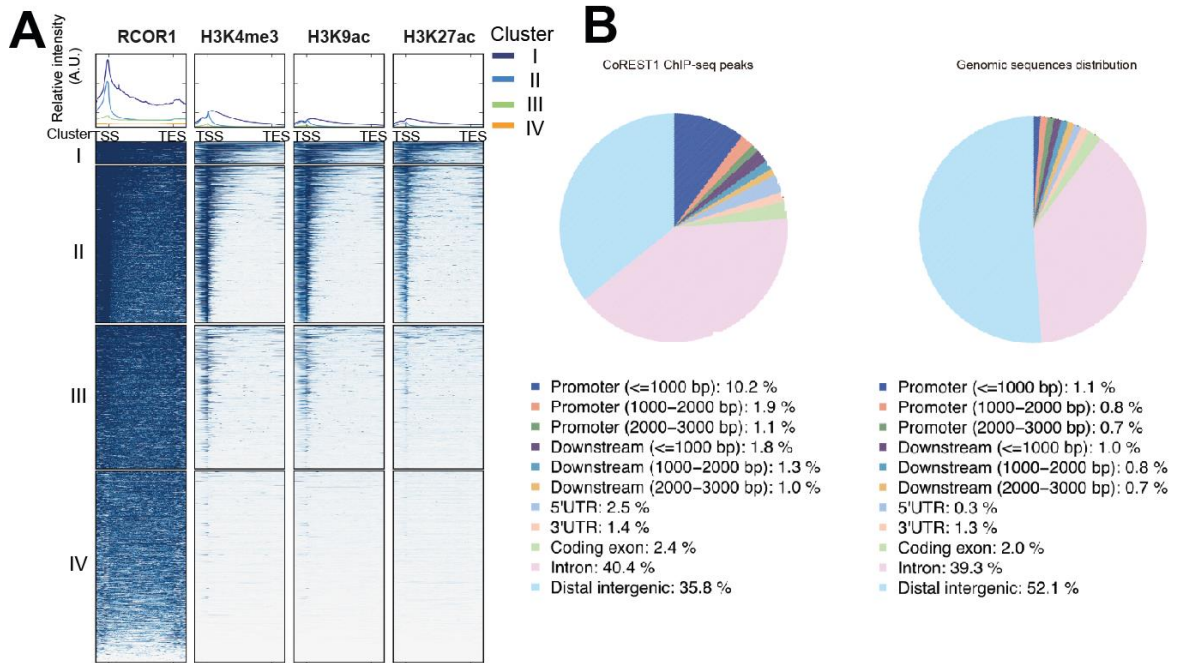


Figure S3.

(A) Metagenomic profiling of RCOR1, H3K4me3, H3K9ac and H3K27ac on RCOR1 clustered genes on CH12 mouse cells.

(B) Pie charts depicting the occupancy of RCOR1 peaks on genomic elements and the natural abundance of those elements on the genome of CH12 cells.

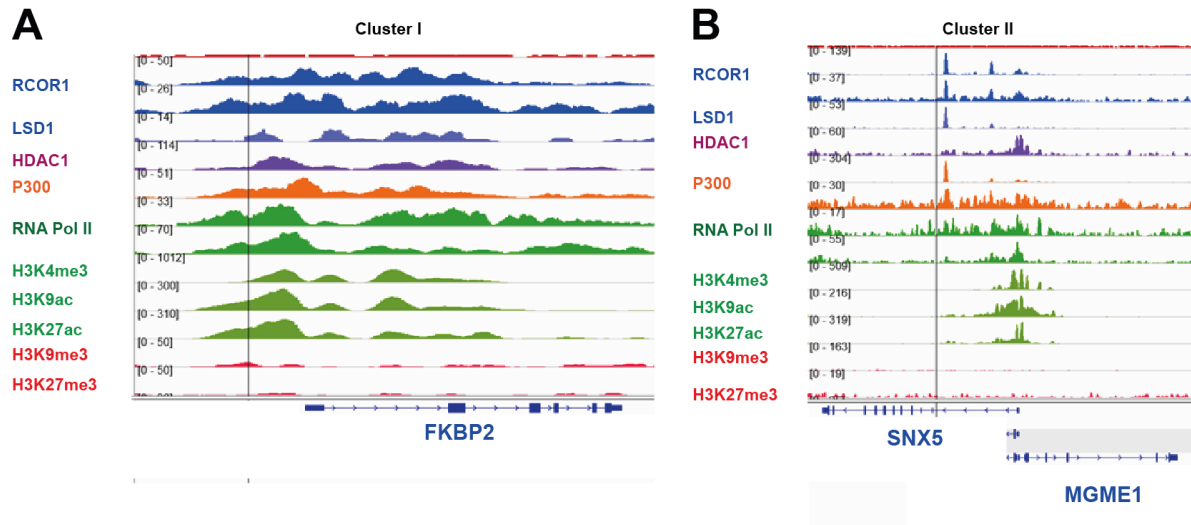


Figure S4.

(A) Representative gene of RCOR1 cluster I.

(B) Representative gene of RCOR1 cluster II.

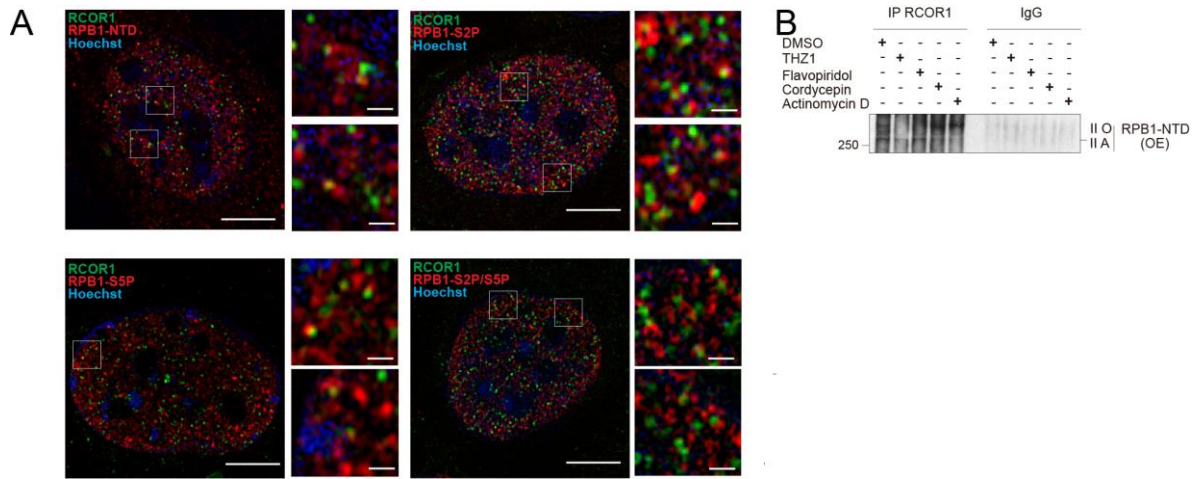


Figure S5.

(A) HT22 cells were stained with double immunolabeling of RCOR1 (green) and different phosphorylated isoforms of RPB1 as shown in red. Right panels show magnified regions of original images. Scale bar is 5 μ m.

(B) Overexposed (OE) western blot image obtained from Main Figure 6.

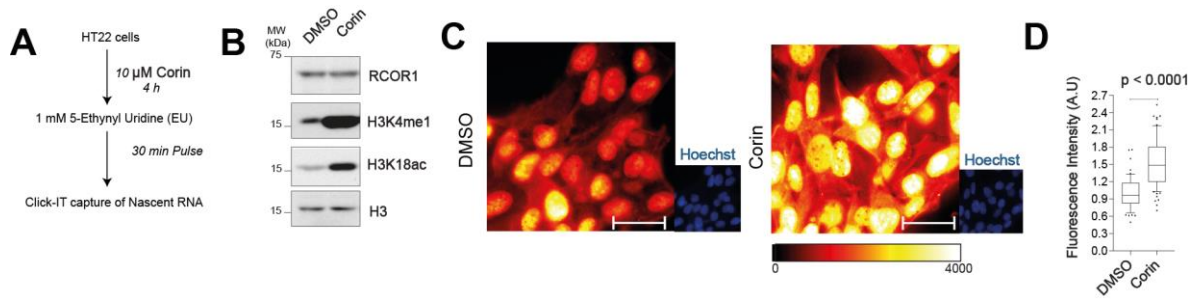


Figure S6.

- (A) Scheme depicting the strategy used to label nascent transcripts in Corin-treated HT22 cells..
- (B) Western blot analysis showing the effect on H3 modifications after treating HT22 cells with Corin.
- (C) Pseudocolor images showing labeling of nascent transcripts in HT22 cells. Scale bar represents 40 μ m.
- (D) Box plots showing quantitation of fluorescent intensity of nascent transcripts

CHAPTER III

RCOR2 is a core component of nuclear speckles and stabilizes

SRSF2

COVER LETTER

09/03/2020

Santiago, Chile

Nucleic Acids Research

Editorial Office

Dear editors:

We are very excited to submit the manuscript entitled “RCOR2 is a core component of nuclear speckles and stabilizes SRSF2” by Carlos Rivera, Fabián Guzmán, Duxan Arancibia, Daniel Verbel, Gianluca Merello, Jeannie T. Lee and María Estela Andrés to be considered as Research Article. We strongly believe that our manuscript provides high-novelty findings that will interest a large audience in the fields of Epigenetics, Nuclear Bodies, Chromatin Modifications and Gene Expression Regulation.

This investigation is the result of a successful collaboration with Dr. Jeannie T. Lee at Massachusetts General Hospital – Harvard Medical School, Boston, MA, USA. The aim of this work is to characterize the nature of nuclear granules formed by the REST co-repressor 2 (RCOR2), a transcriptional regulator which is essential for maintenance of stem cell pluripotency and necessary for the development of central nervous system. With the use of high

resolution microscopy and biochemical approaches, we describe a unique constitutive localization of RCOR2 in nuclear speckles, which resulted to be highly resistant to different cellular stresses even when its integrity is RNA-dependent. Importantly, we describe this protein as a regulator of the stability of nuclear speckles by controlling SRSF2 (the most studied nuclear speckle marker) steady-state levels.

We could define a novel non-canonical function of RCOR2 beyond chromatin-bound regulation of transcription, we believe it will motivate further studies in the field. We declare this manuscript is original, it has not been published before nor it is being currently submitted to any other research journal. Finally, we thank you in advance for considering our manuscript and sincerely hope you will find it compelling.

Sincerely,

María Estela Andrés

Cellular and Molecular Biology Department

Pontifical Catholic University of Chile

RCOR2 is a core component of nuclear speckles and stabilizes SRSF2

Carlos Rivera^{1,2,3}, Fabián Guzmán^{1,†}, Duxan Arancibia^{1,†}, Daniel Verbel¹, Gianluca Merello¹,
Jeannie T. Lee^{2,3} & María Estela Andrés^{1,*}

¹ Department of Cellular and Molecular Biology, Faculty of Biological Sciences, Pontificia Universidad Católica de Chile, Santiago 8330025, Chile.

² Department of Molecular Biology, Massachusetts General Hospital, Boston, MA 02114, USA.

³ Department of Genetics, The Blavatnik Institute, Harvard Medical School, Boston, MA 02114, USA

† Equally contributing authors.

Author contributions: C.R., F.G., D.A., D.V., and G.M. performed research. C.R., D.A., J.T.L., M.E.A. designed research, analyzed data, and wrote the manuscript.

* To whom correspondence should be addressed: María Estela Andrés, Ph.D. Department of Cellular and Molecular Biology, Faculty of Biological Sciences, Pontificia Universidad Católica de Chile. Avenida Del Libertador Bernardo O'Higgins 340, Santiago 8331150, Chile. Telephone: (562) 23542559; e-mail: mandres@bio.puc.cl

Keywords: CoREST, CoREST2, RCOR2, nuclear speckles, membrane-less organelles, SC35, SRSF2, transcription, splicing.

ABSTRACT

Transcription and splicing processes can co-occur into condensates or nuclear bodies, compartmentalizing these processes without the need of any membrane. Inspired by its unique biochemical properties and subcellular distribution, we aimed to characterize the nature of nuclear granules formed by REST co-repressor 2 (RCOR2), a transcriptional co-repressor essential for pluripotency maintenance and central nervous system development. We reveal that most of the RCOR2 proteins are specifically recruited into nuclear speckles in various cell lines and tissues. High-resolution microscopy shows that RCOR2 is enriched at the core region of the speckle and surrounded by poly-adenylated RNAs. RCOR2 localization is highly stable since it resisted cellular stress conditions that impact nuclear speckle morphology and composition. Remarkably, the knockdown of RCOR2 by RNA interference (RNAi) leads to a decrease in the steady-state levels of serine/arginine-rich splicing factor 2 (SRSF2/SC35) the most studied core component of nuclear speckles. As SRSF2 can impact transcriptional and splicing activities, and RCOR2 regulates its stability, we define a novel non-canonical function of RCOR2 beyond chromatin-bound regulation of transcription.

INTRODUCTION

Eukaryotic gene expression requires the coordination of macromolecular complexes to ensure the appropriate synthesis and processing of RNAs. Coactivator and co-repressor complexes recruited into chromatin through protein-protein interactions with transcription factors and transcriptional machinery, modulate transcription by inducing covalent histone modifications and physical displacement of nucleosomes, causing a local change in chromatin accessibility (Millard, Watson, Fairall, et al. 2013).

The RCOR (CoREST) family of transcriptional co-repressors has been characterized based on its ability to silence neuronal genes in non-neuronal cells and during early stages of neuronal differentiation (Ballas et al. 2005a). RCOR co-repressors behave as molecular bridges that bring enzymatic activities to remove transcriptionally-permissive histone modifications. The most stable interactions are established with the H3K4me1/2-demethylase LSD1 (KDM1A), and the histone deacetylases HDAC1 and HDAC2 (Shi et al. 2005). Intriguingly, RCOR2 (CoREST2) and RCOR3 (CoREST3) are weaker repressors than RCOR1 (CoREST, CoREST1), and this feature might be related to their effects on the coordination of LSD1 and HDAC1/2 activities (Barrios et al. 2014). Accordingly, RCOR1 can efficiently stimulate LSD1-mediated H3K4me1/2 demethylation on nucleosomal substrates, while RCOR2 exerts only a subtle LSD1 stimulation and RCOR3 almost lacks that property (Upadhyay et al. 2014; Yang et al. 2011). This data illustrates the existence of differential biochemical properties among RCOR family members. Interestingly, RCOR2-mediated repression does not require HDAC1/2

activity (Barrios et al. 2014). In addition, *in vivo* evidence have attributed specific functions to RCOR2 in developmental regulation, as it is the only RCOR protein important for the maintenance of stem cell state across the cell cycle and also to achieve pluripotency of reprogramming fibroblasts (Yang et al. 2011). RCOR2 has also been reported to regulate cortex development in mice brain in an RCOR1-independent manner (Wang et al. 2016). However, neuron-specific RCOR2-knock out mice can develop a normal brain unless they lack RCOR1 too (Monaghan et al. 2017), suggesting that both members could play complementary roles.

Besides the unique biochemical properties already reported for RCOR2 and its biological impact, there is still an increasing need to determine the molecular mechanisms whereby this protein is acting. Since specific immunostaining of RCOR2 is significantly different than other RCOR members (Saez et al. 2015; Wang et al. 2016), biological compartmentalization mechanisms may be involved in the regulation of its specific functions. In this report, we show through microscopy and biochemical approaches that RCOR2 is constitutively recruited to nuclear speckles, also known as interchromatin granule clusters (IGCs). These nuclear bodies are membrane-less organelles formed by assemblies of 20 nm ribonucleoprotein particles connected by narrow fibers (Thiry 1995) that constitute a phase-separated granule with liquid-droplet properties (Zhu and Brangwynne 2015). They are enriched in pre-mRNA splicing factors and localize close to subnuclear territories where active transcription is occurring (Spector and Lamond 2011). We describe RCOR2 as a core component that stabilizes nuclear speckles, suggesting this protein might impact pre-mRNA processing. Our findings expand the canonical roles associated with RCOR2, adding a new

layer to biological processes where a co-repressor protein can be involved.

MATERIALS AND METHODS

Animals. Adult C57BL/6 mice were maintained on a 12-h-light/12-h-dark cycle with food and water available ad libitum. The procedures were conducted following national and institutional policies (Comisión Nacional de Investigación Científica y Tecnológica [CONICYT] and Pontificia Universidad Católica de Chile).

Cell culture. HT22, HeLa and HEK293-T cells were cultured in Dulbecco's Modified Eagle's Medium (DMEM, Gibco) supplemented with 10% fetal bovine serum (FBS, Gibco) and 1% Penicillin/Streptomycin. Cells grew at 37°C in an atmosphere containing 5% CO₂.

Antibodies. Rabbit polyclonal anti-RCOR2 (Sigma HPA021638), anti-Coilin antibody (Genetex, GTX112570), anti-H3K9me3 (Abcam, ab8898), anti-HP1 α (Cell Signaling, #2616S), anti-LSD1 (Abcam, ab17721), and anti-GAPDH (Cell Signaling, #2118S). Rabbit monoclonal anti-HA (Cell Signaling, #3724S). Mouse monoclonals anti-SC35/SRSF2 (Genetex GTX11826), anti-SC35/SRSF2 (Sigma SAB4200725), and anti-Nucleophosmin (Abcam, ab10530).. Alexa Fluor® 488 AffiniPure Fab Fragment Goat Anti-Rabbit IgG (H+L) (Jackson ImmunoResearch, 111-547-003). AlexaFluor 594-conjugated donkey anti-rabbit IgG antibody (Invitrogen, Thermo Fisher, R37119). AlexaFluor 488-conjugated donkey anti-mouse IgG antibody (Invitrogen, Thermo Fisher, R37114).

Cell Immunofluorescence. Cells were fixed and permeabilized as previously shown (Saez et al. 2015). For double labeling of RCOR2 and markers of nuclear bodies with antibodies raised in the same species, we performed anti-RCOR2 incubation first, then we used an 10X excess (20 μ g/mL) of monovalent Alexa Fluor 488 affinity-purified Fab fragment anti-Rabbit IgG

(H+L) (Jackson ImmunoResearch, 111-547-003), according to manufacturer instructions. After five consecutive 5 min 1X PBS washes, we incubated cells with the second primary antibody and second secondary antibody according to the regular protocol. For tissue immunofluorescence, we followed classical procedures (Saez et al. 2015).

Poly(A)-RNA In situ hybridization. Coverslips were rinsed, post-fixed and dehydrated through 2 min sequential incubations in 70, 80, 90 y 100% V/V Ethanol. We used 1 ng/ μ L Oligo-dT₍₅₀₎ probe in Hybes buffer (2X SSC pH 7.0, 10% m/V dextran sulphate, 25% V/V formamide, 100 ng/ μ L mouse cot-1 DNA). After denaturation, probe was added to the dried slides for 2 hours at RT. Cells were washed 3 times in 4X SSC, 3 times in 2X SSC, and then subjected to DNA staining and mounting.

Microscopy: Images were acquired on an Olympus DS-Fi2 epifluorescence microscope, using 40X and 100X Olympus UplanFI oil immersion objectives, a Nikon DS-fi2 camera and the Q-Imaging capture software. For confocal acquisition, it was carried out at Unidad de Microscopía Avanzada (UMA), Pontificia Universidad Católica de Chile. Cells were imaged on a Nikon Eclipse C2 Si Confocal Spectral Microscope with NIS-Elements C software. High-resolution confocal images were acquired at Massachusetts General Hospital (MGH) Program in Membrane Biology (PMB) Microscopy Core Facility on a Zeiss LSM 800 Airyscan confocal microscope, with Airyscan acquisition mode and conventional super-resolution processing.

Image analyses. Colocalization analyses were performed on ImageJ software (NIH, Baltimore, MD) by using the JACoP (Just another colocalization plugin) plugin (Bolte and Cordelieres 2006) to determine thresholded Manders' coefficients and Van Steensel parameters for single Z-stacks of images. Fluorescence intensity was measured using raw integrated densities of each

cell over background measurements. Intensities were normalized as the percentage of total fluorescence counts. The spatial correlation of the fluorescence intensities of three-color images was performed on ImageJ by drawing a 10-15 μm line and then measuring the fluorescence intensity of each channel every 0.0155 μm . Intensities were normalized as the percentage of total fluorescence counts.

Immunoprecipitation. Cells were lysed in Immunoprecipitation buffer (20 mM Tris-HCl pH 7.5, 150 mM NaCl, 1 mM EDTA, 1 mM EGTA, 1% NP40, 1 mM PMSF, 1 $\mu\text{g}/\text{mL}$ leupeptin and 1 $\mu\text{g}/\text{mL}$ aprotinin). Sonication was applied to improve the solubilization of chromatin-bound material. Binding and elution reactions were performed as previously described (Gomez et al. 2008; Saez et al. 2018).

RNA immunoprecipitation (RIP). Nuclear pellets were prepared and incubated in RIP-Nuclear Lysis buffer (1x PBS pH 7.7, 1% NP40, 0.5% sodium deoxycholate, 100 U/mL Superase In RNase Inhibitor (Thermo-Fisher Scientific) and 1x protease inhibitor cocktail (Roche)) for 30 min with rotation at 4 °C. RIP was performed as previously described (Jeon and Lee 2011). Bound RNAs were recovered with Trizol LS (Thermo-Fisher Scientific) and purified using Direct-zol RNA Miniprep Plus Kit (Zymo Research). MALAT1 and 7SK were detected by qPCR using the following primer pairs: MALAT1 Forward: GCATGCCAGTGTGCAAGAAA, Reverse: ACCCGCAAAGGCCTACATAC. 7SK Forward: CCCTGCTAGAACCTCCAAAC, Reverse: TGGAGTCTTGGAAGCTTGACT.

Subcellular fractionation and sequential extraction of chromatin-bound proteins. Cytosolic extracts were prepared as previously described (Saavedra, Marty-Lombardi, and Loyola 2018). Nuclei were collected and washed 3 times in hypotonic buffer, then were

sequentially resuspended in nuclear extraction buffers (20 mM Tris, pH 7.9, 25% glycerol, 1.5 mM MgCl₂, 0.2 mM EDTA, 0.5 mM DTT, 0.5 mM PMSF and 1X protease inhibitor complex (Roche)), starting with 100 mM NaCl and increasing salt concentration by steps of 100 mM until 600 mM NaCl was reached. For each step, nuclei were incubated for 7 minutes at 4 °C and then centrifuged at 4000 x g for 5 additional minutes. Supernatants were collected and cleared by centrifugation at 15000 x g for 30 minutes at 4 °C.

RNA interference. HEK293T cells were transfected for 48h with RCOR2 siRNA (Santa Cruz, sc-96631) at a ratio of 33 pmol every μ L of Lipofectamine 2000®. For shRNA RNA experiments, the FUX-off lentiviral plasmid (FUGW H1) (Leal-Ortiz et al. 2008) was used to clone an shRNA against RCOR2 obtained from pGeneClip^(TM) plasmid (Promega, Madison, WI). For this, 100 pmol of each oligo were annealed in 100 mM potassium acetate, 30 mM HEPES, and 2 mM magnesium acetate; pH 7.4. The annealed oligos were phosphorylated using T4 polynucleotide kinase (New England Biolabs), introduced in the plasmid and verified by sequencing. Then, FUX-off lentiviral plasmid was packaging in lentiviral particles and HT22 cells were transduced for 96h to perform cell immunofluorescence.

RESULTS

The RCOR2-LSD1 complex is specifically compartmentalized at nuclear speckles.

While examining published RCOR2 immunofluorescence studies made on murine brain and neuronal primary cultures, we noticed an intriguing subcellular distribution of RCOR2 showing a nuclear punctate pattern (Saez et al. 2015; Wang et al. 2016). This observation raised the possibility that RCOR2 may be recruited to some type of nuclear body or chromatin condensate. To test this hypothesis, we carried out double immunofluorescence labeling of RCOR2 and protein markers for nucleoli (nucleophosmin), Cajal bodies (Coilin), pericentric heterochromatin (Heterochromatin protein 1 α , HP1 α ; and H3K9me3), and nuclear speckles (serine and arginine enriched splicing factor 2, SRSF2/SC35) in HT22 cells (**Figure 1**). As expected, RCOR2 showed an intranuclear punctate distribution, which seemed to be located at the interchromatin space since it was excluded from regions with intense Hoechst staining (**Figure 1A**). RCOR2 puncta were excluded from nuclear territories occupied by nucleoli, Cajal bodies, and chromocenters (pericentric heterochromatin), as showed by nucleophosmin, coilin, and H3K9me3/HP1 α co-staining, respectively (**Figure 1A-D**). Quantification of RCOR2 colocalization with these bodies showed less than 8.5% of its fluorescence signal overlapping them (**Figure 1F**), and no correlation between their fluorescence intensity profiles (**Figure 1A-D**). Surprisingly, when we analyzed the co-staining between RCOR2 and nuclear speckles by SRSF2 (also known as SC35) immunofluorescence, we found a strong correlation of their

intensities and about 74% of RCOR2 signals overlapping SRSF2 territories (**Figure 1E-F**). In this context, we detected a partial correlation of fluorescence intensities between LSD1 and SRSF2 (**Figure 1G and Supplementary Figure 1A**), and around 20% of LSD1 signals overlapping SRSF2 speckles (data not shown). These results suggest that a significant amount of the RCOR2-LSD1 complex is compartmentalized at nuclear speckles in interphasic cells.

RCOR2 associates with nuclear speckles inside its core region.

SRSF2 forms the core region of nuclear speckles, while both a subset of polyadenylated pre-mRNAs and exon-junction processing complexes are enriched at the periphery of SRSF2 core domains (Daguenet et al. 2012; Hall et al. 2006). We aimed to determine at which region of the nuclear speckle architecture RCOR2 is recruited. To this end, we examined the colocalization between RCOR2 and SRSF2 at high resolution by Airyscan confocal microscopy with a 2D super-resolution acquisition mode, which can achieve ~120 nm resolution in XY planes (Kolossoff et al. 2018). We detected a strong colocalization between both marks (**Figure 2A**), indicating that RCOR2 is near SRSF2. Therefore, RCOR2 recruitment occurs in the core region of nuclear speckles.

To further inquire about the position of RCOR2 in the architecture of nuclear speckles, we established an immuno-RNA FISH protocol that enabled us to perform a triple fluorescence labeling of RCOR2, SRSF2 and poly-adenylated RNA (poly(A)-RNA) (**Figure 2B**). Previous studies suggested that poly(A)-RNAs are distributed between speckles and the nucleoplasmic space (Carter, Taneja, and Lawrence 1991). At conventional confocal resolution, RCOR2,

SRSF2, and poly(A)-RNAs colocalized at nuclear speckles (**Supplementary Figure 1B**), and poly(A)-RNAs form fiber-like structures, which appear connecting different speckles (**Supplementary Figure 1B**). Super-resolution acquisition mode of Airyscan confocal microscopy enabled us to confirm that poly(A)-RNAs decorated the periphery of RCOR2-SRSF2-containing nuclear speckles, verifying that RCOR2 is located at the speckle core (**Figure 2B**). RCOR2 and SRSF2 appeared to be in close physical contact with poly(A)-RNA, since no space was observed between them (**Figure 2B and Supplementary Figure 1B**).

Next, we performed a biochemical fractionation to first separate the cytosolic and nuclear fractions, and then extract the nuclear proteins sequentially by incubations of increasing salt concentration (**Figure 2C**). In these conditions, RCOR2 is distributed in two main subnuclear fractions, the first one was extracted between 250 and 350 mM NaCl and the second one resisted all the salt-induced extractions, remaining enriched in the chromatin pellet (**Figure 2C**). SRSF2 proteins were mostly extracted between 250 and 350 mM NaCl, similar to the nuclear-soluble fraction of RCOR2, further strengthening the existence of a stable complex between the two proteins (**Figure 2C**). To test if RCOR2 establishes physical interaction with SRSF2, we performed RCOR2 co-immunoprecipitation assays with endogenous proteins in different cell types. In cell lines (**Figure 2D and Supplementary Figure 1C**) their interaction was confirmed by detecting these proteins as constituents of the same immunocomplex (**Figure 2D**) in conditions where the LSD1 demethylase, a bona fide RCOR2 binding partner, was precipitated as well (**Figure 2D and Supplementary Figure 1C**). This interaction was also observed when co-immunoprecipitation of RCOR2 was carried out on native protein extracts of mice brain (**Figure 2E**). As expected, RCOR2 and SRSF2 double labeling performed on

brain slices confirmed their colocalization. Surprisingly, nuclear speckles in neurons were bigger than the regular-sized ones commonly found in widely used cell lines, reaching sizes even larger than two μm (**Figure 2F**). Similar results were observed in mice liver slices, where nuclear speckles were also bigger than in cell lines (**Supplementary Figure 1D**). Consequently, RCOR2 and SRSF2 are in close proximity inside nuclear speckle cores, forming a stable and biochemically detectable complex.

RCOR2 recruitment to nuclear speckles is stabilized by RNA

Nuclear speckle components are organized in sub-compartmentalized layers in a hierarchized and ordered fashion (Fei et al. 2017), with some factors, such as the stress response protein Gadd45, recruited in an RNA-dependent manner (Sytnikova et al. 2011). But others, like SRSF2, are not (Spector, Fu, and Maniatis 1991). To test whether RNA molecules stabilize RCOR2 at nuclear speckles, we analyzed RCOR2 localization after partial digestion of RNA, by treating permeabilized cells with DNase-free RNase A, before fixation. We carried out triple labeling of RCOR2, SRSF2, and poly(A) RNAs which allowed us to correlate RCOR2 levels with remaining RNA content in cells of the same samples. Under control conditions, the permeabilization and subsequent mock treatment did not change the subnuclear distribution of RCOR2 and SRSF2 (**Supplementary Figure 2A**). However, under RNase A treatment, cells that lost more than 80% of their poly(A)-RNAs showed around 60% decrease RCOR2 fluorescence intensity (**Figure 3A, 3B**). Also, SRSF2 fluorescence intensity dropped around 40%, indicating an RNA partial dependence on its nuclear speckle localization. These data suggest that RCOR2 is recruited or stabilized into nuclear speckles by RNA. Consequently, we

tested if RCOR2 is an RNA-binding protein by subjecting native, chromatin-free cell extracts of HT22 cells to poly(A)-RNA pull-down using oligo-dT-conjugated beads (**Figure 3C**). In conditions where a control protein (GAPDH) that does not bind RNA was not pulled down, we detected strong enrichment of RCOR2 in the beads, pulling down more than 30% of the input protein (**Figure 3C**), indicating that RCOR2 binds poly(A)-RNA in cells. Finally, we tested if RCOR2 can interact with non-coding RNAs that are enriched in speckles by native RNA immunoprecipitation (RIP) assays (**Figure 3C**). In conditions where no DNA was amplified by qPCR, we detected a specific interaction between RCOR2 with MALAT1 and RCOR2 with 7SK (**Figure 3C**).

Chemical perturbation of nuclear speckle architecture does not alter RCOR2 recruitment to nuclear speckles

The architecture of nuclear speckles changes significantly with the inhibition of transcription (Kim et al. 2019). Consistently, variations in nuclear speckle sizes result of speckle fusion and over-recruitment of nucleoplasmic factors. Our previous data showing that RCOR2 localizes in the nuclear speckle core prompted us to compare the stability of its compartmentalization with that of SRSF2 when transcription is inhibited. To this end, we treated HeLa cells with actinomycin D, which blocks transcriptional elongation. As expected, nuclear speckles became bigger and rounder (**Figure 4A, B, and supplementary Figure 2B**). RCOR2 remained recruited to these bodies, as measured by its colocalization with SRSF2 (**Figure 4B, 4E**). Thus, the compartmentalization of RCOR2 at nuclear speckles resisted the

inhibition of transcription.

We also tested the effect of isoginkgetin, a biflavonoid that inhibits the recruitment of the U4/U6/U5 snRNP complex into the spliceosome, by blocking its assembly at an early stage of the splicing cycle (O'Brien et al. 2008). The exposure of cells to low and high concentrations of Isoginkgetin caused a decrease in nuclear speckle sizes (**Figure 4F**), probably increasing the nucleoplasmic availability of speckle-bound factors (**Figure 4C and Supplementary Figure 2C**). Meanwhile, the signal for RCOR2 remained similar to controls and colocalizing with SRSF2 (**Figure 4C, 4E**). This data suggests that a fraction of SRSF2 proteins is released from the nuclear speckles when splicing is inhibited, but the majority of RCOR2 remains associated with SRSF2 inside the nuclear speckles.

Finally, we tested tubercidin to induce disassembly of the nuclear speckles. This adenosine analog was discovered by its ability to displace poly(A)-RNA from the nucleus and to cause dispersion of some splicing factors from nuclear speckles (Kurogi et al. 2014). Recently, it was shown that tubercidin can also cause stress granule formation and mRNA export defects (Hochberg-Laufer, Schwed-Gross, et al. 2019). In our model, tubercidin caused a dramatic dispersion of SRSF2 to the nucleoplasm and cytoplasm (**Figure 4D**), with some recruitment of this splicing factor to cytoplasmic granules (**Figure 4D**). Surprisingly, RCOR2 distribution was not affected, being still compartmentalized in speckles-like subnuclear structures. These data suggest that RCOR2 localization at the speckle cores might be even more stable than that of SRSF2.

RCOR2 stabilizes the architecture of nuclear speckles

Altogether, our previous data suggest that RCOR2 may have a role in structuring nuclear speckles. To test this idea, we performed knockdown of this protein with siRNA in HEK293T cells, achieving almost a 60% decrease in RCOR2 protein level (**Figure 5A**). Surprisingly, concomitant with the RCOR2 knockdown, we detected a siRNA concentration-dependent reduction in SRSF2 (**Figure 5A**), suggesting that RCOR2 stabilizes the SRSF2 protein. Next, we aimed to test if RCOR2 knockdown could affect nuclear speckle assembly. To this end, we performed an shRNA-mediated knockdown of RCOR2 in HT22 cells, and we observed a strong decrease in the fluorescence intensity of both RCOR2 and SRSF2 (**Figure 5B**). However, the punctate pattern of the remaining levels of both proteins was not modified under RCOR2 knockdown, which indicates that RCOR2 may be stabilizing the levels of SRSF2 splicing factor inside the nuclear speckles. Previous studies have demonstrated that nuclear speckle factors are degraded upon hyperacetylation (Chen, Huang, et al. 2018; Edmond et al. 2011), and under HDAC inhibition SRSF2 becomes hyperacetylated triggering its proteasomal degradation (Edmond et al. 2011). Interestingly, we found that under HDAC inhibition RCOR2, but not RCOR1, is degraded (**Supplementary Figure 3A, 3B**), evidencing a similar behavior to speckle bound proteins specific for RCOR2 in the RCOR co-repressor family. This suggests that RCOR2-SRSF2 interaction could be preventing SRSF2 degradation.

DISCUSSION

In this work, we report microscopic and biochemical evidence showing that RCOR2 is a core component of nuclear speckles that stabilizes their architecture. These findings open a new layer of biological phenomena linked to RCOR2 specific functions in the regulation of gene expression, beyond its canonical role as a transcriptional co-repressor at the chromatin level. Although some proteins that behave as transcriptional co-repressors, such as the methyl-CpG binding protein 2 (MeCP2) (Salichs et al. 2009) and Nuclear receptor co-repressor 2 (N-CoR2) (Wu et al. 2001), have been identified as components of nuclear speckles (Salichs et al. 2009), their role there is unknown. To our knowledge, this is the first characterization of a repressor protein presenting a non-canonical function inside nuclear speckles.

Sub-nuclear distribution equilibrium of RCOR2 reflecting a novel non-canonical function

Classical reports suggest that many factors associated with nuclear speckles, especially the ones involved in pre-mRNA processing, are dynamically distributed between speckles and the nucleoplasm. They propose the nucleoplasmic pool as a subpopulation available to act directly in pre-mRNA processing while transcription is occurring. In this sense, nuclear speckles would act as their storage site (Kruhlak et al. 2000; Phair and Misteli 2000). This idea has been strengthened by live-cell fluorescence microscopy data showing an increase in the speed of pre-mRNA processing when nuclear speckles are disassembled. This correlated with

an increase in nuclear speckle factors available in the nucleoplasm (Hochberg-Laufer, Neufeld, et al. 2019). Considering its specific biochemical features and functions among RCOR proteins, RCOR2 should be understood as a member that evolved particular functions (Barrios et al. 2014; Wang et al. 2016; Yang et al. 2011).

This report adds novel specific features to this protein. We showed in different biological systems, ranging from cell lines to murine tissues, that RCOR2 is concentrated inside the nucleus and highly enriched in nuclear speckles, being around 3 times more abundant in these bodies than in the nucleoplasmic fraction. This property seems to be specific for this RCOR-family member since the immunostaining of RCOR1 and RCOR3 does not show similar punctate patterns (Saez et al. 2015). Therefore, the evidence of RCOR2 compartmentalization reflects the existence of a distribution equilibrium of RCOR2 proteins between two different nuclear liquid phases: nuclear speckles and the nucleoplasm, which is displaced towards the nuclear speckle fraction at steady state. We speculate that nucleoplasmic RCOR2 may constitute a fraction available to act on chromatin to repress transcription, while the speckle-bound fraction could be a reservoir pool, but also a different subpopulation where RCOR2 exerts specific functions by stabilizing these bodies.

RCOR2 impact on gene expression: beyond chromatin?

RCOR2 forms a stable complex with LSD1, which is different from the classical LSD1-RCOR1-HDAC1/2 complex, since RCOR2 shows a weak interaction with HDACs (Barrios et al. 2014; Yang et al. 2011). Interestingly, we showed that around 20% of LSD1 colocalizes

with nuclear speckles and it can be detected as part of the same immunocomplex when RCOR2 is immunoprecipitated. These data indicate that a proportion of the RCOR2-LSD1 complex is present in nuclear speckles. However, whether this complex is being stored as an inactive complex inside the nuclear speckles or it is regulating gene expression is an unexplored topic. Regarding the suspected, but not confirmed active role of nuclear speckles on transcription and RNA processing, two recent elegant studies addressed this at a genome-wide scale, by focusing on the measurement of distances and detection of high-order interactions between chromosomal regions and nuclear bodies: tyramide signal amplification sequencing (TSA-seq) (Chen, Zhang, et al. 2018) and split-pool recognition of interactions by tag extension (SPRITE) (Quinodoz et al. 2018). Both revealed a huge subset of highly expressed genes and super-enhancers enriched close to nuclear speckles (Chen, Zhang, et al. 2018; Quinodoz et al. 2018).

Interestingly, a recent study confirmed by sophisticated microscopy approaches that the spatial association of nascent transcripts with nuclear speckles significantly enhances their transcription yield, presumably by some kind of steric protection against nascent-RNA degradation (Kim, Venkata, et al. 2020). In this sense, since RCOR2-LSD1 complex behaves as a bona fide repressor (Barrios et al. 2014; Yang et al. 2011), and our data suggests that it is excluded from nuclear compartments where transcription is silenced, such as pericentric heterochromatin, nucleolus and nuclear lamina, we propose that besides its stabilizing function at nuclear speckles, the RCOR2-LSD1 complex could also be acting by dampening the transcriptional enhancement that nuclear speckles produce on some genes, or by antagonizing the presence of lysine methyltransferases in nuclear speckles (Saitoh et al. 2004), that dimethylate H3K4, the substrate that LSD1 demethylates when bound to RCOR proteins

(Upadhyay et al. 2014). Another interesting possibility is that the cell developed mechanisms to sequester the RCOR2-LSD1 complex at the core region of speckles to prevent their repressive functions when enhancement of transcription is needed at nuclear speckle-proximal genes in chromatin.

An RNA component allows for the localization of RCOR2 at the core of nuclear speckles

We showed by high-resolution microscopy that RCOR2 localizes at the center of nuclear speckles, surrounded by poly(A)-RNAs that decorate their periphery. We were able to biochemically detect physical interactions of RCOR2 and SRSF2, and between RCOR2 and speckle associated non-coding RNAs MALAT1 and 7SK, confirming that RCOR2 is a stable component of nuclear speckles whose interactions are still detectable after cell and tissue lysis. We found a strong enrichment of RCOR2 at fractions where poly(A)-RNAs were precipitated, which correlate with our microscopy findings since we could not detect physical separation between the RCOR2 and poly(A)-RNAs even at high resolution, motivating us to propose RCOR2 as an RNA binding protein. RNA-binding properties of RCOR2 must be important for its nuclear speckle localization, given that RNase A treatment significantly reduced the levels of the protein inside the nucleus. This supports that RNAs stabilize RCOR2 inside nuclear speckles. Further studies will focus on which RNAs are the strongest binding partners of RCOR2 and how their interactions may impact the RCOR2 function.

Stability of nuclear speckle-bound RCOR2: even higher than splicing factors

The speckle-core localization of RCOR2 was highly stable since we attempted with different pharmacological treatments to change the architecture of nuclear speckles and it resisted all of them. As an initial approach, we inhibited transcription with actinomycin D, which blocks transcription at elongation steps by intercalating itself with DNA regions where RNA polymerase II is hyperphosphorylated (Steurer et al. 2018). Transcription inhibitors induce larger and rounder shapes in nuclear speckles (Spector, Fu, and Maniatis 1991). In this context, we observed that under actinomycin D treatment, RCOR2 colocalization with SRSF2 was significantly increased, supporting that RCOR2 distribution equilibrium is displaced towards nuclear speckles when transcription is inhibited. Additionally, this evidence suggests that some nucleoplasmic fraction of RCOR2 may be recruited back to nuclear speckles when transcription elongation is blocked. On the other hand, when we inhibit splicing with Isoginkgetin, we could not detect any change in the colocalization of RCOR2 and SRSF2, even when a 60% reduction of speckle sizes was proven.

Isoginkgetin causes an accumulation of the intermediate complex A in the spliceosome assembly pathway, preventing the formation of the catalytically active spliceosome and generation of lariat products (O'Brien et al. 2008). Since RCOR2 localization at nuclear speckles was not affected, we would discard an eventual involvement of RCOR2 in spliceosome assembly. Finally, even when SRSF2 was displaced from nuclear speckles under treatment with the only known drug that induces splicing factor disassembly from nuclear speckles, tubercidin, RCOR2 remained as a nuclear punctate pattern. Altogether, our data evidenced a strong stability

of RCOR2 inside nuclear speckle cores, which seemed to be even higher than classical speckle markers.

RCOR2 stabilizes nuclear speckles

Splicing factors like SRSF2 are recruited to nuclear speckles when phosphorylated at their RS motif (Sacco-Bubulya and Spector 2002). The family of RS containing proteins participates actively to regulate important events in almost all stages of RNA maturation, ranging from constitutive/alternative splicing to mRNA export and translation (Shepard and Hertel 2009). Beyond the fact that SRSF2 is the classical molecular marker of nuclear speckles, its loss of function by mutations has been widely linked to complex clinical phenomena such as cancer and immune diseases (Kedzierska et al. 2016; Cheng et al. 2016). Hence, our findings can significantly impact SRSF2 signaling, as the knockdown of RCOR2 decreased the steady-state levels of SRSF2 and its abundance in nuclear speckles. It has been demonstrated that SRSF2 is degraded by the proteasome in an acetylation dependent mechanism, driven by Tip60 mediated acetylation of SRSF2 lysine 52 (Edmond et al. 2011). Interestingly, we found that under global HDAC inhibition, RCOR2 levels are decreased, suggesting that RCOR2 may experience a similar degradation mechanism as SRSF2. Therefore, based on our results, we can speculate that RCOR2-mediated SRSF2 stabilization could be linked to the prevention of acetylation-dependent SRSF2 degradation.

ACKNOWLEDGEMENTS

We thank Dr. Ekaterina Nizovtseva and Dr. Verónica Noches for critical reading of the manuscript. Unidad de Microscopía Avanzada (UMA), Pontificia Universidad Católica de Chile, Chile, and the Massachusetts General Hospital (MGH) Program in Membrane Biology (PMB) Microscopy Core Facility for the use of confocal imaging instruments.

FUNDING:

This work was supported by the Agencia Nacional de Investigación y Desarrollo (ANID) [FONDECYT Regular Grants #1150200, #1191152 to MEA, Ph.D. Fellowship #21161044 to CR, Ph.D. Fellowship #21150971 to DA] and FRAXA Research Foundation and National Institutes of Health (N.I.H) (R01-HD097665) grants to J.T.L.

DECLARATION OF COMPETING INTERESTS: J.T.L. is a co-founder of Translate Bio and Fulcrum Therapeutics, and also serves as Advisor to Skyhawk Therapeutics.

SUPPLEMENTARY DATA STATEMENT

Supplementary data are available at NAR online.

FIGURES

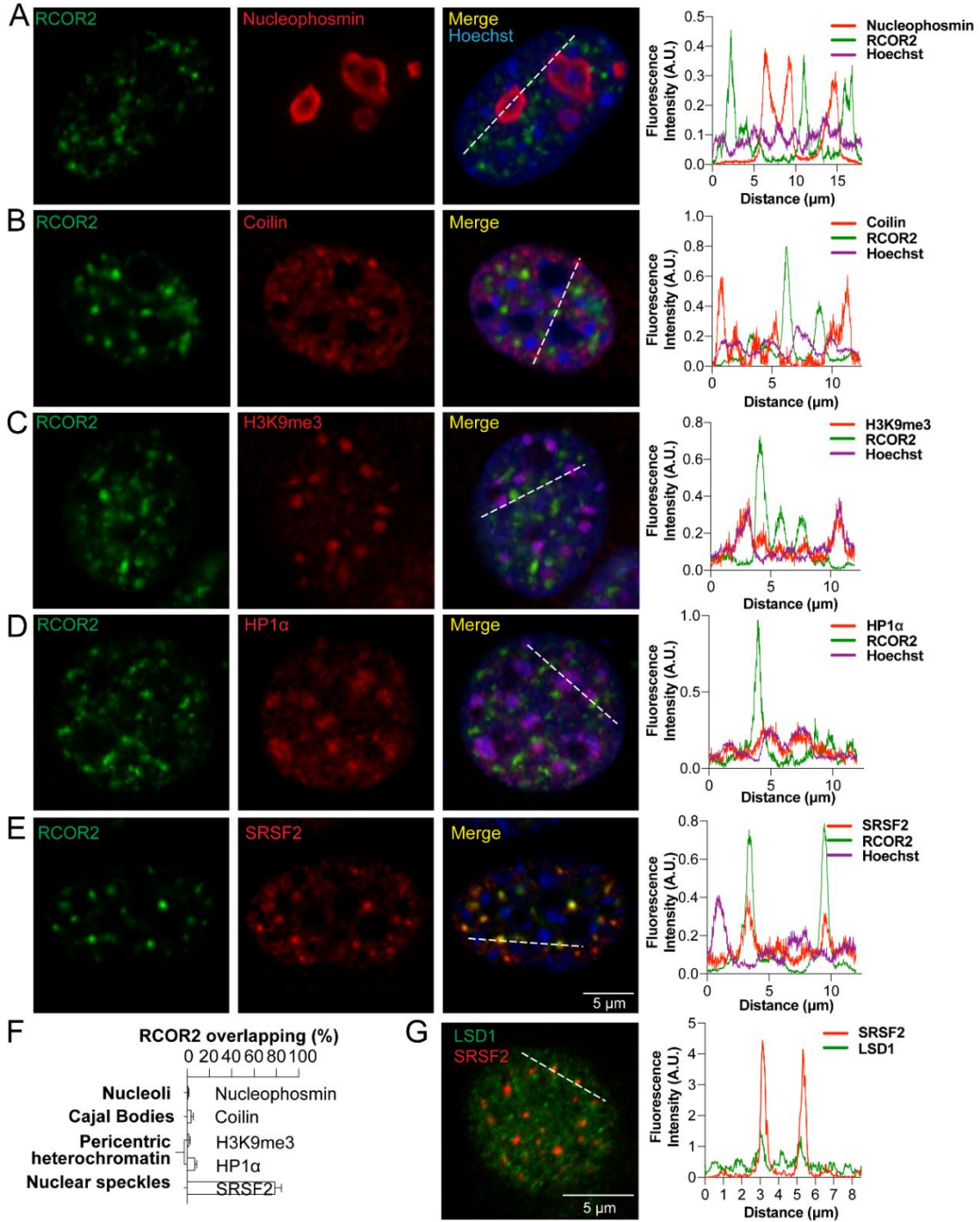


Figure 1. RCOR2 colocalizes with nuclear speckles.

Figure 1. RCOR2 colocalizes with nuclear speckles.

(A-E) HT22 cells were stained with double immunolabeling of RCOR2 (green) and nucleophosmin (A), Coilin (B), H3K9me3 (C), HP1 α (D) or SRSF2 (E) as molecular markers of nuclear bodies or chromatin condensates (red). For each staining procedure, the spatial correlation of both fluorophores plus Hoechst staining was tracked according to the white dashed lines. Right-sided plots show their normalized fluorescence intensity plotted against the position on the dashed line. Images are representative of three independent stainings.

(F) RCOR2 overlapping degree is expressed as the percentage of thresholded RCOR2 pixels overlapping territories of red channel pixels. Percentages were calculated based on RCOR2 thresholded Manders coefficients analyzed by JACoP ImageJ-plugin on independent stainings.

(G) Double immunolabeling of LSD1 (green) and SRSF2 (red). The right-sided plot shows their normalized fluorescence intensity plotted against the position on the dashed line. The image is representative of two independent stainings.

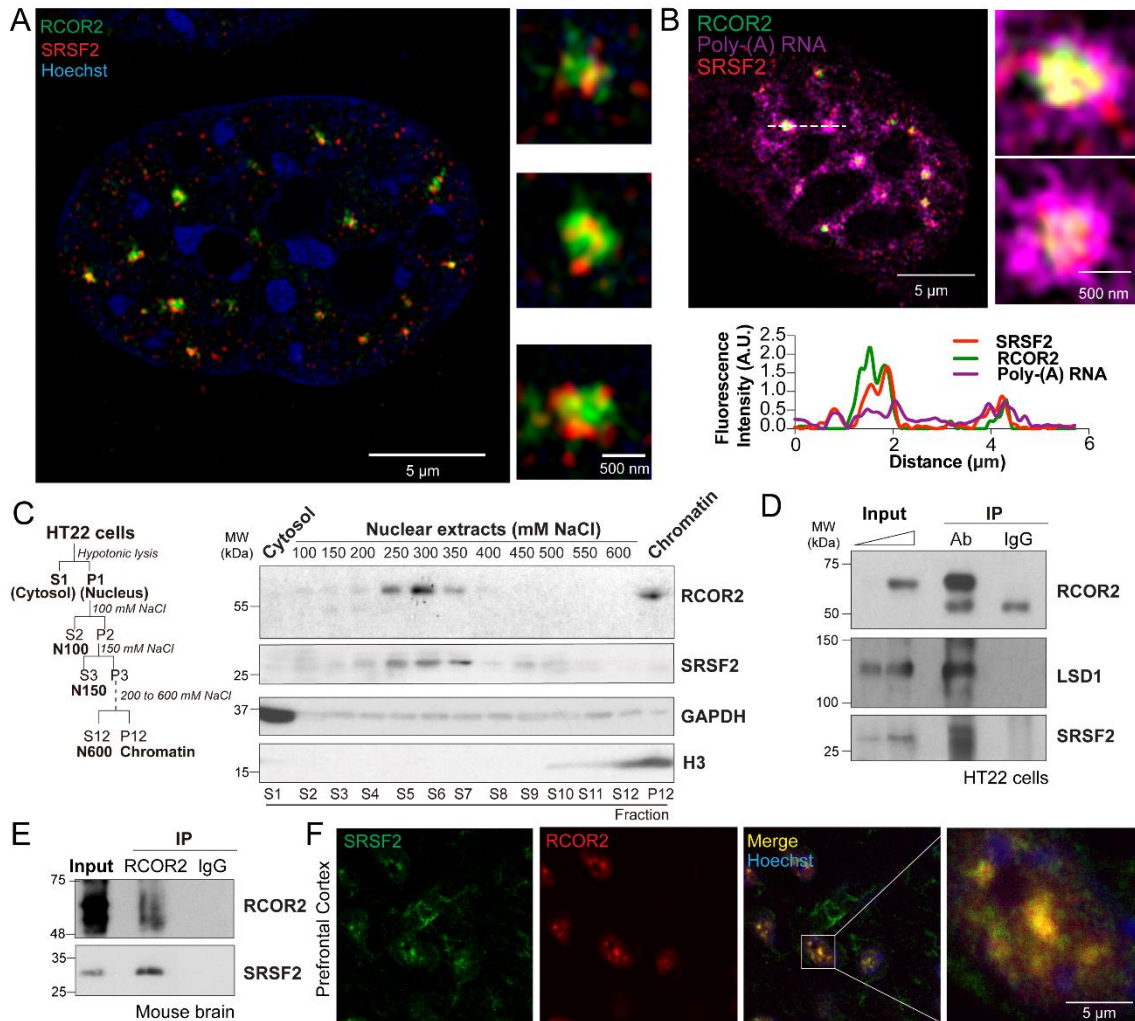


Figure 2. RCOR2 associates with nuclear speckles at their core region.

Figure 2. RCOR2 associates with nuclear speckles at their core region.

(A) RCOR2 (green) and SRSF2 (red) immunolabeling visualized at super-resolution confocal acquisition. Hoechst is visualized in blue color. Right panels show zoomed-in individual nuclear speckles.

(B) Merged representation of RCOR2 (green), SRSF2 (red), and Poly(A)-RNA (magenta) triple immunostaining at super-resolution confocal acquisition. Right panels show zoomed-in individual nuclear speckles. The bottom plot shows the normalized fluorescence intensity of each channel plotted against the position on the dashed line. The image is representative of 4 independent stainings.

(C) Biochemical fractionation of HT22 cells by sequential salt extraction of nuclear proteins. The left schematic workflow indicates the overall procedure, showing how cytosolic (S1), nuclear (P1), and chromatin fractions (P12) were obtained. For sequential nuclear extractions, nuclear extracts at different salt concentrations are labelled as N100, where N means nuclear extract and 100 means 100 mM NaCl. Right panels show western blot analysis of RCOR2 and SRSF2 abundance on cytosolic, nuclear and chromatin fractions. GAPDH and H3 were assayed as cytosolic and chromatin markers. Western blot is representative of two independent experiments.

(D) Western blot analysis of co-immunoprecipitation of RCOR2, LSD1, and SRSF2 in HT22 native extracts. Increasing concentrations of protein inputs were loaded as shown. Ab: Antibody used to immunoprecipitate RCOR2. IgG: Immunoglobulin G used as a specificity control. Figure is representative of 4 independent experiments.

(E) Western blot confirmation of co-immunoprecipitation of RCOR2 and SRSF2 in mouse

brain native extracts. Ab: Antibody used for immunoprecipitation of RCOR2. IgG: Immunoglobulin G used as a specificity control.

(F) Tissue immunofluorescence labeling of SRSF2 (green) and RCOR2 (red) in prefrontal cortex slices. The merged image includes Hoechst DNA staining (blue). The right panel shows a zoomed-in nucleus, illustrating the bigger sizes of speckles found in brain tissues.

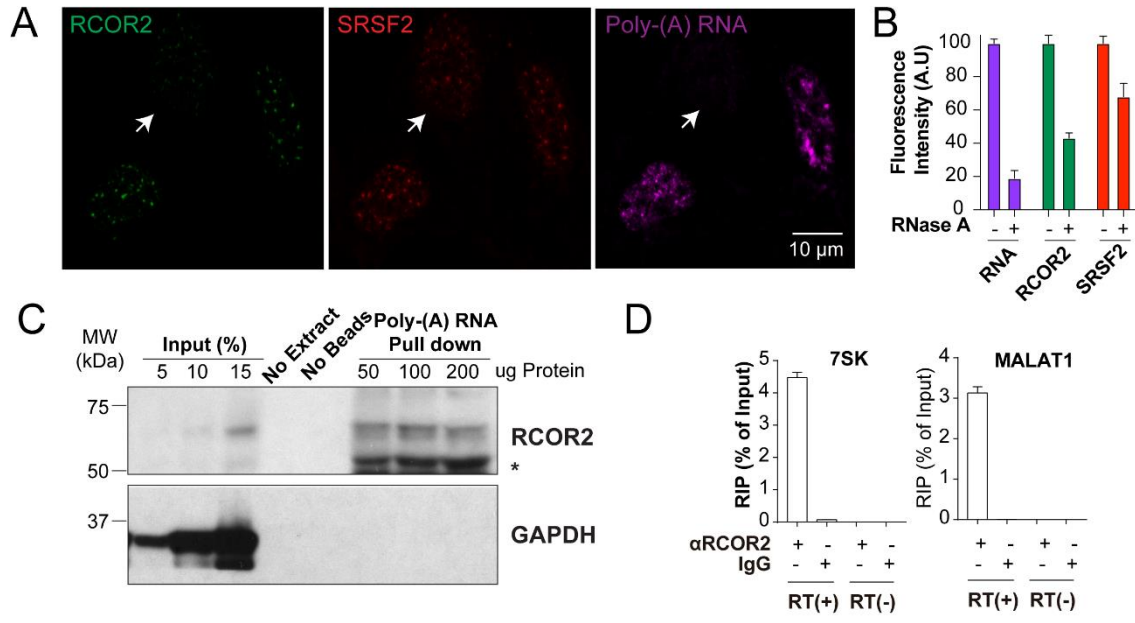


Figure 3. An RNA component stabilizes RCOR2 at nuclear speckles.

Figure 3. An RNA component stabilizes RCOR2 at nuclear speckles.

(A) RCOR2 (green), SRSF2 (red), and poly(A)-RNA (magenta) labeling of RNase A treated cells visualized at regular confocal acquisition. Arrows indicate a representative cell that lost its RNA content after RNase A treatment.

(B) Quantification of normalized cell fluorescence intensity for each channel of cells mock-treated and RNase A-treated. Quantifications included 20 cells from 3 biological replicates.

(C) Western blot analysis of RCOR2 and GAPDH to test their coprecipitation after poly(A)-pull-down. Increasing concentrations of protein input were loaded to estimate enrichment after pull down. No loaded extract and extract without beads were subjected to the same procedure as specificity controls.

(D) Real-time quantitative PCR results showing 7SK and MALAT1 fragment amplification after performing RNA immunoprecipitation with an anti-RCOR2 antibody. IgG was used as specificity control and qPCR without reverse transcription (RT(-)) was analyzed to discard eventual DNA concentration after immunoprecipitations. Results are representative of two different biological replicates.

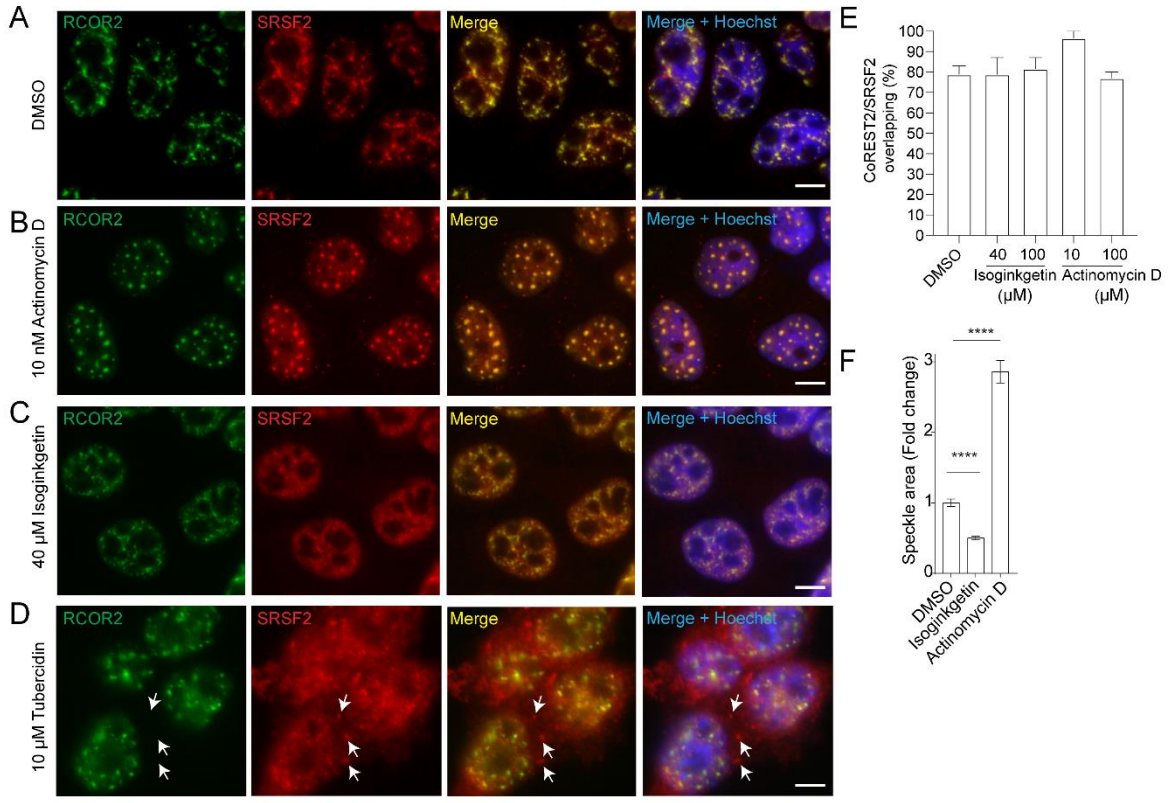


Figure 4. RCOR2 nucleation in speckles is highly stable.

Figure 4. RCOR2 nucleation in speckles is highly stable.

(A-D) HeLa cells were stained against RCOR2 (green) and SRSF2 (red) after treatments with DMSO vehicle (A), actinomycin D (B), Isoginkgetin (C) and tubercidin (D). Arrows indicate cytoplasmic SRSF2 aggregates. Images are representative of two independent experiments.

(E) RCOR2 overlapping degree is expressed as the percentage of thresholded RCOR2 pixels overlapping SRSF2 territories. Percentages were calculated based on RCOR2 thresholded Manders coefficients analyzed by JACoP ImageJ-plugin on independent stainings.

(F) Speckle area quantitation under isoginkgetin and actinomycin D treatments. The area was measured in 10 cells measuring areas of 10 speckles per cell on each condition. Results were normalized against DMSO control values. Unpaired t-tests were performed for each condition against mock-treated cells to estimate statistical significance. **** p<0.001.

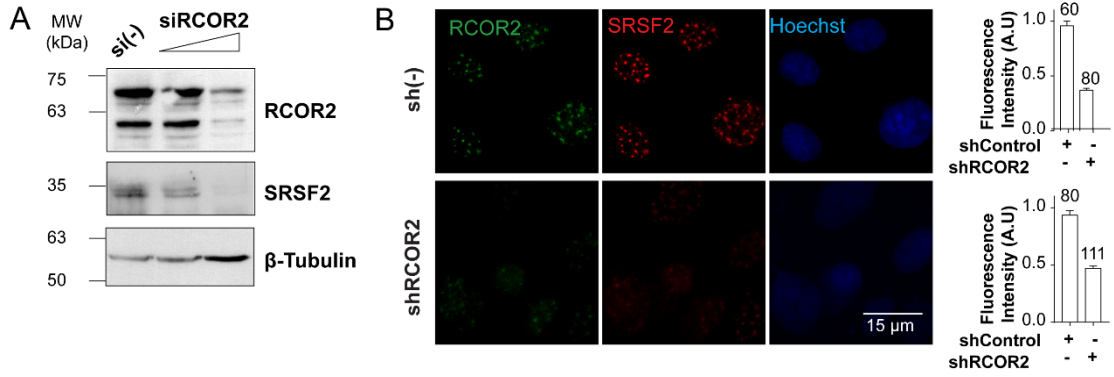


Figure 5. RCOR2 regulates SRSF2 stability.

Figure 5. RCOR2 regulates SRSF2 stability.

(A) Western blot analysis of SRSF2 and RCOR2 levels under RCOR2 knockdown in HEK293T cells. Equal protein quantities were loaded for scrambled control (si(-)) and RCOR2 siRNA (siRCOR2) conditions. β -Tubulin was assayed as a loading control.

(B) RCOR2 (green) and SRSF2 (red) immunofluorescent labeling of HT22 transduced with lentiviral packed shRNAs-coding plasmids. Hoechst DNA staining is showed in blue. Images are representative of two independent transductions. Total cell fluorescence intensities were plotted in the right panels to evaluate the efficiency of the RCOR2 knockdown and its effect over SRSF2 levels. Numbers over each bar represent the total number of cells measured for each condition.

REFERENCES

1. Millard, C.J., Watson, P.J., Fairall, L. and Schwabe, J.W. (2013) An evolving understanding of nuclear receptor coregulator proteins. *J Mol Endocrinol*, **51**, T23-36.
2. Ballas, N., Grunseich, C., Lu, D.D., Speh, J.C. and Mandel, G. (2005) REST and its co-repressors mediate plasticity of neuronal gene chromatin throughout neurogenesis. *Cell*, **121**, 645-657.
3. Shi, Y.J., Matson, C., Lan, F., Iwase, S., Baba, T. and Shi, Y. (2005) Regulation of LSD1 histone demethylase activity by its associated factors. *Mol Cell*, **19**, 857-864.
4. Barrios, A.P., Gomez, A.V., Saez, J.E., Ciossani, G., Toffolo, E., Battaglioli, E., Mattevi, A. and Andres, M.E. (2014) Differential properties of transcriptional complexes formed by the CoREST family. *Mol Cell Biol*, **34**, 2760-2770.
5. Upadhyay, G., Chowdhury, A.H., Vaidyanathan, B., Kim, D. and Saleque, S. (2014) Antagonistic actions of Rcor proteins regulate LSD1 activity and cellular differentiation. *Proc Natl Acad Sci U S A*, **111**, 8071-8076.
6. Yang, P., Wang, Y., Chen, J., Li, H., Kang, L., Zhang, Y., Chen, S., Zhu, B. and Gao, S. (2011) RCOR2 is a subunit of the LSD1 complex that regulates ESC property and substitutes for SOX2 in reprogramming somatic cells to pluripotency. *Stem Cells*, **29**, 791-801.

7. Wang, Y., Wu, Q., Yang, P., Wang, C., Liu, J., Ding, W., Liu, W., Bai, Y., Yang, Y., Wang, H. *et al.* (2016) LSD1 co-repressor Rcor2 orchestrates neurogenesis in the developing mouse brain. *Nat Commun*, **7**, 10481.
8. Monaghan, C.E., Nechiporuk, T., Jeng, S., McWeeney, S.K., Wang, J., Rosenfeld, M.G. and Mandel, G. (2017) REST co-repressors RCOR1 and RCOR2 and the repressor INSM1 regulate the proliferation-differentiation balance in the developing brain. *Proc Natl Acad Sci U S A*, **114**, E406-E415.
9. Saez, J.E., Gomez, A.V., Barrios, A.P., Parada, G.E., Galdames, L., Gonzalez, M. and Andres, M.E. (2015) Decreased Expression of CoREST1 and CoREST2 Together with LSD1 and HDAC1/2 during Neuronal Differentiation. *PLoS One*, **10**, e0131760.
10. Thiry, M. (1995) The interchromatin granules. *Histol Histopathol*, **10**, 1035-1045.
11. Zhu, L. and Brangwynne, C.P. (2015) Nuclear bodies: the emerging biophysics of nucleoplasmic phases. *Curr Opin Cell Biol*, **34**, 23-30.
12. Spector, D.L. and Lamond, A.I. (2011) Nuclear speckles. *Cold Spring Harb Perspect Biol*, **3**.
13. Bolte, S. and Cordelieres, F.P. (2006) A guided tour into subcellular colocalization analysis in light microscopy. *J Microsc*, **224**, 213-232.
14. Gomez, A.V., Galleguillos, D., Maass, J.C., Battaglioli, E., Kukuljan, M. and Andres, M.E. (2008) CoREST represses the heat shock response mediated by HSF1. *Mol Cell*, **31**, 222-231.

15. Saez, J.E., Arredondo, C., Rivera, C. and Andres, M.E. (2018) PIASgamma controls stability and facilitates SUMO-2 conjugation to CoREST family of transcriptional co-repressors. *Biochem J*, **475**, 1441-1454.
16. Jeon, Y. and Lee, J.T. (2011) YY1 tethers Xist RNA to the inactive X nucleation center. *Cell*, **146**, 119-133.
17. Saavedra, F., Marty-Lombardi, S. and Loyola, A. (2018) Characterization of Posttranslational Modifications on Histone Variants. *Methods Mol Biol*, **1832**, 21-49.
18. Leal-Ortiz, S., Waites, C.L., Terry-Lorenzo, R., Zamorano, P., Gundelfinger, E.D. and Garner, C.C. (2008) Piccolo modulation of Synapsin1a dynamics regulates synaptic vesicle exocytosis. *J Cell Biol*, **181**, 831-846.
19. Dagueneat, E., Baguet, A., Degot, S., Schmidt, U., Alpy, F., Wendling, C., Spiegelhalter, C., Kessler, P., Rio, M.C., Le Hir, H. *et al.* (2012) Perispeckles are major assembly sites for the exon junction core complex. *Mol Biol Cell*, **23**, 1765-1782.
20. Hall, L.L., Smith, K.P., Byron, M. and Lawrence, J.B. (2006) Molecular anatomy of a speckle. *Anat Rec A Discov Mol Cell Evol Biol*, **288**, 664-675.
21. Kolossov, V.L., Sivaguru, M., Huff, J., Luby, K., Kanakaraju, K. and Gaskins, H.R. (2018) Airyscan super-resolution microscopy of mitochondrial morphology and dynamics in living tumor cells. *Microsc Res Tech*, **81**, 115-128.
22. Carter, K.C., Taneja, K.L. and Lawrence, J.B. (1991) Discrete nuclear domains of poly(A) RNA and their relationship to the functional organization of the nucleus. *J Cell Biol*, **115**, 1191-1202.

23. Fei, J., Jadhava, M., Harmon, T.S., Li, I.T.S., Hua, B., Hao, Q., Holehouse, A.S., Reyer, M., Sun, Q., Freier, S.M. *et al.* (2017) Quantitative analysis of multilayer organization of proteins and RNA in nuclear speckles at super resolution. *J Cell Sci*, **130**, 4180-4192.
24. Sytnikova, Y.A., Kubarenko, A.V., Schafer, A., Weber, A.N. and Niehrs, C. (2011) Gadd45a is an RNA binding protein and is localized in nuclear speckles. *PLoS One*, **6**, e14500.
25. Spector, D.L., Fu, X.D. and Maniatis, T. (1991) Associations between distinct pre-mRNA splicing components and the cell nucleus. *EMBO J*, **10**, 3467-3481.
26. Kim, J., Han, K.Y., Khanna, N., Ha, T. and Belmont, A.S. (2019) Nuclear speckle fusion via long-range directional motion regulates speckle morphology after transcriptional inhibition. *J Cell Sci*, **132**.
27. O'Brien, K., Matlin, A.J., Lowell, A.M. and Moore, M.J. (2008) The biflavonoid isoginkgetin is a general inhibitor of Pre-mRNA splicing. *J Biol Chem*, **283**, 33147-33154.
28. Kurogi, Y., Matsuo, Y., Mihara, Y., Yagi, H., Shigaki-Miyamoto, K., Toyota, S., Azuma, Y., Igarashi, M. and Tani, T. (2014) Identification of a chemical inhibitor for nuclear speckle formation: implications for the function of nuclear speckles in regulation of alternative pre-mRNA splicing. *Biochem Biophys Res Commun*, **446**, 119-124.

29. Hochberg-Laufer, H., Schwed-Gross, A., Neugebauer, K.M. and Shav-Tal, Y. (2019) Uncoupling of nucleo-cytoplasmic RNA export and localization during stress. *Nucleic Acids Res*, **47**, 4778-4797.
30. Chen, Y., Huang, Q., Liu, W., Zhu, Q., Cui, C.P., Xu, L., Guo, X., Wang, P., Liu, J., Dong, G. *et al.* (2018) Mutually exclusive acetylation and ubiquitylation of the splicing factor SRSF5 control tumor growth. *Nat Commun*, **9**, 2464.
31. Edmond, V., Moysan, E., Khochbin, S., Matthias, P., Brambilla, C., Brambilla, E., Gazzeri, S. and Eymin, B. (2011) Acetylation and phosphorylation of SRSF2 control cell fate decision in response to cisplatin. *EMBO J*, **30**, 510-523.
32. Salichs, E., Ledda, A., Mularoni, L., Alba, M.M. and de la Luna, S. (2009) Genome-wide analysis of histidine repeats reveals their role in the localization of human proteins to the nuclear speckles compartment. *PLoS Genet*, **5**, e1000397.
33. Wu, X., Li, H., Park, E.J. and Chen, J.D. (2001) SMRTE inhibits MEF2C transcriptional activation by targeting HDAC4 and 5 to nuclear domains. *J Biol Chem*, **276**, 24177-24185.
34. Kruhlak, M.J., Lever, M.A., Fischle, W., Verdin, E., Bazett-Jones, D.P. and Hendzel, M.J. (2000) Reduced mobility of the alternate splicing factor (ASF) through the nucleoplasm and steady state speckle compartments. *J Cell Biol*, **150**, 41-51.
35. Phair, R.D. and Misteli, T. (2000) High mobility of proteins in the mammalian cell nucleus. *Nature*, **404**, 604-609.

36. Hochberg-Laufer, H., Neufeld, N., Brody, Y., Nadav-Eliyahu, S., Ben-Yishay, R. and Shav-Tal, Y. (2019) Availability of splicing factors in the nucleoplasm can regulate the release of mRNA from the gene after transcription. *PLoS Genet*, **15**, e1008459.
37. Chen, Y., Zhang, Y., Wang, Y., Zhang, L., Brinkman, E.K., Adam, S.A., Goldman, R., van Steensel, B., Ma, J. and Belmont, A.S. (2018) Mapping 3D genome organization relative to nuclear compartments using TSA-Seq as a cytological ruler. *J Cell Biol*, **217**, 4025-4048.
38. Quinodoz, S.A., Ollikainen, N., Tabak, B., Palla, A., Schmidt, J.M., Detmar, E., Lai, M.M., Shishkin, A.A., Bhat, P., Takei, Y. *et al.* (2018) Higher-Order Inter-chromosomal Hubs Shape 3D Genome Organization in the Nucleus. *Cell*, **174**, 744-757 e724.
39. Kim, J., Venkata, N.C., Hernandez Gonzalez, G.A., Khanna, N. and Belmont, A.S. (2020) Gene expression amplification by nuclear speckle association. *J Cell Biol*, **219**.
40. Saitoh, N., Spahr, C.S., Patterson, S.D., Bubulya, P., Neuwald, A.F. and Spector, D.L. (2004) Proteomic analysis of interchromatin granule clusters. *Mol Biol Cell*, **15**, 3876-3890.
41. Steurer, B., Janssens, R.C., Geverts, B., Geijer, M.E., Wienholz, F., Theil, A.F., Chang, J., Dealy, S., Pothof, J., van Cappellen, W.A. *et al.* (2018) Live-cell analysis of endogenous GFP-RPB1 uncovers rapid turnover of initiating and promoter-paused RNA Polymerase II. *Proc Natl Acad Sci U S A*, **115**, E4368-E4376.

42. Sacco-Bubulya, P. and Spector, D.L. (2002) Disassembly of interchromatin granule clusters alters the coordination of transcription and pre-mRNA splicing. *J Cell Biol*, **156**, 425-436.
43. Shepard, P.J. and Hertel, K.J. (2009) The SR protein family. *Genome Biol*, **10**, 242.
44. Kedzierska, H., Poplawski, P., Hoser, G., Rybicka, B., Rodzik, K., Sokol, E., Boguslawska, J., Tanski, Z., Fogtman, A., Koblowska, M. *et al.* (2016) Decreased Expression of SRSF2 Splicing Factor Inhibits Apoptotic Pathways in Renal Cancer. *Int J Mol Sci*, **17**.
45. Cheng, Y., Luo, C., Wu, W., Xie, Z., Fu, X. and Feng, Y. (2016) Liver-Specific Deletion of SRSF2 Caused Acute Liver Failure and Early Death in Mice. *Mol Cell Biol*, **36**, 1628-1638.

SUPPLEMENTARY INFORMATION**RCOR2 is a core component of nuclear speckles and stabilizes
SRSF2**

Carlos Rivera^{1,2,3}, Fabián Guzmán^{1,†}, Duxan Arancibia^{1,†}, Daniel Verbel¹, Gianluca Merello¹,
Jeannie T. Lee^{2,3} & María Estela Andrés^{1,*}

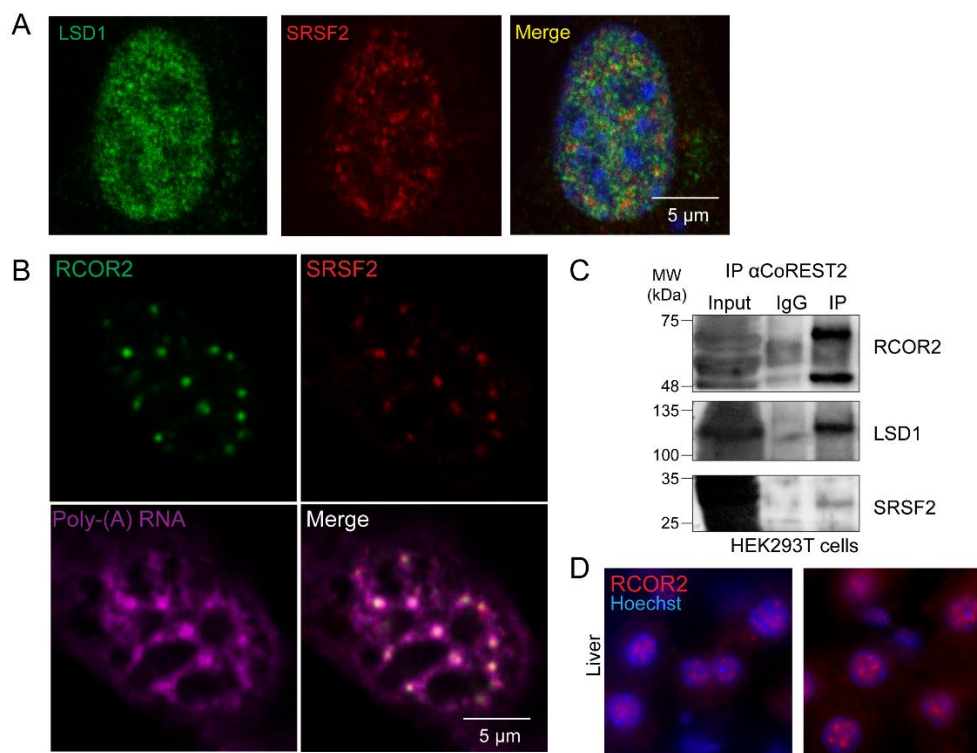


Figure S1.

(A) Immunostaining of LSD1 (green) and SRSF2 (red) in HT22 cells. Merged image is showed including Hoechst DNA staining in blue, showing partial colocalization of LSD1 in nuclear speckles.

(B) Confocal images for validation of our triple staining of RCOR2 (green), SRSF2 (red), and Poly(A)-RNA (magenta). Merged image is included.

(C) Western blot analysis of co-immunoprecipitation of RCOR2, LSD1, and SRSF2 in HEK cells.

(D) RCOR2 and Hoechst staining in mouse liver tissue slices showing the speckled pattern for RCOR2.

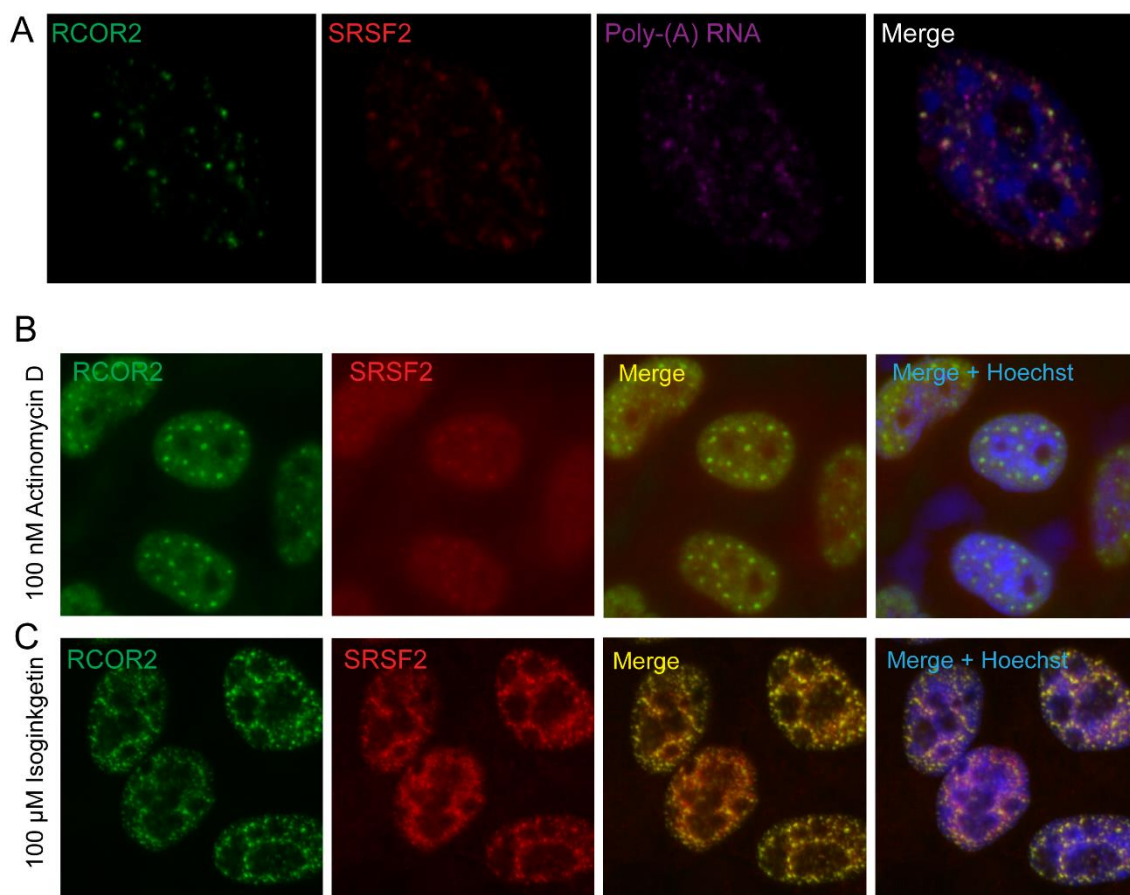


Figure S2.

(A) Confocal images of RCOR2 (green), SRSF2 (red), and Poly(A)-RNA (magenta) triple staining in permeabilized, mock-treated HT22 cells before fixation. The merged image includes Hoechst DNA staining.

(B-C) HeLa cells were stained against RCOR2 (green) and SRSF2 (red) after treatments with high doses of actinomycin D (B) and Isoginkgetin (C). Images are representative of two independent experiments.

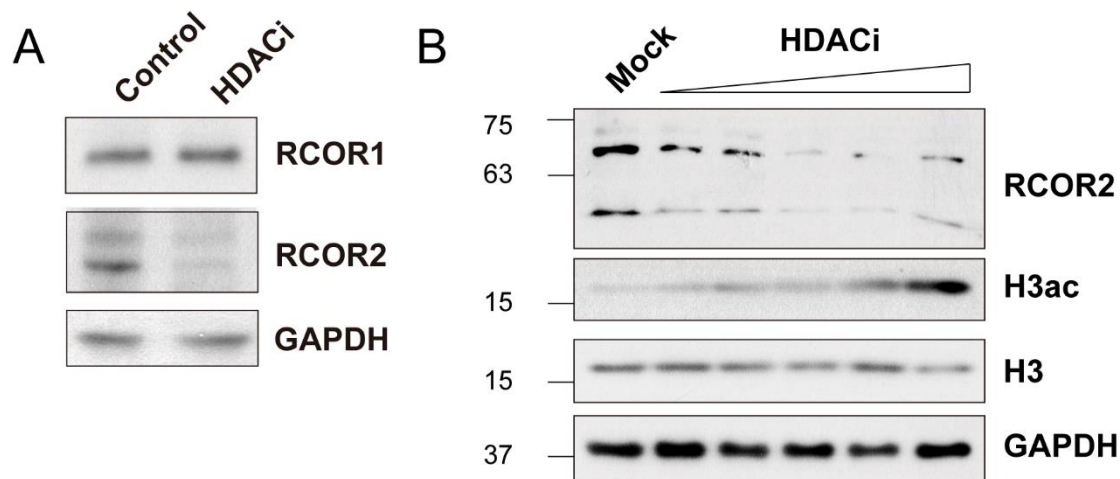


Figure S3.

(A) Western blot analyses of RCOR1, RCOR2, and GAPDH in HT22 cells after were 24 h treatment with HDAC inhibitor Sodium Butyrate 5 mM.

(B) Western blot analyses of RCOR2, H3ac, total H3, and GAPDH in HT22 cells after treatment with increasing concentrations of HDAC inhibitors (1 to 20 mM).

CHAPTER IV

GENERAL DISCUSSION

DISCUSSION

Insights from the evolution of co-repressor proteins

The molecular evolution of highly regulated gene expression patterns has been linked to the appearance of complex mechanisms of transcriptional control. This includes pathways that exert a negative effect on the production or activity of transcriptional machinery and/or activator complexes. In addition, the presence of paralogous genes coding for co-repressor proteins such as CtBP, TLE, SMRT, N-COR, and RCOR depicts the evolutionary trend to diversify mechanisms of transcriptional repression. One possible explanation has been discussed in the literature and suggests the existence of paralogue genes as ways to regulate tissue-specific gene expression patterns (Payankulam, Li, and Arnosti 2010). However, diversification of biological functions is also possible. For instance, different CtBP co-repressors have differential subcellular distribution, suggesting their activity is differentially regulated (Bergman et al. 2006), and distinct N-COR proteins generated by alternative splicing produce differential repressive functions by targeting different transcription factors (Goodson, Jonas, and Privalsky 2005). The RCOR family of transcriptional co-repressors is not an exception. Despite their highly conserved functional domains, they elicit particular functions. RCOR1 has the highest repressive capacity of the family, RCOR2-mediated repression is an HDAC-independent mechanism, and RCOR3 can compete for binding LSD1, preventing RCOR1-mediated LSD1 stimulation (Barrios et al. 2014; Upadhyay et al. 2014).

Our laboratory found that RCOR1 and RCOR2 are segregated in different subnuclear domains excluded from DNA dense regions (Rivera et al., unpublished), suggesting they might be acting on euchromatin or the nucleoplasmic space. This work addressed relevant questions that emerged from these observations, focusing on characterizing the subnuclear localization, chromatin-binding properties, and roles of the co-repressors RCOR1 and RCOR2 in the cell nucleus. We found novel, non-canonical roles exerted by both proteins, which in part provide evidence to the prevalent paradox in the field regarding the molecular functions of co-repressors in transcriptional permissive chromatin domains. The findings expand the variety of pathways where RCOR co-repressors have been attributed to.

On the subcellular distribution of RCOR1 and RCOR2

The two scientific articles derived from this investigation showed the existence of different subcellular populations of RCOR1 and RCOR2. On the one hand, RCOR1 showed three central subcellular populations: A cytosolic one, a nuclear soluble which was extracted at 250 mM NaCl and a chromatin-bound, salt-resistant subpopulation. On the other hand, RCOR2 showed two main subpopulations inside cells, both restricted to the nucleus. This protein was mostly extracted at 250 mM NaCl, and immunostaining showed that 75% of it is constitutively recruited to nuclear speckles. Considering that RCOR1 does not colocalize with RCOR2, it prompts us to propose that the speckle-binding property of RCOR2 is a specific feature for this protein that is not present in RCOR1, supporting the evolutionary diversification of protein functions in this family of co-repressor proteins.

Interestingly, from the co-existence of different subcellular populations of RCOR proteins, we can point out various interpretations. First, if these subpopulations are part of the same molecular pathway targeting soluble RCOR proteins to chromatin at different stages of their life cycle, it could reflect that the cytoplasmic abundance of the proteins represents their newly synthesized pool waiting to be transported to the nucleus. In the same way, once imported to the nucleus, RCOR1 proteins can establish a dynamic distribution between the nucleoplasm and chromatin and RCOR2 proteins between the nucleoplasm, chromatin, and nuclear speckles. Second, since it is not known if RCOR proteins can be transported retrogradely to the cytoplasmic compartment, we could also suggest that the cytosolic population represent a specific compartment where RCOR proteins are acting in a non-canonical way, probably by mediating deacetylation or demethylation reactions in non-histone substrates or in newly-synthesized histone proteins. Third, the differential extractability of two subnuclear populations of both RCOR1 and RCOR2 could reflect more than just distribution between nucleoplasm and chromatin or nuclear bodies. By this, I mean that the soluble population detected in our studies could also represent a chromatin-bound fraction of RCOR proteins, which is mostly recruited to chromatin or nuclear speckles by electrostatic interactions, and thus they could be easily extracted by moderate hypertonic buffers. Finally, since we detected the presence of nuclear lamina markers in the chromatin fraction, we can also suggest that RCOR proteins saw there could also be enriched in these subnuclear domains. Further studies are required to address these questions emerging from our findings.

Interestingly, it has been suggested that BHC80 and PHF21 can stabilize RCOR1 complexes in chromatin (Gocke and Yu 2008; Lan et al. 2007). However, in our models, these proteins were selectively extracted in the nuclear soluble fraction (data not shown), suggesting that additional factors might be stabilizing the chromatin-bound pool of RCOR co-repressors.

On the interaction between RCOR1 and RNA Polymerase II

Little evidence has been reported regarding the interaction of subunits of co-repressor complexes with the RNA Pol II. The transcriptional co-repressor MMTR (MAT1-mediated transcriptional repressor) was found to interact with the general transcription factor TFIIF which harbors the helicase activity necessary for RNA Pol II initiation of transcription. Remarkably, this co-repressor interacts with HDAC1 and induces inhibition of RNA Pol II phosphorylation (Kang et al. 2007). Other transcription repressive proteins have been linked to RNA Pol II function, such as the repressor TRIM28, which stabilizes the pausing of RNA Pol II, inhibiting transcription elongation (Bunch et al. 2014). In this present work, we provide evidence showing that the RCOR1-LSD1-HDAC1 complex interacts with the transcriptional machinery. We found RCOR1 is recruited to Pol II after initiation and before and during productive elongation, suggesting that the complex could be acting by repressing transcription at the level of promoter-proximal pausing and elongation. It is not known yet if these roles are mutually exclusive along different epigenomic regions. However, the existence of distinct clusters of RCOR1 in chromatin, characterized by differential distribution between the TSS and gene body regions, could represent different loci where the complex is acting at the level of promoter proximal-pausing and/or elongation. We followed this interaction as a function of co-

precipitation induced by RCOR1 immunoprecipitation, both in total extracts prepared with sonication or by MNased chromatin templates. Both techniques generate chromatin-soluble fragments, so in these ways, we can not distinguish if the interaction is direct. Additional research needs to be designed to provide answers to these questions.

Interestingly, we found that the inhibition of the enzymes linked to RCOR1 by the small-molecule dual-inhibitor Corin upregulates the acetylation levels of RPB1. This RPB1 post-translational modification has been linked both to promoter-proximal pausing and elongation, and it is correlated with genes that are actively expressed (Dias et al. 2015; Schroder et al. 2013). Surprisingly, this increased acetylation was detected only in the hypo-phosphorylated variant of RPB1, suggesting that the complex is regulating the acetylation of initiating Pol II and/or is accumulating acetylated Pol II as a mechanism to promote dephosphorylation of RPB1. Further studies are needed to gain mechanistic insights about this phenomenon.

On the non-canonical role of RCOR1 in euchromatin gene repression

As we previously discussed, we were able to demonstrate a preferential localization of RCOR1 in euchromatin domains where active gene expression is occurring. Microscopy, biochemical, and 3D chromosome models constrained by Hi-C datasets supported these statements. Our results under modulation of RCOR1 levels in cells suggested that RCOR1 is repressing transcription in genes that are synthesized in a short time window. Flavopiridol-blocking of transcription in promoter-proximal stages induced a global inhibition of RNA Pol II-mediated transcription, as we can notice in the fluorescent images of nascent transcripts, where the remaining signals mostly come from nucleolar compartments. Recovery experiments

by washing out the inhibitor in RCOR1 down-regulated cells demonstrated a faster recovery of global transcriptional activity, suggesting RCOR1 as a regulator of the release of promoter-proximal pausing and/or elongation speed. Further studies are needed to confirm this hypothesis.

Remarkably, overexpression of RCOR1 produced a global decrease in nascent transcript synthesis, suggesting that RCOR1 could also be playing a role in the regulation of gene expression beyond RNA Pol II-mediated transcription. In support of this, the Corin inhibitor also produced an increase in nucleolar transcription. However, RCOR1 immunostainings suggested exclusion from nucleolar compartments. A possible explanation could be transient active recruitment of the complex to these regions that cannot be tracked by the methodologies used in this study.

Although cluster I of RCOR1-bound genes supports the role of RCOR1 inactive chromatin, an interesting observation also emerged from the identification of cluster II of RCOR1. These genes are enriched in bidirectional promoters, which could suggest eventual participation of the complex in the repression of bidirectional transcription. Future follow-up studies are going to be carried out to unveil this eventual mechanism.

Altogether, these results provided novel ways to explain how RCOR1 is recruited to active regions of the genome and unveil it as a rheostat or dampener of global RNA synthesis.

On the molecular assemblies of RCOR proteins

Previous studies performed in our laboratory showed that both RCOR1 and RCOR2 proteins, when immunostained, display a punctate distribution pattern inside the nucleus (Saez et al. 2015). Our preliminary data showed that RCOR1 and RCOR2 are segregated, supporting they mark different nuclear territories. The screening of nuclear bodies confirmed that RCOR2 is targeted at nuclear speckles. Thus, we can suggest that RCOR1 clusters represent other types of nuclear body or chromatin condensates. Interestingly, both RCOR1 and RCOR2 harbor different compositional-biased domains. RCOR1 has an N-terminal-rich domain, and RCOR2 has a C-terminal Proline-rich domain. These domains are commonly over-represented in proteins that display phase-separation processes in cells (Darling, Zaslavsky, and Uversky 2019). Therefore, it will be interesting to test if RCOR co-repressors can perform phase separation processes by themselves or, at least, be recruited to these biological condensates through interaction with their compositional-biased domains.

Unlike RCOR1, RCOR2 has not been characterized in depth. In this regard, our findings relating this co-repressor to the regulation of the stability of components of nuclear speckles contribute to this lack of fundamental information to understand its biological functions.

Conclusive remarks

This study unveiled novel, non-canonical roles of RCOR1 and RCOR2 transcriptional-co-repressors. We describe them as regulators of cellular functions related to euchromatin rather than chromatin silent domains. We consider this as a paradox since proteins that participate in transcriptional silencing are commonly associated with the establishment and maintenance of heterochromatin domains. However, our evidence unveil RCOR1 as a negative regulator of active transcription and RCOR2 as a factor that stabilizes nuclear speckle components. We propose that both proteins can negatively impact global gene expression, RCOR1 by inhibiting the transition to elongation of RNA Pol II and RCOR2 as a stabilizer of a speckle-bound, inactive, fraction of splicing factors.

UNCATEGORIZED REFERENCES

- Abrajano, J. J., I. A. Qureshi, S. Gokhan, A. E. Molero, D. Zheng, A. Bergman, and M. F. Mehler. 2010. ' co-repressor for element-1-silencing transcription factor preferentially mediates gene networks underlying neural stem cell fate decisions', *Proc Natl Acad Sci U S A*, 107: 16685-90.
- Abrajano, J. J., I. A. Qureshi, S. Gokhan, D. Zheng, A. Bergman, and M. F. Mehler. 2009. 'REST and CoREST modulate neuronal subtype specification, maturation and maintenance', *PLoS One*, 4: e7936.
- Ali, I., D. G. Ruiz, Z. Ni, J. R. Johnson, H. Zhang, P. C. Li, M. M. Khalid, R. J. Conrad, X. Guo, J. Min, J. Greenblatt, M. Jacobson, N. J. Krogan, and M. Ott. 2019. 'Crosstalk between RNA Pol II C-Terminal Domain Acetylation and Phosphorylation via RPRD Proteins', *Mol Cell*, 74: 1164-74 e4.
- Almouzni, G., and A. V. Probst. 2011. 'Heterochromatin maintenance and establishment: lessons from the mouse pericentromere', *Nucleus*, 2: 332-8.
- Anastas, J. N., B. M. Zee, J. H. Kalin, M. Kim, R. Guo, S. Alexandrescu, M. A. Blanco, S. Giera, S. M. Gillespie, J. Das, M. Wu, S. Nocco, D. M. Bonal, Q. D. Nguyen, M. L. Suva, B. E. Bernstein, R. Alani, T. R. Golub, P. A. Cole, M. G. Filbin, and Y. Shi. 2019. 'Re-programing Chromatin with a Bifunctional LSD1/HDAC Inhibitor Induces Therapeutic Differentiation in DIPG', *Cancer Cell*, 36: 528-44 e10.
- Andres, M. E., C. Burger, M. J. Peral-Rubio, E. Battaglioli, M. E. Anderson, J. Grimes, J. Dallman, N. Ballas, and G. Mandel. 1999. 'CoREST: a functional co-repressor required

- for regulation of neural-specific gene expression', *Proc Natl Acad Sci U S A*, 96: 9873-8.
- Ballas, N., E. Battaglioli, F. Atouf, M. E. Andres, J. Chenoweth, M. E. Anderson, C. Burger, M. Moniwa, J. R. Davie, W. J. Bowers, H. J. Federoff, D. W. Rose, M. G. Rosenfeld, P. Brehm, and G. Mandel. 2001. 'Regulation of neuronal traits by a novel transcriptional complex', *Neuron*, 31: 353-65.
- Ballas, N., C. Grunseich, D. D. Lu, J. C. Speh, and G. Mandel. 2005a. 'REST and its co-repressors mediate plasticity of neuronal gene chromatin throughout neurogenesis', *Cell*, 121: 645-57.
- . 2005b. 'REST and its co-repressors mediate plasticity of neuronal gene chromatin throughout neurogenesis', *Cell*, 121: 645-57.
- Ballas, N., and G. Mandel. 2005. 'The many faces of REST oversee epigenetic programming of neuronal genes', *Curr Opin Neurobiol*, 15: 500-6.
- Bannister, A. J., and T. Kouzarides. 2011. 'Regulation of chromatin by histone modifications', *Cell Res*, 21: 381-95.
- Barrios, A. P., A. V. Gomez, J. E. Saez, G. Ciossani, E. Toffolo, E. Battaglioli, A. Mattevi, and M. E. Andres. 2014. 'Differential properties of transcriptional complexes formed by the CoREST family', *Mol Cell Biol*, 34: 2760-70.
- Battaglioli, E., M. E. Andres, D. W. Rose, J. G. Chenoweth, M. G. Rosenfeld, M. E. Anderson, and G. Mandel. 2002. 'REST repression of neuronal genes requires components of the hSWI.SNF complex', *J Biol Chem*, 277: 41038-45.

- Benson, L. J., Y. Gu, T. Yakovleva, K. Tong, C. Barrows, C. L. Strack, R. G. Cook, C. A. Mizzen, and A. T. Annunziato. 2006. 'Modifications of H3 and H4 during chromatin replication, nucleosome assembly, and histone exchange', *J Biol Chem*, 281: 9287-96.
- Bergman, L. M., L. Morris, M. Darley, A. H. Mirnezami, S. C. Gunatilake, and J. P. Blaydes. 2006. 'Role of the unique N-terminal domain of CtBP2 in determining the subcellular localisation of CtBP family proteins', *BMC Cell Biol*, 7: 35.
- Bolte, S., and F. P. Cordelieres. 2006. 'A guided tour into subcellular colocalization analysis in light microscopy', *J Microsc*, 224: 213-32.
- Brero, A., H. P. Easwaran, D. Nowak, I. Grunewald, T. Cremer, H. Leonhardt, and M. C. Cardoso. 2005. 'Methyl CpG-binding proteins induce large-scale chromatin reorganization during terminal differentiation', *J Cell Biol*, 169: 733-43.
- Bucevicius, J., J. Keller-Findeisen, T. Gilat, S. W. Hell, and G. Lukinavicius. 2019. 'Rhodamine-Hoechst positional isomers for highly efficient staining of heterochromatin', *Chem Sci*, 10: 1962-70.
- Bunch, H., X. Zheng, A. Burkholder, S. T. Dillon, S. Motola, G. Birrane, C. C. Ebmeier, S. Levine, D. Fargo, G. Hu, D. J. Taatjes, and S. K. Calderwood. 2014. 'TRIM28 regulates RNA polymerase II promoter-proximal pausing and pause release', *Nat Struct Mol Biol*, 21: 876-83.
- Butler, P. J. 1983. 'The folding of chromatin', *CRC Crit Rev Biochem*, 15: 57-91.
- Carter, K. C., K. L. Taneja, and J. B. Lawrence. 1991. 'Discrete nuclear domains of poly(A) RNA and their relationship to the functional organization of the nucleus', *J Cell Biol*, 115: 1191-202.

- Chen, Y., Q. Huang, W. Liu, Q. Zhu, C. P. Cui, L. Xu, X. Guo, P. Wang, J. Liu, G. Dong, W. Wei, C. H. Liu, Z. Feng, F. He, and L. Zhang. 2018. 'Mutually exclusive acetylation and ubiquitylation of the splicing factor SRSF5 control tumor growth', *Nat Commun*, 9: 2464.
- Chen, Y., Y. Zhang, Y. Wang, L. Zhang, E. K. Brinkman, S. A. Adam, R. Goldman, B. van Steensel, J. Ma, and A. S. Belmont. 2018. 'Mapping 3D genome organization relative to nuclear compartments using TSA-Seq as a cytological ruler', *J Cell Biol*, 217: 4025-48.
- Cheng, Y., C. Luo, W. Wu, Z. Xie, X. Fu, and Y. Feng. 2016. 'Liver-Specific Deletion of SRSF2 Caused Acute Liver Failure and Early Death in Mice', *Mol Cell Biol*, 36: 1628-38.
- Chereji, R. V., T. D. Bryson, and S. Henikoff. 2019. 'Quantitative MNase-seq accurately maps nucleosome occupancy levels', *Genome Biol*, 20: 198.
- Craig, J. M. 2005. 'Heterochromatin--many flavours, common themes', *Bioessays*, 27: 17-28.
- Cramer, P., K. J. Armache, S. Baumli, S. Benkert, F. Brueckner, C. Buchen, G. E. Damsma, S. Dengl, S. R. Geiger, A. J. Jasiak, A. Jawhari, S. Jennebach, T. Kamenski, H. Kettenberger, C. D. Kuhn, E. Lehmann, K. Leike, J. F. Sydow, and A. Vannini. 2008. 'Structure of eukaryotic RNA polymerases', *Annu Rev Biophys*, 37: 337-52.
- Cusanovich, D. A., B. Pavlovic, J. K. Pritchard, and Y. Gilad. 2014. 'The functional consequences of variation in transcription factor binding', *PLoS Genet*, 10: e1004226.
- Daguenet, E., A. Baguet, S. Degot, U. Schmidt, F. Alpy, C. Wendling, C. Spiegelhalter, P. Kessler, M. C. Rio, H. Le Hir, E. Bertrand, and C. Tomasetto. 2012. 'Perispeckles are major assembly sites for the exon junction core complex', *Mol Biol Cell*, 23: 1765-82.

- Dar, R. D., B. S. Razooky, A. Singh, T. V. Trimeloni, J. M. McCollum, C. D. Cox, M. L. Simpson, and L. S. Weinberger. 2012. 'Transcriptional burst frequency and burst size are equally modulated across the human genome', *Proc Natl Acad Sci U S A*, 109: 17454-9.
- Darling, A. L., B. Y. Zaslavsky, and V. N. Uversky. 2019. 'Intrinsic Disorder-Based Emergence in Cellular Biology: Physiological and Pathological Liquid-Liquid Phase Transitions in Cells', *Polymers (Basel)*, 11.
- De Koning, L., A. Corpet, J. E. Haber, and G. Almouzni. 2007. 'Histone chaperones: an escort network regulating histone traffic', *Nat Struct Mol Biol*, 14: 997-1007.
- Dias, J. D., T. Rito, E. Torlai Triglia, A. Kukalev, C. Ferrai, M. Chotalia, E. Brookes, H. Kimura, and A. Pombo. 2015. 'Methylation of RNA polymerase II non-consensus Lysine residues marks early transcription in mammalian cells', *Elife*, 4.
- Dixon, J. R., I. Jung, S. Selvaraj, Y. Shen, J. E. Antosiewicz-Bourget, A. Y. Lee, Z. Ye, A. Kim, N. Rajagopal, W. Xie, Y. Diao, J. Liang, H. Zhao, V. V. Lobanenkov, J. R. Ecker, J. A. Thomson, and B. Ren. 2015. 'Chromatin architecture reorganization during stem cell differentiation', *Nature*, 518: 331-6.
- Edmond, V., E. Moysan, S. Khochbin, P. Matthias, C. Brambilla, E. Brambilla, S. Gazzeri, and B. Eymin. 2011. 'Acetylation and phosphorylation of SRSF2 control cell fate decision in response to cisplatin', *EMBO J*, 30: 510-23.
- Fei, J., M. Jдалиha, T. S. Harmon, I. T. S. Li, B. Hua, Q. Hao, A. S. Holehouse, M. Reyer, Q. Sun, S. M. Freier, R. V. Pappu, K. V. Prasanth, and T. Ha. 2017. 'Quantitative analysis of multilayer organization of proteins and RNA in nuclear speckles at super resolution', *J Cell Sci*, 130: 4180-92.

- Fornieris, F., C. Binda, A. Adamo, E. Battaglioli, and A. Mattevi. 2007. 'Structural basis of LSD1-CoREST selectivity in histone H3 recognition', *J Biol Chem*, 282: 20070-4.
- Fornieris, F., C. Binda, M. A. Vanoni, E. Battaglioli, and A. Mattevi. 2005. 'Human histone demethylase LSD1 reads the histone code', *J Biol Chem*, 280: 41360-5.
- Gates, L. A., J. Shi, A. D. Rohira, Q. Feng, B. Zhu, M. T. Bedford, C. A. Sagum, S. Y. Jung, J. Qin, M. J. Tsai, S. Y. Tsai, W. Li, C. E. Foulds, and B. W. O'Malley. 2017. 'Acetylation on histone H3 lysine 9 mediates a switch from transcription initiation to elongation', *J Biol Chem*, 292: 14456-72.
- Gocke, C. B., and H. Yu. 2008. 'ZNF198 stabilizes the LSD1-CoREST-HDAC1 complex on chromatin through its MYM-type zinc fingers', *PLoS One*, 3: e3255.
- Gomez, A. V., D. Galleguillos, J. C. Maass, E. Battaglioli, M. Kukuljan, and M. E. Andres. 2008. 'CoREST represses the heat shock response mediated by HSF1', *Mol Cell*, 31: 222-31.
- Goodson, M., B. A. Jonas, and M. A. Privalsky. 2005. 'co-repressors: custom tailoring and alterations while you wait', *Nucl Recept Signal*, 3: e003.
- Greer, C. B., Y. Tanaka, Y. J. Kim, P. Xie, M. Q. Zhang, I. H. Park, and T. H. Kim. 2015. 'Histone Deacetylases Positively Regulate Transcription through the Elongation Machinery', *Cell Rep*, 13: 1444-55.
- Gunjan, A., J. Paik, and A. Verreault. 2006. 'The emergence of regulated histone proteolysis', *Curr Opin Genet Dev*, 16: 112-8.
- Gurard-Levin, Z. A., J. P. Quivy, and G. Almouzni. 2014. 'Histone chaperones: assisting histone traffic and nucleosome dynamics', *Annu Rev Biochem*, 83: 487-517.

- Hall, L. L., K. P. Smith, M. Byron, and J. B. Lawrence. 2006. 'Molecular anatomy of a speckle', *Anat Rec A Discov Mol Cell Evol Biol*, 288: 664-75.
- Hamiche, A., and M. Shuaib. 2013. 'Chaperoning the histone H3 family', *Biochim Biophys Acta*, 1819: 230-7.
- Harlen, K. M., and L. S. Churchman. 2017. 'The code and beyond: transcription regulation by the RNA polymerase II carboxy-terminal domain', *Nat Rev Mol Cell Biol*, 18: 263-73.
- Hochberg-Laufer, H., N. Neufeld, Y. Brody, S. Nadav-Eliyahu, R. Ben-Yishay, and Y. Shav-Tal. 2019. 'Availability of splicing factors in the nucleoplasm can regulate the release of mRNA from the gene after transcription', *PLoS Genet*, 15: e1008459.
- Hochberg-Laufer, H., A. Schwed-Gross, K. M. Neugebauer, and Y. Shav-Tal. 2019. 'Uncoupling of nucleo-cytoplasmic RNA export and localization during stress', *Nucleic Acids Res*, 47: 4778-97.
- Holmquist, G. 1975. 'Hoechst 33258 fluorescent staining of Drosophila chromosomes', *Chromosoma*, 49: 333-56.
- Huang, Y., S. J. Myers, and R. Dingledine. 1999. 'Transcriptional repression by REST: recruitment of Sin3A and histone deacetylase to neuronal genes', *Nat Neurosci*, 2: 867-72.
- Humphrey, G. W., Y. Wang, V. R. Russanova, T. Hirai, J. Qin, Y. Nakatani, and B. H. Howard. 2001. 'Stable histone deacetylase complexes distinguished by the presence of SANT domain proteins CoREST/kiaa0071 and Mta-L1', *J Biol Chem*, 276: 6817-24.
- Jao, C. Y., and A. Salic. 2008. 'Exploring RNA transcription and turnover in vivo by using click chemistry', *Proc Natl Acad Sci U S A*, 105: 15779-84.
- Jenuwein, T., and C. D. Allis. 2001. 'Translating the histone code', *Science*, 293: 1074-80.

- Jeon, Y., and J. T. Lee. 2011. 'YY1 tethers Xist RNA to the inactive X nucleation center', *Cell*, 146: 119-33.
- Kalin, J. H., M. Wu, A. V. Gomez, Y. Song, J. Das, D. Hayward, N. Adejola, M. Wu, I. Panova, H. J. Chung, E. Kim, H. J. Roberts, J. M. Roberts, P. Prusevich, J. R. Jeliaskov, S. S. Roy Burman, L. Fairall, C. Milano, A. Eroglu, C. M. Proby, A. T. Dinkova-Kostova, W. W. Hancock, J. J. Gray, J. E. Bradner, S. Valente, A. Mai, N. M. Anders, M. A. Rudek, Y. Hu, B. Ryu, J. W. R. Schwabe, A. Mattevi, R. M. Alani, and P. A. Cole. 2018. 'Targeting the CoREST complex with dual histone deacetylase and demethylase inhibitors', *Nat Commun*, 9: 53.
- Kang, B. G., J. H. Shin, J. K. Yi, H. C. Kang, J. J. Lee, H. S. Heo, J. H. Chae, I. Shin, and C. G. Kim. 2007. 'co-repressor MMTR/DMAP1 is involved in both histone deacetylase 1- and TFIID-mediated transcriptional repression', *Mol Cell Biol*, 27: 3578-88.
- Kao, H. Y., M. Downes, P. Ordentlich, and R. M. Evans. 2000. 'Isolation of a novel histone deacetylase reveals that class I and class II deacetylases promote SMRT-mediated repression', *Genes Dev*, 14: 55-66.
- Kedzierska, H., P. Poplawski, G. Hoser, B. Rybicka, K. Rodzik, E. Sokol, J. Boguslawska, Z. Tanski, A. Fogtman, M. Koblowska, and A. Piekuelko-Witkowska. 2016. 'Decreased Expression of SRSF2 Splicing Factor Inhibits Apoptotic Pathways in Renal Cancer', *Int J Mol Sci*, 17.
- Kim, J., K. Y. Han, N. Khanna, T. Ha, and A. S. Belmont. 2019. 'Nuclear speckle fusion via long-range directional motion regulates speckle morphology after transcriptional inhibition', *J Cell Sci*, 132.

- Kim, J., N. C. Venkata, G. A. Hernandez Gonzalez, N. Khanna, and A. S. Belmont. 2020. 'Gene expression amplification by nuclear speckle association', *J Cell Biol*, 219.
- Kim, S. A., N. Chatterjee, M. J. Jennings, B. Bartholomew, and S. Tan. 2015. 'Extranucleosomal DNA enhances the activity of the LSD1/CoREST histone demethylase complex', *Nucleic Acids Res*, 43: 4868-80.
- Kim, S. A., J. Zhu, N. Yennawar, P. Eek, and S. Tan. 2020. 'Crystal Structure of the LSD1/CoREST Histone Demethylase Bound to Its Nucleosome Substrate', *Mol Cell*, 78: 903-14 e4.
- Kolossov, V. L., M. Sivaguru, J. Huff, K. Luby, K. Kanakaraju, and H. R. Gaskins. 2018. 'Airyscan super-resolution microscopy of mitochondrial morphology and dynamics in living tumor cells', *Microsc Res Tech*, 81: 115-28.
- Kornberg, R. D. 1974. 'Chromatin structure: a repeating unit of histones and DNA', *Science*, 184: 868-71.
- Kouzarides, T. 2007. 'Chromatin modifications and their function', *Cell*, 128: 693-705.
- Kraus, W. L., and J. T. Kadonaga. 1998. 'p300 and estrogen receptor cooperatively activate transcription via differential enhancement of initiation and reinitiation', *Genes Dev*, 12: 331-42.
- Kraushaar, D. C., Z. Chen, Q. Tang, K. Cui, J. Zhang, and K. Zhao. 2018. 'The gene repressor complex NuRD interacts with the histone variant H3.3 at promoters of active genes', *Genome Res*, 28: 1646-55.
- Kruhlak, M. J., M. A. Lever, W. Fischle, E. Verdin, D. P. Bazett-Jones, and M. J. Hendzel. 2000. 'Reduced mobility of the alternate splicing factor (ASF) through the nucleoplasm and steady state speckle compartments', *J Cell Biol*, 150: 41-51.

- Kurogi, Y., Y. Matsuo, Y. Mihara, H. Yagi, K. Shigaki-Miyamoto, S. Toyota, Y. Azuma, M. Igarashi, and T. Tani. 2014. 'Identification of a chemical inhibitor for nuclear speckle formation: implications for the function of nuclear speckles in regulation of alternative pre-mRNA splicing', *Biochem Biophys Res Commun*, 446: 119-24.
- Lakowski, B., I. Roelens, and S. Jacob. 2006. 'CoREST-like complexes regulate chromatin modification and neuronal gene expression', *J Mol Neurosci*, 29: 227-39.
- Lan, F., R. E. Collins, R. De Cegli, R. Alpatov, J. R. Horton, X. Shi, O. Gozani, X. Cheng, and Y. Shi. 2007. 'Recognition of unmethylated histone H3 lysine 4 links BHC80 to LSD1-mediated gene repression', *Nature*, 448: 718-22.
- Lan, F., A. C. Nottke, and Y. Shi. 2008. 'Mechanisms involved in the regulation of histone lysine demethylases', *Curr Opin Cell Biol*, 20: 316-25.
- Larson, D. R. 2011. 'What do expression dynamics tell us about the mechanism of transcription?', *Curr Opin Genet Dev*, 21: 591-9.
- Leal-Ortiz, S., C. L. Waites, R. Terry-Lorenzo, P. Zamorano, E. D. Gundelfinger, and C. C. Garner. 2008. 'Piccolo modulation of Synapsin1a dynamics regulates synaptic vesicle exocytosis', *J Cell Biol*, 181: 831-46.
- Lee, J. W., Y. C. Lee, S. Y. Na, D. J. Jung, and S. K. Lee. 2001. 'Transcriptional coregulators of the nuclear receptor superfamily: coactivators and co-repressors', *Cell Mol Life Sci*, 58: 289-97.
- Lee, M. G., C. Wynder, D. A. Bochar, M. A. Hakimi, N. Cooch, and R. Shiekhattar. 2006. 'Functional interplay between histone demethylase and deacetylase enzymes', *Mol Cell Biol*, 26: 6395-402.

- Lee, M., H. Ji, Y. Furuta, J. I. Park, and P. D. McCrea. 2014. 'p120-catenin regulates REST and CoREST, and modulates mouse embryonic stem cell differentiation', *J Cell Sci*, 127: 4037-51.
- Lenstra, T. L., J. Rodriguez, H. Chen, and D. R. Larson. 2016. 'Transcription Dynamics in Living Cells', *Annu Rev Biophys*, 45: 25-47.
- Liu, Z., and R. Tjian. 2018. 'Visualizing transcription factor dynamics in living cells', *J Cell Biol*, 217: 1181-91.
- Loyola, A., and G. Almouzni. 2004. 'Histone chaperones, a supporting role in the limelight', *Biochim Biophys Acta*, 1677: 3-11.
- Loyola, A., T. Bonaldi, D. Roche, A. Imhof, and G. Almouzni. 2006. 'PTMs on H3 variants before chromatin assembly potentiate their final epigenetic state', *Mol Cell*, 24: 309-16.
- Luger, K., A. W. Mader, R. K. Richmond, D. F. Sargent, and T. J. Richmond. 1997. 'Crystal structure of the nucleosome core particle at 2.8 Å resolution', *Nature*, 389: 251-60.
- McKenna, N. J., R. B. Lanz, and B. W. O'Malley. 1999. 'Nuclear receptor coregulators: cellular and molecular biology', *Endocr Rev*, 20: 321-44.
- McKenna, N. J., and B. W. O'Malley. 2001. 'Nuclear receptors, coregulators, ligands, and selective receptor modulators: making sense of the patchwork quilt', *Ann N Y Acad Sci*, 949: 3-5.
- Meller, V. H., S. S. Joshi, and N. Deshpande. 2015. 'Modulation of Chromatin by Noncoding RNA', *Annu Rev Genet*, 49: 673-95.
- Mieczkowski, J., A. Cook, S. K. Bowman, B. Mueller, B. H. Alver, S. Kundu, A. M. Deaton, J. A. Urban, E. Larschan, P. J. Park, R. E. Kingston, and M. Y. Tolstorukov. 2016.

- 'MNase titration reveals differences between nucleosome occupancy and chromatin accessibility', *Nat Commun*, 7: 11485.
- Millard, C. J., P. J. Watson, I. Celardo, Y. Gordiyenko, S. M. Cowley, C. V. Robinson, L. Fairall, and J. W. Schwabe. 2013. 'Class I HDACs share a common mechanism of regulation by inositol phosphates', *Mol Cell*, 51: 57-67.
- Millard, C. J., P. J. Watson, L. Fairall, and J. W. Schwabe. 2013. 'An evolving understanding of nuclear receptor coregulator proteins', *J Mol Endocrinol*, 51: T23-36.
- Monaghan, C. E., T. Nechiporuk, S. Jeng, S. K. McWeeney, J. Wang, M. G. Rosenfeld, and G. Mandel. 2017. 'REST co-repressors RCOR1 and RCOR2 and the repressor INSM1 regulate the proliferation-differentiation balance in the developing brain', *Proc Natl Acad Sci U S A*, 114: E406-E15.
- Narita, T., B. T. Weinert, and C. Choudhary. 2019. 'Functions and mechanisms of non-histone protein acetylation', *Nat Rev Mol Cell Biol*, 20: 156-74.
- O'Brien, K., A. J. Matlin, A. M. Lowell, and M. J. Moore. 2008. 'The biflavonoid isoginkgetin is a general inhibitor of Pre-mRNA splicing', *J Biol Chem*, 283: 33147-54.
- Ocampo, J., F. Cui, V. B. Zhurkin, and D. J. Clark. 2016. 'The proto-chromatosome: A fundamental subunit of chromatin?', *Nucleus*, 7: 382-7.
- Payankulam, S., L. M. Li, and D. N. Arnosti. 2010. 'Transcriptional repression: conserved and evolved features', *Curr Biol*, 20: R764-71.
- Phair, R. D., and T. Misteli. 2000. 'High mobility of proteins in the mammalian cell nucleus', *Nature*, 404: 604-9.
- Pilotto, S., V. Speranzini, M. Tortorici, D. Durand, A. Fish, S. Valente, F. Forneris, A. Mai, T. K. Sixma, P. Vachette, and A. Mattevi. 2015. 'Interplay among nucleosomal DNA,

- histone tails, and co-repressor CoREST underlies LSD1-mediated H3 demethylation', *Proc Natl Acad Sci U S A*, 112: 2752-7.
- PLIMPTON, S. 1995. 'FAST PARALLEL ALGORITHMS FOR SHORT-RANGE MOLECULAR-DYNAMICS', *Journal of Computational Physics*, 117: 1-19.
- Probst, A. V., and G. Almouzni. 2008. 'Pericentric heterochromatin: dynamic organization during early development in mammals', *Differentiation*, 76: 15-23.
- Quinodoz, S. A., N. Ollikainen, B. Tabak, A. Palla, J. M. Schmidt, E. Detmar, M. M. Lai, A. A. Shishkin, P. Bhat, Y. Takei, V. Trinh, E. Aznauryan, P. Russell, C. Cheng, M. Jovanovic, A. Chow, L. Cai, P. McDonel, M. Garber, and M. Guttman. 2018. 'Higher-Order Inter-chromosomal Hubs Shape 3D Genome Organization in the Nucleus', *Cell*, 174: 744-57 e24.
- Ramirez, F., F. Dundar, S. Diehl, B. A. Gruning, and T. Manke. 2014. 'deepTools: a flexible platform for exploring deep-sequencing data', *Nucleic Acids Res*, 42: W187-91.
- Rivera, C., Z. A. Gurard-Levin, G. Almouzni, and A. Loyola. 2014. 'Histone lysine methylation and chromatin replication', *Biochim Biophys Acta*.
- Rivera, C., F. Saavedra, F. Alvarez, C. Diaz-Celis, V. Ugalde, J. Li, I. Forne, Z. A. Gurard-Levin, G. Almouzni, A. Imhof, and A. Loyola. 2015. 'Methylation of histone H3 lysine 9 occurs during translation', *Nucleic Acids Res*, 43: 9097-106.
- Saavedra, F., S. Marty-Lombardi, and A. Loyola. 2018. 'Characterization of Posttranslational Modifications on Histone Variants', *Methods Mol Biol*, 1832: 21-49.
- Saavedra, F., C. Rivera, E. Rivas, P. Merino, D. Garrido, S. Hernandez, I. Forne, I. Vassias, Z. A. Gurard-Levin, I. E. Alfaro, A. Imhof, G. Almouzni, and A. Loyola. 2017. 'PP32 and

- SET/TAF-Ibeta proteins regulate the acetylation of newly synthesized histone H4', *Nucleic Acids Res*, 45: 11700-10.
- Sacco-Bubulya, P., and D. L. Spector. 2002. 'Disassembly of interchromatin granule clusters alters the coordination of transcription and pre-mRNA splicing', *J Cell Biol*, 156: 425-36.
- Saez, J. E., C. Arredondo, C. Rivera, and M. E. Andres. 2018. 'PIASgamma controls stability and facilitates SUMO-2 conjugation to CoREST family of transcriptional co-repressors', *Biochem J*, 475: 1441-54.
- Saez, J. E., A. V. Gomez, A. P. Barrios, G. E. Parada, L. Galdames, M. Gonzalez, and M. E. Andres. 2015. 'Decreased Expression of CoREST1 and CoREST2 Together with LSD1 and HDAC1/2 during Neuronal Differentiation', *PLoS One*, 10: e0131760.
- Saijo, K., B. Winner, C. T. Carson, J. G. Collier, L. Boyer, M. G. Rosenfeld, F. H. Gage, and C. K. Glass. 2009. 'A Nurr1/CoREST pathway in microglia and astrocytes protects dopaminergic neurons from inflammation-induced death', *Cell*, 137: 47-59.
- Saitoh, N., C. S. Spahr, S. D. Patterson, P. Bubulya, A. F. Neuwald, and D. L. Spector. 2004. 'Proteomic analysis of interchromatin granule clusters', *Mol Biol Cell*, 15: 3876-90.
- Saleque, S., J. Kim, H. M. Rooke, and S. H. Orkin. 2007. 'Epigenetic regulation of hematopoietic differentiation by Gfi-1 and Gfi-1b is mediated by the cofactors CoREST and LSD1', *Mol Cell*, 27: 562-72.
- Salichs, E., A. Ledda, L. Mularoni, M. M. Alba, and S. de la Luna. 2009. 'Genome-wide analysis of histidine repeats reveals their role in the localization of human proteins to the nuclear speckles compartment', *PLoS Genet*, 5: e1000397.

- Schroder, S., E. Herker, F. Itzen, D. He, S. Thomas, D. A. Gilchrist, K. Kaehlcke, S. Cho, K. S. Pollard, J. A. Capra, M. Schnolzer, P. A. Cole, M. Geyer, B. G. Bruneau, K. Adelman, and M. Ott. 2013. 'Acetylation of RNA polymerase II regulates growth-factor-induced gene transcription in mammalian cells', *Mol Cell*, 52: 314-24.
- Shepard, P. J., and K. J. Hertel. 2009. 'The SR protein family', *Genome Biol*, 10: 242.
- Shi, Y. J., C. Matson, F. Lan, S. Iwase, T. Baba, and Y. Shi. 2005. 'Regulation of LSD1 histone demethylase activity by its associated factors', *Mol Cell*, 19: 857-64.
- Shi, Y., J. Sawada, G. Sui, B. Affar el, J. R. Whetstine, F. Lan, H. Ogawa, M. P. Luke, Y. Nakatani, and Y. Shi. 2003. 'Coordinated histone modifications mediated by a CtBP co-repressor complex', *Nature*, 422: 735-8.
- Shin, H., T. Liu, A. K. Manrai, and X. S. Liu. 2009. 'CEAS: cis-regulatory element annotation system', *Bioinformatics*, 25: 2605-6.
- Simpson, R. T. 1978. 'Structure of the chromatosome, a chromatin particle containing 160 base pairs of DNA and all the histones', *Biochemistry*, 17: 5524-31.
- Song, Y., L. Dagil, L. Fairall, N. Robertson, M. Wu, T. J. Ragan, C. G. Savva, A. Saleh, N. Morone, M. B. A. Kunze, A. G. Jamieson, P. A. Cole, D. F. Hansen, and J. W. R. Schwabe. 2020. 'Mechanism of Crosstalk between the LSD1 Demethylase and HDAC1 Deacetylase in the CoREST Complex', *Cell Rep*, 30: 2699-711 e8.
- Spector, D. L., X. D. Fu, and T. Maniatis. 1991. 'Associations between distinct pre-mRNA splicing components and the cell nucleus', *EMBO J*, 10: 3467-81.
- Spector, D. L., and A. I. Lamond. 2011. 'Nuclear speckles', *Cold Spring Harb Perspect Biol*, 3.
- Steurer, B., R. C. Janssens, B. Geverts, M. E. Geijer, F. Wienholz, A. F. Theil, J. Chang, S. Dealy, J. Pothof, W. A. van Cappellen, A. B. Houtsmuller, and J. A. Marteijn. 2018.

- 'Live-cell analysis of endogenous GFP-RPB1 uncovers rapid turnover of initiating and promoter-paused RNA Polymerase II', *Proc Natl Acad Sci U S A*, 115: E4368-E76.
- Strahl, B. D., and C. D. Allis. 2000. 'The language of covalent histone modifications', *Nature*, 403: 41-5.
- Suganuma, T., and J. L. Workman. 2008. 'Crosstalk among Histone Modifications', *Cell*, 135: 604-7.
- Sytnikova, Y. A., A. V. Kubarenko, A. Schafer, A. N. Weber, and C. Niehrs. 2011. 'Gadd45a is an RNA binding protein and is localized in nuclear speckles', *PLoS One*, 6: e14500.
- Tagoh, H., S. Melnik, P. Lefevre, S. Chong, A. D. Riggs, and C. Bonifer. 2004. 'Dynamic reorganization of chromatin structure and selective DNA demethylation prior to stable enhancer complex formation during differentiation of primary hematopoietic cells in vitro', *Blood*, 103: 2950-5.
- Thiry, M. 1995. 'The interchromatin granules', *Histol Histopathol*, 10: 1035-45.
- Trojer, P., and D. Reinberg. 2007. 'Facultative heterochromatin: is there a distinctive molecular signature?', *Mol Cell*, 28: 1-13.
- Tunnacliffe, E., and J. R. Chubb. 2020. 'What Is a Transcriptional Burst?', *Trends Genet*, 36: 288-97.
- Upadhyay, G., A. H. Chowdhury, B. Vaidyanathan, D. Kim, and S. Saleque. 2014. 'Antagonistic actions of Rcor proteins regulate LSD1 activity and cellular differentiation', *Proc Natl Acad Sci U S A*, 111: 8071-6.
- Vicent, G. P., A. S. Nacht, R. Zaurin, J. Font-Mateu, D. Soronellas, F. Le Dily, D. Reyes, and M. Beato. 2013. 'Unliganded progesterone receptor-mediated targeting of an RNA-

- containing repressive complex silences a subset of hormone-inducible genes', *Genes Dev*, 27: 1179-97.
- Vignali, M., A. H. Hassan, K. E. Neely, and J. L. Workman. 2000. 'ATP-dependent chromatin-remodeling complexes', *Mol Cell Biol*, 20: 1899-910.
- Wang, Y., X. Li, and H. Hu. 2014. 'H3K4me2 reliably defines transcription factor binding regions in different cells', *Genomics*, 103: 222-8.
- Wang, Y., Q. Wu, P. Yang, C. Wang, J. Liu, W. Ding, W. Liu, Y. Bai, Y. Yang, H. Wang, S. Gao, and X. Wang. 2016. 'LSD1 co-repressor Rcor2 orchestrates neurogenesis in the developing mouse brain', *Nat Commun*, 7: 10481.
- Wang, Z., C. Zang, K. Cui, D. E. Schones, A. Barski, W. Peng, and K. Zhao. 2009. 'Genome-wide mapping of HATs and HDACs reveals distinct functions in active and inactive genes', *Cell*, 138: 1019-31.
- Wen, Y. D., V. Perissi, L. M. Staszewski, W. M. Yang, A. Krones, C. K. Glass, M. G. Rosenfeld, and E. Seto. 2000. 'The histone deacetylase-3 complex contains nuclear receptor co-repressors', *Proc Natl Acad Sci U S A*, 97: 7202-7.
- Wu, X., H. Li, E. J. Park, and J. D. Chen. 2001. 'SMRTE inhibits MEF2C transcriptional activation by targeting HDAC4 and 5 to nuclear domains', *J Biol Chem*, 276: 24177-85.
- Yang, M., C. B. Gocke, X. Luo, D. Borek, D. R. Tomchick, M. Machius, Z. Otwinowski, and H. Yu. 2006. 'Structural basis for CoREST-dependent demethylation of nucleosomes by the human LSD1 histone demethylase', *Mol Cell*, 23: 377-87.
- Yang, P., Y. Wang, J. Chen, H. Li, L. Kang, Y. Zhang, S. Chen, B. Zhu, and S. Gao. 2011. 'RCOR2 is a subunit of the LSD1 complex that regulates ESC property and substitutes for SOX2 in reprogramming somatic cells to pluripotency', *Stem Cells*, 29: 791-801.

- You, A., J. K. Tong, C. M. Grozinger, and S. L. Schreiber. 2001. 'CoREST is an integral component of the CoREST- human histone deacetylase complex', *Proc Natl Acad Sci U S A*, 98: 1454-8.
- Zaborowska, J., S. Egloff, and S. Murphy. 2016. 'The pol II CTD: new twists in the tail', *Nat Struct Mol Biol*, 23: 771-7.
- Zhang, J., J. Parvin, and K. Huang. 2012. 'Redistribution of H3K4me2 on neural tissue specific genes during mouse brain development', *BMC Genomics*, 13 Suppl 8: S5.
- Zhang, T., G. Wei, C. J. Millard, R. Fischer, R. Konietzny, B. M. Kessler, J. W. R. Schwabe, and N. Brockdorff. 2018. 'A variant NuRD complex containing PWWP2A/B excludes MBD2/3 to regulate transcription at active genes', *Nat Commun*, 9: 3798.
- Zhang, X., H. Wen, and X. Shi. 2012. 'Lysine methylation: beyond histones', *Acta Biochim Biophys Sin (Shanghai)*, 44: 14-27.
- Zhao, X., J. Su, F. Wang, D. Liu, J. Ding, Y. Yang, J. W. Conaway, R. C. Conaway, L. Cao, D. Wu, M. Wu, Y. Cai, and J. Jin. 2013. 'Crosstalk between NSL histone acetyltransferase and MLL/SET complexes: NSL complex functions in promoting histone H3K4 dimethylation activity by MLL/SET complexes', *PLoS Genet*, 9: e1003940.
- Zhu, L., and C. P. Brangwynne. 2015. 'Nuclear bodies: the emerging biophysics of nucleoplasmic phases', *Curr Opin Cell Biol*, 34: 23-30.
- Zhu, L. J., C. Gazin, N. D. Lawson, H. Pages, S. M. Lin, D. S. Lapointe, and M. R. Green. 2010. 'ChIPpeakAnno: a Bioconductor package to annotate ChIP-seq and ChIP-chip data', *BMC Bioinformatics*, 11: 237.
- Zibetti, C., A. Adamo, C. Binda, F. Forneris, E. Toffolo, C. VerPELLI, E. Ginelli, A. Mattevi, C. Sala, and E. Battaglioli. 2010. 'Alternative splicing of the histone demethylase

LSD1/KDM1 contributes to the modulation of neurite morphogenesis in the mammalian nervous system', *J Neurosci*, 30: 2521-32.